Spring 6-30-1976

The effects of optical path perturbations during recording on a reconstructed holographic image

Stevan Israel Feldman
New Jersey Institute of Technology

Copyright Warning & Restrictions

The copyright law of the United States (Title 17, United States Code) governs the making of photocopies or other reproductions of copyrighted material.

Under certain conditions specified in the law, libraries and archives are authorized to furnish a photocopy or other reproduction. One of these specified conditions is that the photocopy or reproduction is not to be "used for any purpose other than private study, scholarship, or research." If a, user makes a request for, or later uses, a photocopy or reproduction for purposes in excess of "fair use" that user may be liable for copyright infringement,

This institution reserves the right to refuse to accept a copying order if, in its judgment, fulfillment of the order would involve violation of copyright law.

Please Note: The author retains the copyright while the New Jersey Institute of Technology reserves the right to distribute this thesis or dissertation

Printing note: If you do not wish to print this page, then select "Pages from: first page # to: last page #" on the print dialog screen

THE EFFECTS OF OPTICAL PATH PERTURBATIONS DURING RECORDING ON A RECONSTRUCTED HOLOGRAPHIC IMAGE

BY

STEVAN ISRAEL FELDMAN

A DISSERTATION

PRESENTED IN PARTIAL FULFILLMENT OF

THE REQUIREMENTS FOR THE DEGREE

OF

DOCTOR OF SCIENCE IN ELECTRICAL ENGINEERING

AT

NEW JERSEY INSTITUTE OF TECHNOLOGY

Newark, New Jersey

1976

ABSTRACT

The effects of optical path perturbations occurring during recording on the reconstructed image of a hologram are investigated. It is shown that such variations of optical path are equivalent to conditions of holographic interferometry which can be classified in three categories: 1) object motion alone, 2) film motion alone, and 3) simultaneous film and object motion; all motions are defined with respect to the stationary reference source during the recording of the hologram.

The theory concerning the effects of object motion alone on the radiance distribution of a reconstructed holographic image has already been developed by previous researchers and is reviewed. This theory is extended to cover the other two above mentioned categories. Quasi-monochromatic conditions are assumed throughout. Experimental verification of the theory is presented for the cases of step object motion, step film motion, simultaneous step film and object motion, simultaneous staircase film and object motion, and simultaneous step film - staircase object motion.

Holographic recording conditions under which a step change in refractive index occurs in a slab of the medium separating the mechanically stationary object and film during the hologram recording are analyzed. It is shown

that, within the assumptions of paraxial conditions and small optical path perturbations, these conditions are equivalent to the occurrence of a mechanical step film motion during the hologram recording.

Extension of this interpretation and of the resulting analysis technique to the study of the effects of turbulence in the optical path medium during recording on the reconstructed holographic image yields results in accordance with the predictions of conventional turbulence analysis techniques. Several promising applications of the new technique are indicated. These include simulation of turbulence under controlled conditions in the laboratory. In addition, application of the theory to the measurement of atmospheric turbulence distributions from holographic data is broadly indicated and some advantages of this novel approach over the present state of the art are enumerated.

APPROVAL OF DISSERTATION

THE EFFECTS OF OPTICAL PATH

PERTURBATIONS DURING RECORDING

ON A RECONSTRUCTED

HOLOGRAPHIC IMAGE

BY

STEVAN ISRAEL FELDMAN

FOR

DEPARTMENT OF ELECTRICAL ENGINEERING

NEW JERSEY INSTITUTE OF TECHNOLOGY

BY

FACULTY COMMITTEE

APPROVED: _____ CHAIRMAN

_____

_____

_____

_____

NEWARK, NEW JERSEY

JUNE, 1976

PREFACE

During the past ten years, holography has been emerging as an important technical tool for a large variety of scientific, engineering and medical applications. In many instances, holographic techniques are by far the most practical, sometimes the only practical means of obtaining useful data for design and analysis. The investigation presented in this thesis is mainly concerned with the detection and study of optical path disturbances occurring during holographic recording in the medium between object and holographic plate and whose nature is either deterministic or stochastic.

A resume of the historical development of holography and a description of some basic holographic techniques and properties are presented in chapter I. The presentation is intended to establish a coherent method of notation, and in so doing, presents certain holographic phenomena from a sometimes unusual point of view. Particular emphasis is placed on those specific concepts (such as the hologram's sensitivity to the degree of coherence) that are especially important and relevant to the investigation presented.

To this end a detailed analysis of the split beam holographic process employing partially coherent quasi-monochromatic radiation during the formation of the hologram

is offered. Concepts from the classical theory of coherence are applied to a description of the holographic process, and establish the groundwork for consideration of the effects of motions during recording on holography (chapter II).

The theory describing the effects of object motion during recording, on the reconstructed holographic image is reviewed in chapter III and expressed in generalized form. This theory is then extended to include motion of the holographic film plate during recording. It is shown that this new extension of the theory can be used not only to study the effects of simultaneous film and object motion, but also to establish a novel method of holographic interferometry capable of simulating, detecting, and identifying complicated optical disturbances in the medium between the holographic plate and the object.

The specific analysis of the effects of random (turbulent) disturbances in the medium interposed between the object and recording planes during hologram formation is the subject of chapter IV. A novel approach to the computation of the effects of random perturbations of optical path on the reconstructed image is developed. In particular, it is shown that predictions obtained by this new approach are in accordance with results obtained by other investigators using conventional turbulence analysis. Suggestions

concerning the possibility offered by this method of achieving simulation of turbulence effects under controlled laboratory conditions are indicated.

A detailed study of the effects of simultaneous film and object motion with respect to a stationary reference source during the hologram exposure is presented in chapter V. A general expression for the modified complex degree of coherence for this case is developed. The effects of such motion on the reconstructed image are analyzed and computations are made for several special types of simultaneous laws of motions. On the basis of this discussion it is proved that this technique affords a practical, approximate means of computing the modified complex degree of coherence, and it is finally shown that it permits the analysis of complicated motion effects for certain classes of object-film motions by simpler, more practical means than heretofore available.

The theories concerning film motion and simultaneous film and object motion are extended to the three dimensional case in chapter VI. This is shown to be useful for the further interpretation of the observed fringe spacing in the reconstructed image.

Original experimental verification of the theory is presented in chapter VII, where the theoretical predictions of the theory concerning object, film, and several cases of simultaneous object and film motion are verified to within experimental error.

Conclusions and recommendations for future work are presented in chapter VIII.

ACKNOWLEDGMENT

I would like to thank Professor Mauro Zambuto for his encouragement, inspiration, critiques and valuable suggestions throughout this study.

Further, this research would not have been possible without the facilities provided by the Electrical Engineering Department of New Jersey Institute of Technology.

TABLE OF CONTENTS

LIST OF FIGURES

LIST OF TABLES

CHAPTER I

BASIC CONCEPTS OF HOLOGRAPHY

The past ten years has seen a large research and development effort concentrated on improving the techniques and devising new applications for holography. Indeed holography, in its more spectacular aspects, as a method of lensless three-dimensional photography, has become quite familiar and popular with the general public. Less generally known, outside a circle of specialists, are some holographic applications of a more specific technical value which make the process an immensely important tool for a large variety of scientific, engineering and medical applications.

This thesis is concerned with investigating one such application which falls within the realm of "holographic interferometry." Thanks to its ability to detect the distribution not only in intensity but in phase of wavefronts, holography can be used as a particularly sensitive, powerful, and convenient tool for the "visualization" of "phase objects." To this end, a large effort has been directed towards applying holography to the study of small displacements, distortions and laws of motion[1] (holographic interferometry). Our investigation will be further concerned with the application of holographic interferometry

to the detection and study of optical path disturbances whose nature is either deterministic or stochastic.

In this chapter we shall present a fast resume of the historical development of holography and a description of some basic holographic techniques and properties. The presentation will emphasize specific aspects and concepts, such as, sensitivity to the degree of coherence, the characteristic function, etc. because of their importance and relevance to the development of this investigation as presented in later chapters.

It must be emphasized that this resume is not intended to be complete, nor particularly rigorous in presentation. It is intended to recall some fundamental properties of the holographic process in a form suited to our purposes. It will serve to introduce a coherent form of notation and present certain phenomena from a sometimes unusual point of view because of envisioned further developments. The resume is not intended to substitute for a more complete and general understanding of the holographic process which can be obtained from the abundant literature.[2,3,4,5,6,7] Indeed we shall often offer no more than a hint and a reference to well known facts and well developed theories, without reproducing their proofs or specifically indicating the limitations implied in their statements. If at this time, more detailed information is required, the reader is again

referred to discussions such as those offered by Born and Wolf[8] or De Velis and Reynolds[9] et. al.

1.1 The History of Holography

Wavefront reconstruction (holography) is a two step, lensless imaging technique conceived by D. Gabor[10,11], in 1948 to deal with problems associated with electron lens distortion in electron microscopes. He proposed the recording of the pattern resulting from the interference between the Fresnel diffraction, by a suitable object, of the illuminating radiation, and a reference radiation. Naturally, for the interference to have sufficient visibility for recording, the two radiations should have a high degree of coherence. In the original proposed geometry, the reference radiation was provided by the undiffracted portion of the illuminating radiation (refer to figure 1-1). This, of course, restricted the types of objects to those which allow a large portion of the incident radiation to pass undiffracted, i.e., objects with a small subject area compared to the total area of illumination. A photographic record was then formed of the resulting interference pattern across the recording plane. This record was termed "hologram" and had little resemblance to a conventional photographic image of the subject.

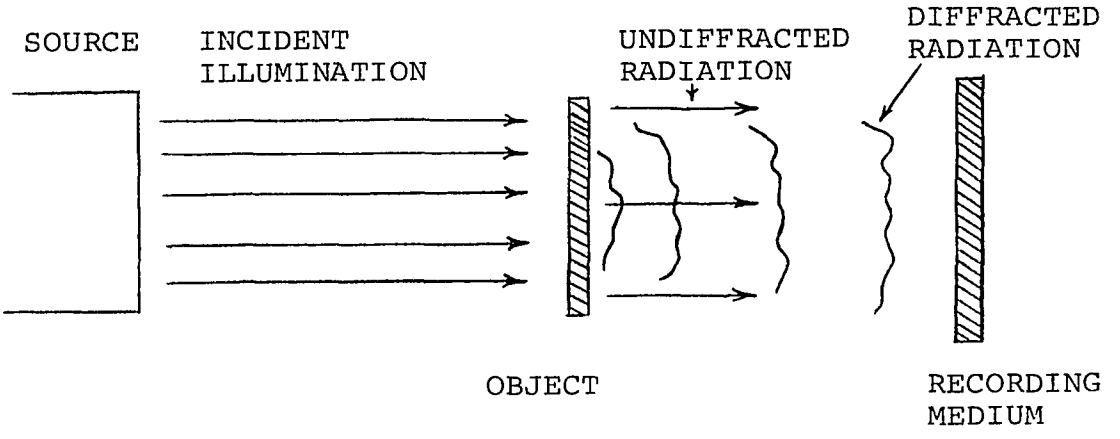

Figure 1-1

Geometry for the formation and reconstruction of a Gabor type hologram

The hologram was then placed in a geometry, with respect to the reconstruction source, such that the illuminating wavefront, at the processed hologram plane, was identical (except for a possible amplitude difference) to the reference wavefront existing across the hologram plane during recording. The diffraction of the incident radiation by the hologram resulted in transmitted wavefronts appearing downstream (opposite the source side) of the hologram. These transmitted wavefronts contained a replica of the original object wavefront which existed in the hologram plane at the time of recording, a conjugate wavefront which is sometimes referred to as a "ghost image" and wavefronts related to the illuminating source.

Gabor's initial experimental work was limited by a lack of sufficiently intense and coherent sources of radiation. Furthermore, his original holograms, while confirming the validity of the holographic process, suffered from very poor image quality because both the desired and the ghost images were formed on the same optical axis, although these images were formed in different planes. Also, optical imperfections such as dust on the photographic plate (or glass bubbles) resulted in additionally degraded image quality.

Holography remained a laboratory curiosity for many years until E. Leith and J. Upatnieks, of the University of Michigan, using a laser as the source of coherent radiation, produced good quality holographic images. Their technique involved introducing two variations in the holographic process.[12,13] The first improvement resulted from the use of a reference beam forming an angle with the recording plane (an off axis reference beam). This procedure is called split beam holography. The second improvement was obtained by the use of diffuse illumination of the object.

The use of an off axis reference beam requires a greater degree of coherence between the object and illuminating beams to produce an interference pattern across the holcgram plane. This technique was impractical before the laser, which is a source of highly coherent light, was available. The split beam holographic technique results, upon reconstruction, in a spatial (angular) separation of the two images (desired and conjugate image) so that either can be viewed without the annoying interference associated with having both images on the same axis.

Secondly, the use of diffuse illumination greatly reduced the deleterious effects of local optical imperfections in the recording system due to dust specs or glass bubbles. The use of diffuse illumination essentially

spreads the object illumination across the whole recording plane making the local imperfections much less obtrusive when viewing the reconstructed image. Diffuse illumination and split beam techniques also obviate the necessity to print the hologram in order to obtain a positive image.

The impressive results obtained by these techniques spurred new interest in wavefront reconstruction as an imaging technique. Further research by many continued to improve image quality and produced vast numbers of proposed engineering applications for the process, many of which show great promise of coming to fruition.

1.2 A Description of the Holographic Process

A typical split beam hologram recording geometry is depicted in figure 1-2 where S is a monochromatic source of radiation, H is the hologram recording plane, O is a suitable diffusely reflecting object, U_O represents the rediffused object wave, U_R the reference wave and M is a mirror used to direct the reference wave towards the hologram plane. In the discussion to follow, the reference beam will be assumed to be collimated (a plane wave) and perfectly monochromatic to simplify the computations.

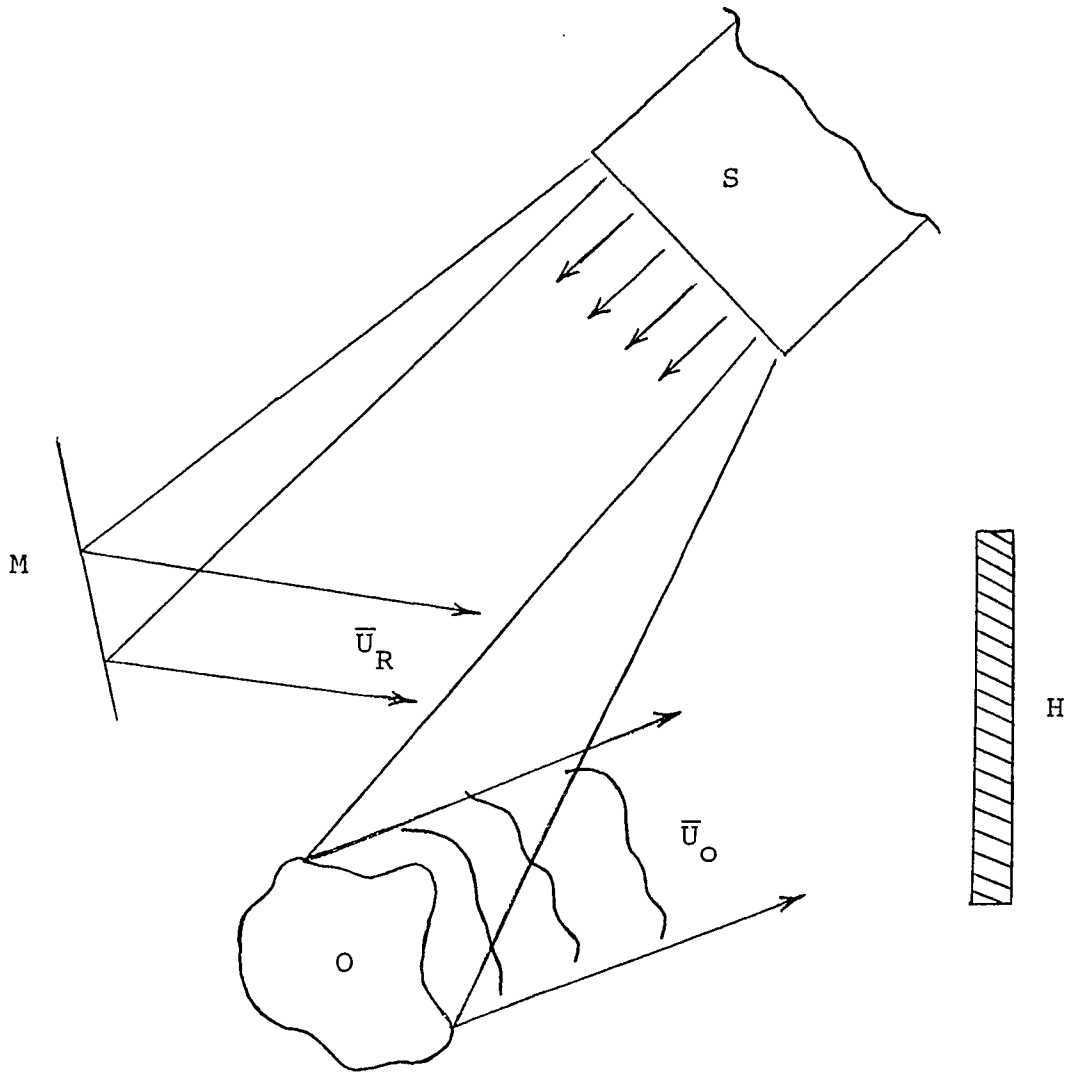

Figure 1-2

A typical hologram (split-beam) geometry with S the monochromatic source, O the object, M a mirror, $\bar{U}_R$ the reference beam, $\bar{U}_O$ the object beam and H the recording medium.

Let x_h and y_h be the coordinates of a point in the recording plane, then, the distribution of the complex amplitude of the reference wavefront on the hologram plane can be represented by,

$$\overline{R}(x_h, y_h) = R(x_h, y_h)\, e^{j\,\phi_R\,(x_h, y_h)} \qquad (1\text{-}1)$$

where $\overline{R}(x_h, y_h)$ is the complex amplitude (amplitude and phase) of the analytic signal $\overline{V}(P, t)$. As usual in holography, use is made of the analytic signal and complex amplitude representation of an electromagnetic wave. The reader is reminded that $\overline{V}(P, t)$ is a scalar quantity representing the appropriate electromagnetic field vector of the radiation. The analytic signal representation for an electromagnetic field vector essentially is a complex function whose real and imaginary terms form a Hilbert transform[14,15,16] and whose real part describes the amplitude and phase of the electromagnetic field disturbance at point P and time t. The use of the analytic signal representation is analogous to the use of an exponential to represent functions which vary as a cosine function.

The use of a scalar quantity to represent the electromagnetic field is justified whenever we can imply certain conditions, for instance that all radiation under consideration is polarized in the same direction.[17] In this case, knowledge of the magnitude and phase of the field as a

function of position and time will completely describe the field.[18] If deemed necessary to consider polarization effects, the formulation must then include the full vector nature of the field.[19] This level of complexity will not be required for the investigation to be discussed here.

Considering equation 1-1, $R(x_h, y_h)$ is a real quantity and $\phi_R(x_h, y_h)$ is a relative phase function which, for a collimated reference beam, depends on the angle between the reference beam and the recording plane. For a collimated reference beam, normal to the recording plane, the phase factor $\phi_R(x_h, y_h)$ would be a constant which could be arbitrarily set to zero.

The complex amplitude distribution in the recording plane due to an object point m is,

$$\bar{O}_m(x_h, y_h) = O_m(x_h, y_h)\, e^{j\,\phi_o(x_h, y_h, m)} \qquad (1\text{-}2)$$

where $O_m(x_h, y_h)$ is a real quantity and $\phi_o(x_h, y_h, m)$ is the relative phase of the radiation coming from point m on the object at the hologram plane point x_h, y_h.

The complex amplitude at a point x_h, y_h in the recording plane due to the superposition of the radiation from the object point m and the reference beam is,

$$\bar{U}(x_h, y_h) = \bar{O}_m(x_h, y_h) + \bar{R}(x_h, y_h) \qquad (1\text{-}3)$$

and the corresponding intensity is

$$I(x_h, y_h) = |\bar{U}(x_h, y_h)|^2$$

$$= |\bar{O}_m(x_h, y_h) + \bar{R}(x_h, y_h)|^2$$

$$= |\bar{O}_m|^2 + |\bar{R}|^2$$

$$+ O_m R\, e^{j(\phi_o - \phi_R)} + O_m R\, e^{j(\phi_R - \phi_o)}. \qquad (1\text{-}4)$$

Then, considering x_h and y_h as running variables, equation 1-4 describes the intensity distribution of the interference of the reference and object wavefronts in the recording plane for the case (here considered for convenience) where the "object" is a single point.

When a photographic plate is placed in the plane H and exposed to this intensity distribution, the exposure* can be expressed as

$$E = \int_0^T |\bar{O}_m + \bar{R}|^2\, dt$$

$$= E_o + E_R + O_m R T \left\{ \frac{1}{T} \int_0^T e^{j(\phi_o - \phi_R)} dt \right.$$

$$\left. + \frac{1}{T} \int_0^T e^{j(\phi_R - \phi_o)} dt \right\} \qquad (1\text{-}5)$$

*the integral of the light intensity reaching the photographic plate over the time during which the plate is exposed to the light is called the exposure.[20]

where E_o and E_R represent the exposure due to the object and reference wavefronts respectively acting alone and an assumption of time invariance of the object and reference beam amplitudes during exposure has been made. In addition, the frequency of both the object and reference wavefronts has also been assumed to be time invariant over the period of exposure (assumed monochromatic radiation). Equation 1-5 can be written as,

$$E = E_o + E_R + \sqrt{E_o E_R}\left\{\overline{G}_{mR}(T) + \overline{G}_{mR}^{*}(T)\right\}$$

$$= E_o + E_R + \sqrt{E_o E_R\, G_{mR}(T)}\left\{e^{j\delta} + e^{-j\delta}\right\} \qquad (1\text{-}6)$$

where $\delta = \phi_o - \phi_R$ and $G_{mR}(T) = |G_{mR}(T)|^2$ is the square of the absolute value of the modified complex degree of coherence that existed between the radiation from the object point m and the reference radiation at the time of exposure providing the quasi-monochromatic hypothesis is satisfied*. The processed film plate is termed a hologram, and is the final result of the formation stage of the holographic process. It should be indicated that the hologram plate bears little resemblance to a photographic image of

*more will be presented concerning this area in chapter 2. For this example the quasi-monochromatic hypothesis is satisfied due to the monochromacity of the object and reference wavefronts. Further definition of this nomenclature can be obtained in a paper by M. Lurie[21] if required by the reader.

the object. Rather, what one observes when looking at the processed plate with ordinary incoherent illumination is a pattern of light and dark fringes.

With proper processing of the photographic plate, the amplitude transmittance of the processed hologram can be made proportional to the exposure ($\gamma = -2$)**. When this hologram is illuminated with a reconstruction beam of complex amplitude distribution at the hologram plate of

$$\bar{r}(x_h, y_h) = r(x_h, y_h)\, e^{j\,\phi_r\,(x_h,\, y_h)} \qquad (1\text{-}7)$$

the complex amplitude distribution $\bar{\Omega}$ downstream of the hologram is[20],

$$\bar{\Omega} = K \{ \bar{r}\,(E_o + E_R) + r\, e^{j\,(\phi_r + \delta)} \sqrt{E_o E_R G_{mR}(T)} + r\, e^{j\,(\phi_r - \delta)} \sqrt{E_o E_R G_{mR}(T)} \} \qquad (1\text{-}8)$$

where K is a constant of proportionality due to the film processing.

**the transmittance is proportional to $E(x_h, y_h)^{-\gamma/2}$ where γ is the slope of the H and D curve for the photographic film[22] and $E(x_h, y_h)$ is the exposure. For a more complete discussion of this subject see Appendix I, for the moment we will assume that the film processing is controlled to produce a gamma of minus two resulting in a transmittance function linear in exposure.

Equations 1-5 and 1-6 imply that for time invariant $\phi_o(x_h, y_h)$ and $\phi_R(x_h, y_h)$ the quantity $G_{mR}(T)$ is equal to unity. Recalling that $\delta = \phi_o - \phi_R$, we have that equation 1-8 becomes, under these conditions,

$$\bar{\Omega} = K \{ \bar{r}(E_o + E_R) + r\, e^{j(\phi_r + \phi_o - \phi_R)} \sqrt{E_o E_R} + r\, e^{j(\phi_r - \phi_o + \phi_R)} \sqrt{E_o E_R} \}. \qquad (1\text{-}9)$$

Further, if $\phi_r(x_h, y_h) \equiv \phi_R(x_h, y_h)$; that is, if the reconstruction and reference wavefronts at the hologram plate are identical except for a possible amplitude difference, the complex amplitude distribution downstream of the hologram is,

$$\bar{\Omega} = K \{ r(E_o + E_R)\, e^{j\phi_R} + r\sqrt{E_o E_R}\, e^{j\phi_o} + r\sqrt{E_o E_R}\, e^{j(2\phi_R - \phi_o)} \} \qquad (1\text{-}10)$$

The first term of equation 1-10 consists of an undiffracted beam of light which represents the reconstruction source and can be considered a noise term. The last term is a diffracted beam of light giving rise to a "complementary" (because of the negative sign of ϕ_o) image of the object.

The middle term is of particular interest to us because it is proportional to the wavefront originally generated by the object beam across the hologram plane during the recording of the hologram.

An observer viewing the hologram from a properly oriented point of view will perceive no difference between the reconstructed wave proceeding from this wavefront and which forms a virtual image of the object, and the original object wave. The two will appear identical. Therefore, the viewer, looking at the hologram, sees an image both in depth (i.e., he must refocus his eyes when changing radial distance from the hologram), and in perspective (i.e., he can change his point of view by moving angularly with respect to the hologram). Consequently, the reconstructed image appears optically indistinguishable from the original object.

If, during the recording of the hologram, $\phi_O - \phi_R$ is not constant as previously assumed, several conditions can exist which will be indicated and discussed in detail in a later chapter. First, suppose that ϕ_O varies in time and ϕ_R remains time invariant; this is a condition of partially coherent object light and completely coherent reference light (this situation is encountered and discussed in chapter 3 under the heading of "object motion"). Under

quasi-monochromatic conditions, as we shall see, the reconstruction of the complex amplitude distribution downstream of the hologram becomes,

$$\overline{\Omega} = K \{ r(E_o + E_R)\, e^{j\,\phi_R} + r\sqrt{E_o\, E_R\, G_{mR}(T)}\, e^{j\,\phi_o} + r\sqrt{E_o\, E_R\, G_{mR}(T)}\, e^{j(2\phi_R - \phi_o)} \qquad (1\text{-}11)$$

which is identical to the complex amplitude distribution for constant $\phi_o - \phi_R$ except that the amplitude of the image terms are now proportional to $\sqrt{G_{mR}(T)}$. The intensity of an image point m' then is now proportional to $G_{mR}(T)$.

The computation of $G_{mR}(T)$ for conditions of object motion is covered in detail in chapter three. Essentially, the phase shift generated at the hologram plane, computed by determining the change in optical path between the object point m and the hologram, due to the point m experiencing a motion during the hologram exposure, will be a non-constant value dependent on the nature of the object's law of motion. Consequently, $G_{mR}(T)$ is both a function of the object point under consideration and of its law of motion.

The second case of interest occurs when both ϕ_O and ϕ_R are time varying during the hologram exposure. Such a situation is encountered for conditions involving film plate motion. Again, this subject will be further discussed and analyzed in detail in chapter three under film plate motion.

REFERENCES

1. M. Zambuto and M. Lurie, Applied Optics, 9, 2066 (1970)

2. H.M.A. El-Sum, Science and Technology, 71, 50 (1967)

3. Grant R. Fowles, Introduction to Modern Optics, Holt, Rinehart and Winston, Inc., 144 (1968)

4. E. Leith and J. Upatnieks, J. Opt. Soc. Am., 52, 1123 (1962)

5. R.J. Collier, C.B. Burckhardt, L.H. Lin, Optical Holography, Academic Press, (1971)

6. W.T. Cathey, Optical Information Processing and Holography, Wiley-Interscience, (1974)

7. H.M. Smith, Principles of Holography, Wiley-Interscience, (1969)

8. M. Born and E. Wolf, Principles of Optics, third edition, Pergamon Press, N.Y., 453 (1965)

9. J.B. De Velis and G.O. Reynolds, Theory and Applications of Holography, Addison-Wesley Publishing Company, (1967)

10. D. Gabor, Nature, 161, 777 (1948)

11. D. Gabor, Nature, 162, 764 (1948)

12. E. Leith and J. Upatnieks, J. Opt. Soc. Am., 53, 1377 (1963)

13. E. Leith and J. Upatnieks, J. Opt. Soc. Am., 54, 1295 (1964)

14. Philip F. Panter, Modulation, Noise, and Spectral Analysis, McGraw-Hill Book Company, 198 (1965)

15. M.J. Beran and G.B. Parrent Jr., Theory of Partial Coherence, Prentice-Hall Inc., 12 (1965)

16. Edward L. O'Neill, Introduction to Statistical Optics, Addison-Wesley Publishing Company, 15 (1963)

17. M. Born and E. Wolf, op. cit., 387

18. M. Born and E. Wolf, op. cit., 387

19. M. Born and E. Wolf, op. cit., 387

20. C.E. Mees and T.H. James, Theory of the Photographic Process, The MacMillan Company, 318 (1966)

21. M. Lurie, J. Opt. Soc. Am., 56, 1369 (1966)

22. Kodak Plates and Films, Eastman Kodak Company, 2 (1973)

23. Grant R. Fowles, op. cit., 145

CHAPTER II

AN ANALYSIS OF THE HOLOGRAPHIC PROCESS

A more detailed discussion of the split beam holographic process employing partially coherent quasi-monochromatic radiation during the hologram formation stage will be presented. We will summarize a large volume of work[1,2,3] and present an analysis applying concepts from the classical theory of coherence to a description of the holographic process.[4] These concepts are essential when considering the effects of motions, during recording, on the holographic process. This particular subject will be discussed with great detail in a later chapter.

Again, this resume is intended to present to the reader a background in the basic concepts of holography. The discussion will initially highlight some important results from the classical theory of coherence and then apply some of these results to a description of the holographic process. If a rigorous presentation of the subject matter is of interest, the reader is referred to either Born and Wolf[5] or De Velis and Reynolds[6].

2.1 Classical Theory of Coherence

Consider an optical disturbance at point P and time t to be represented by the analytic signal $\overline{V}(P, t)$. An important property of this radiation is its coherence which is computed as the correlation of the analytic signal at a particular space-time point in the radiation field with the radiation at a second space-time point in the field. The mutual coherence function is defined as[7]

$$\Gamma(P_1, P_2, \tau) \equiv \Gamma_{12}(\tau) = \langle \overline{V}(P_1, t)\ \overline{V}^*(P_2, t + \tau) \rangle \qquad (2\text{-}1)$$

where $\langle V \rangle = \underset{T\to\infty}{\text{Lim}}\ \frac{1}{T}\int_0^T V dt$, and $\overline{V}(P_1, t)$ is the analytic signal representing the optical disturbance at point P_1 and at time t, while $\overline{V}(P_2, t + \tau)$ is the analytic signal representing the optical disturbance at point P_2 and at a time τ later than t, and the * denotes the complex conjugate function. In the commonly accepted nomenclature of stationary random processes, $\Gamma_{12}(\tau)$ is termed the cross-correlation function of $\overline{V}(P_1, t)$ and $\overline{V}(P_2, t)$.

The propagation of the mutual coherence function in vacuum can be shown to satisfy two coupled wave equations[8] given by

$$\nabla_1^2 \Gamma(P_1, P_2, \tau) = \frac{1}{C^2} \frac{\partial^2 \Gamma(P_1, P_2, \tau)}{\partial \tau^2}$$

$$\nabla_2^2 \Gamma(P_1, P_2, \tau) = \frac{1}{C^2} \frac{\partial^2 \Gamma(P_1, P_2, \tau)}{\partial \tau^2} \qquad (2\text{-}2)$$

where C is the speed of light and ∇_k^2 is the Laplacian operator with respect to the coordinates of P_K.

The coherence of radiation is generally classified as spatial and temporal coherence where temporal coherence refers to the autocorrelation of the radiation measured at one (and the same) space point and spatial coherence the cross-correlation of radiation at two points in the wave field measured at the same time. Specifically, the temporal coherence, $\Gamma_{11}(\tau)$ is,

$$\Gamma_{11}(\tau) = \langle \bar{V}(P_1, t)\ \bar{V}^*(P_1, t + \tau) \rangle \qquad (2\text{-}3)$$

and the spatial coherence $\Gamma_{12}(o)$ is

$$\Gamma_{12}(o) = \langle \bar{V}(P_1, t)\ \bar{V}^*(P_2, t) \rangle . \qquad (2\text{-}4)$$

Observe that as is well known[9], $\Gamma_{11}(o)$, the autocorrelation of the function $\bar{V}(P_1, t)$ with zero time shift, is the intensity of the radiation at point P_1. As a direct consequence of equation 2-3, it can be shown that a wave containing only one frequency (a rigorously monochromatic wave) must be temporally coherent while a non-monochromatic

wave cannot be completely coherent. This is a consequence of applying the Wiener-Khinchin theorem[10] to equation 2-3.

In practice, convenience dictates the use of the normalized mutual coherence function, termed the "complex degree of coherence", and defined as[11]

$$\gamma_{12}(\tau) \equiv \Gamma_{12}(\tau)/\sqrt{\Gamma_{11}(o)\ \Gamma_{22}(o)}\ . \qquad (2\text{-}5)$$

Application of the Schwartz Inequality[12] leads to the conclusion that $|\gamma_{12}(\tau)|$ is a bounded function with bounds of zero and unity.[13] The implications of the bounds are that the condition $|\gamma_{12}(\tau)| = 1$ for all τ indicates a completely coherent field and complete incoherence implies $|\gamma_{12}(\tau)| = 0$ for all $\tau \neq 0$. When $|\gamma_{12}(\tau)|$ lies between these extremes, the radiation is termed partially coherent.[14] As an example, the laser is a source of highly coherent (but not completely coherent) light, the sun is a source of partially coherent light and a frosted incandescent light bulb, if viewed at short distance, is a source of low coherence light where the coherence referred to in these examples is the temporal coherence of the radiation.

Although a physically realizable source cannot be monochromatic (completely temporally coherent)[15], many sources are available which can produce radiation of very

narrow spectral width compared to the mean frequency of the radiation, $\bar{\nu}$ i.e., $\Delta\nu << \bar{\nu}$, $\Delta\nu$ being the frequency deviation from the mean. Radiation of this type is defined as narrowband radiation.[16] In addition, narrowband radiation is termed "quasi-monochromatic" when the path length difference between the source point S and observation points P_1 and P_2 is such that

$$\Delta\ell = \overline{SP}_1 - \overline{SP}_2 << C/\Delta\nu \qquad (2\text{-}6)$$

where C is the speed of light.[17] Equation 2-6 can also be expressed as

$$\frac{1}{\tau} >> \Delta\nu = \Delta\omega/2\pi \qquad (2\text{-}7)$$

which is also a useful relationship. In equation 2-7, $\tau = \Delta\ell/C^*$ where $\Delta\ell$ is the difference in path from the source to the two observation points; τ is the time shift equivalent of the path difference and $\Delta\omega = 2\pi\Delta\nu$. Note that narrowband radiation which satisfies the quasi-monochromatic condition for one experiment may not satisfy the quasi-monochromatic conditions in a different set of circumstances,

*this is the case for two different space points but all that is necessary is to have two different space-time points, i.e., the condition could also be for measurements at the same point in the field taken at two different times.

i.e., the restrictions imposed on τ depend on the particular computation and it is not a basic property of the light.

When quasi-monochromatic conditions prevail, the complex degree of coherence can be accurately approximated by [18]

$$\gamma_{12}(\tau) \approx \gamma_{12}(o)\ e^{-j\omega\tau}. \qquad (2\text{-}8)$$

It is important to note that quasi-monochromatic radiation is temporally coherent radiation[19] over the interval τ since

$$|\gamma_{11}(\tau)| \approx |\gamma_{11}(o)\ e^{j\omega\tau}| = |\gamma_{11}(o)| \qquad (2\text{-}9)$$

and

$$|\gamma_{11}(o)| = \Gamma_{11}(o)/\sqrt{\Gamma_{11}(o)\ \Gamma_{11}(o)}$$

$$= 1$$

2.2 A Description of the Holographic Process Employing Partially Coherent Quasi-Monochromatic Radiation

A discussion of the holographic process will be presented essentially following a compilation from the work of Born and Wolf[19A], De Velis and Reynolds[20], Lurie and Zambuto[21], and many others[22,23] with changes in notation for our specific purposes. This section is presented

primarily to obtain a set of relationships suitable for the computation of the effect of partial coherence on holography, a concept already introduced in chapter I, which is basic to the holographic process and central to our study.

The quasi-monochromatic hypothesis previously discussed was introduced to allow the use of a single frequency mathematical representation for the radiation of interest. This hypothesis also allows the formulation of the description of wave propagation in terms of a single wave equation resulting in the computation becoming a simple boundary value problem.[24] This method is of course preferred to the more rigorous approach which requires the solution of two coupled wave equations.[25] It must be indicated that the simplified method does not always adequately describe the process under consideration. Fortunately, for our study, the rigorous method of formulation will not be necessary.

In describing the holographic process, we must first be able to determine the distribution of radiation in a plane removed from the source plane which contains a known distribution of radiation. Then, consider $\psi(\bar{x})$ to represent the radiation of interest in the x, y plane, and $\psi_i(\bar{\xi})$ the source radiation in the ξ, η plane. Let $\bar{\xi}$ be a position vector in the ξ, η plane (the source plane) and $\bar{x}$ a position vector in the x, y plane. Let $G(\bar{\xi}, \bar{x})$

represent the appropriate Green's function which satisfies the boundary conditions, in the source plane, of $G(\bar{\xi}, \bar{x}) = 0$ for $Z = o$ and $\partial G/\partial n$, the derivative of the Green's function along the normal to the wavefront, exists. Then, to obtain the desired distribution of radiation $\psi(\bar{x})$ from the known distribution of radiation $\psi_i(\bar{\xi})$ requires the evaluation of the following integral[26],

$$\psi(\bar{x}) = \int \psi_i(\bar{\xi}) \partial G(\bar{\xi}, \bar{x})/\partial n \, d\bar{\xi}. \qquad (2\text{-}10)$$

Figure 2-1 indicates the geometry used to calculate the Green's function which satisfies the boundary conditions in the ξ, η plane. The Green's function in this case is given by

$$G(\bar{\xi}, \bar{x}) = \frac{e^{jkr}}{4\pi r} - \frac{e^{jkr'}}{4\pi r'} \qquad (2\text{-}11)$$

where r is the distance from the source (a point in the plane of known distribution) to a point in the plane on which we wish to know the new distribution of radiation, and r' is the mirror image of r, i.e., for $r = f(x, y, z)$, $r' = f(x, y, -z)$.

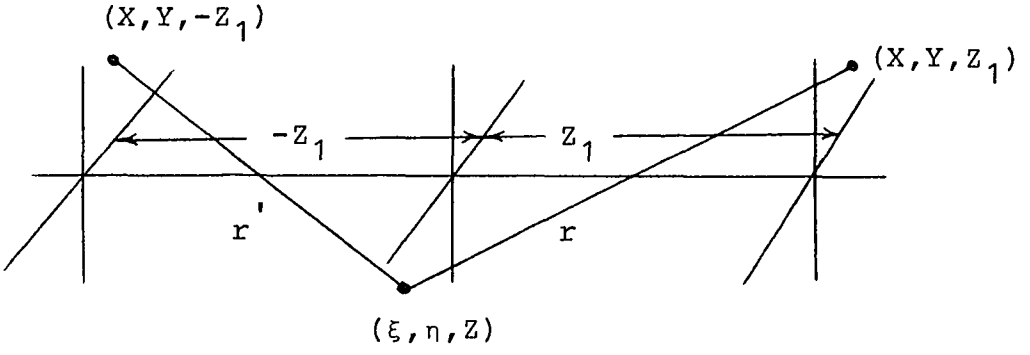

Figure 2-1

The geometry for the calculation of the Green's function.

After some manipulation, equation 2-10 reduces to

$$\psi(\bar{x}) = -\frac{jk}{2\pi Z_1} \int_{\bar{\xi}} \psi_i(\bar{\xi})\ e^{jkr(\bar{\xi},\ \bar{x})}\ d\bar{\xi} \qquad (2\text{-}12)$$

where the usual geometric and small angle assumptions associated with the paraxial approximation have been invoked[28]. Equation 2-12 can now be applied to computing the distribution of radiation in a plane different from a source plane when given the source distribution.

Consider now a typical split beam hologram geometry represented in figure 2-2 where the conditions of the quasi-monochromatic hypothesis is satisfied. Let the reference radiation be defined by,

$$V_R(t) = A_R\ e^{j\omega t} \qquad (2\text{-}13)$$

and let

$$V(\bar{\xi},\ Z,\ t) = A(\bar{\xi},\ Z)\ e^{j[\omega t + \theta(\bar{\xi},\ Z)]} \qquad (2\text{-}14)$$

represent the radiation from a typical object point $m = [\xi,\ \eta,\ Z]$ with the condition that as ξ, η, Z vary, V represents the analytic signal for the different object points. Note that the reference radiation is considered to be coherent and a plane wave, and the object under consideration has a distribution in the ξ, η plane and in depth.

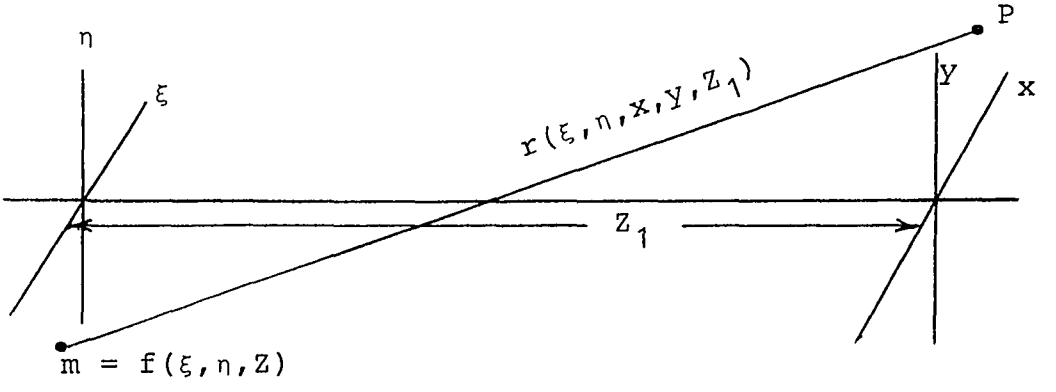

Figure 2-2

Typical hologram geometry for the formation stage of the holographic process.

The analytic signal representing the radiation in the x, y plane at point P, which is removed from the ξ, η plane by a distance Z_1 can be found using equation 2-12. The distribution is found to be,

$$V_P(\bar{x}, Z_1, t) = A_R\, e^{j(\omega t + kZ_1)}$$

$$- \iiint_{\bar{\xi},\, Z} \frac{jk}{2\pi r(\bar{\xi}, \bar{x}, Z)} A(\bar{\xi}, Z) \; X$$

$$e^{j[\omega t + \theta(\bar{\xi}, Z) + kr(\bar{\xi}, \bar{x}, Z)]}\, d\bar{\xi}\, dZ \quad (2\text{-}15)$$

where $k = 2\pi/\lambda$, λ the average wavelength of the quasi-monochromatic radiation. The object wave (the second term of equation 2-15) is the diffracted object illumination at $P = [x, y]$ in the x, y plane. The distance from the object point m to the recording point P is

$$r(\bar{\xi}, \bar{x}, Z) = \sqrt{(\xi - x)^2 + (\eta - y)^2 + (Z - Z_1)^2}.$$

The record of the intensity distribution in the interference pattern formed by the coherent addition of these wavefronts (object and reference) across the recording medium is a hologram. This record will, after proper processing, have an amplitude transmittance proportional to the energy distribution across the recording plane. More precisely, if χ_P is the amplitude transmittance of

the hologram at point P[29] and K is a constant of proportionality related to the film response and the point intensity, then

$$\chi_P = K \int_0^T |V_P(\bar{x}, Z_1, t)|^2 \, dt. \qquad (2\text{-}16)$$

The hologram transmittance at each point, $P(\bar{x})$, becomes (under proper processing conditions)*

$$\chi_P = K|A_R|^2 T + KT \left| \iiint_{\bar{\xi}, Z} \frac{jk\, A(\bar{\xi}, Z)}{2\pi r(\bar{\xi}, \bar{x}, Z)} \, X \right.$$

$$\left. e^{j[kr(\bar{\xi}, \bar{x}, Z) + \theta(\bar{\xi}, Z) - kZ_1]} d\bar{\xi} \, dZ \right|^2$$

$$+ K \int_0^T \left\{ \iiint_{\bar{\xi}, Z} \frac{jk\, A(\bar{\xi}, Z) A_R}{2\pi r(\bar{\xi}, \bar{x}, Z)} \, X \right.$$

$$e^{j[kr(\bar{\xi}, \bar{x}, Z) - kZ_1 + \theta(\bar{\xi}, Z)]} d\bar{\xi} \, dZ$$

$$- \iiint_{\bar{\xi}, Z} \frac{jk\, A(\bar{\xi}, Z) A_R}{2\pi r(\bar{\xi}, \bar{x}, Z)} \, X$$

$$\left. e^{j[kZ_1 - kr(\bar{\xi}, \bar{x}, Z) - \theta(\bar{\xi}, Z)]} d\bar{\xi} \, dZ \right\} dt \qquad (2\text{-}17)$$

where the quantity $A(\bar{\xi}, Z)$ is the amplitude distribution of the object radiation in the object plane.

*for a more detailed description of this process see appendix I.

Consider for the moment, the integrand of equation 2-17. Let

$$V_m(t + \tau) \equiv V(\bar{\xi}, t + \tau) \equiv A(\bar{\xi}, Z)\ e^{j[\theta(\bar{\xi}, Z) + \omega(t + \tau)]} \tag{2-18}$$

with

$$\frac{k}{\omega}\ [r(\bar{\xi}, \bar{x}, Z) - Z_1] = \frac{1}{C}\ [r(\bar{\xi}, \bar{x}, Z) - Z_1] \equiv \tau \tag{2-19}$$

and τ is the time delay due to the difference in optical path between the reference source and point P, and the object point m and P. Combining equations 2-17 and 2-18 gives

$$\begin{aligned} V(\bar{\xi}, t + \tau) &= A(\bar{\xi}, Z)\ e^{j[\theta(\bar{\xi}, Z) + \omega t + \omega\tau]} \\ &= A(\bar{\xi}, Z)\ e^{\,j\{\theta(\bar{\xi}, Z) + k[r(\bar{\xi}, \bar{x}, Z) - Z_1]\}} \end{aligned} \tag{2-20}$$

and,

$$\chi_P = K|A_R|^2 T + KT \left| \iint_{\bar{\xi},\, Z} \frac{jk\ A(\bar{\xi}, Z)}{2\pi r(\bar{\xi}, \bar{x}, Z)}\ X \right.$$

$$\left. e^{j[kr(\bar{\xi}, \bar{x}, Z) + \theta(\bar{\xi}, Z) - kZ_1]} d\bar{\xi}\ dZ \right|^2$$

$$+ K \int_0^T \left\{ \iiint_{\bar{\xi},\, Z} \frac{jk}{2\pi r(\bar{\xi},\, \bar{x},\, Z)} V_R^*(t) V(\bar{\xi},\, t + \tau) d\bar{\xi}\, dZ \right.$$

$$\left. - \iiint_{\bar{\xi},\, Z} \frac{jk}{2\pi r(\bar{\xi},\, \bar{x},\, Z)} V_R(t) V^*(\xi,\, t + \tau) d\bar{\xi}\, dZ \right\} dt \qquad (2\text{-}21)$$

Defining the time average over a period T as

$$\langle \cdot \rangle_T = \frac{1}{T} \int_0^T \cdot\, dt \qquad (2\text{-}22)$$

and accounting for the finite time average by introducing a "modified"complex degree of coherence [30], we have

$$G_{mR}(\tau) = \frac{V_R^*(t) V(\bar{\xi},\, t + \tau)}{\sqrt{I_R\, I_{\bar{\xi}}}}$$

$$G_{mR}(\tau) \equiv \frac{V_R^*(t) V_m(t + \tau)}{\sqrt{I_R\, I_m}} \qquad (2\text{-}23)$$

equation 2-21 becomes

$$\chi_P = K|A_R|^2T + KT \left| \iiint_{\bar{\xi},\, Z} \frac{jk\, A(\bar{\xi},\, Z)}{2\pi r(\bar{\xi},\, \bar{x},\, Z)} \; X \right.$$

$$\left. e^{j[kr(\bar{\xi},\, \bar{x},\, Z) + \theta(\bar{\xi},\, Z) - kZ_1]} d\bar{\xi}\, dZ \right|^2$$

$$+ KA_RT \iiint_{\bar{\xi},\, Z} \frac{jk}{2\pi r(\bar{\xi},\, \bar{x},\, Z)} G_{mR}(\tau) A(\bar{\xi},\, Z) d\bar{\xi}\, dZ$$

$$- KA_RT \iiint_{\bar{\xi},\, Z} \frac{jk}{2\pi r(\bar{\xi},\, \bar{x},\, Z)} G^*_{mR}(\tau) A(\bar{\xi},\, Z) d\bar{\xi}\, dZ \qquad (2\text{-}24)$$

Recalling that quasi-monochromatic radiation is assumed, we can state that

$$G_{mR}(\tau) = |G_{mR}(o)|\, e^{j[\omega\tau + \theta(\bar{\xi},\, Z)]} \qquad (2\text{-}25)$$

where $|G_{mR}(o)|$ is the magnitude of the modified complex degree of coherence between the radiation leaving the object point m and the reference radiation.

The hologram transmission, under conditions of quasi-monochromatic conditions becomes

$$\chi_P = K|A_R|^2T + KT \left| \iiint_{\bar{\xi},\, Z} \frac{jk\, A(\bar{\xi},\, Z)}{2\pi r(\bar{\xi},\, \bar{x},\, Z)} \; X \right.$$

$$\left. e^{j[kr(\bar{\xi},\, \bar{x},\, Z) + \theta(\bar{\xi},\, Z) - kZ_1]} d\bar{\xi}\, dZ \right|^2$$

$$+ KA_R T \iiint_{\bar{\xi},\, Z} \frac{jk\, |G_{mR}(o)|}{2\pi r(\bar{\xi},\, \bar{x},\, Z)} e^{j[\omega\tau + \theta(\bar{\xi},\, Z)]} A(\bar{\xi},\, Z) d\bar{\xi}\, dZ$$

$$- KA_R T \iiint_{\bar{\xi},\, Z} \frac{jk\, |G_{mR}(o)|}{2\pi r(\bar{\xi},\, \bar{x},\, Z)} e^{-j[\omega\tau + \theta(\bar{\xi},\, Z)]} A(\bar{\xi},\, Z) d\bar{\xi}\, dZ. \qquad (2\text{-}26)$$

Recognize the similarity between equation 2-26 and the equivalent statement in chapter I (equation 1-6) employing the characteristic function. Again, equation 2-24 assumes that $r(\bar{\xi},\, \bar{x},\, Z)$ remains constant with respect to time, a point already introduced in chapter one and, a point which will be discussed at length in a later chapter when motion of the object during the hologram exposure is considered.

The image reconstruction process employs an illuminating wavefront identical to the reference wavefront used during recording. This implies that the characteristics of the reconstructing source, with respect to the hologram, are related to the reference source employed for formation of the hologram. Image reconstruction is then accomplished by illuminating the hologram with the reconstructing beam and viewing the radiation diffracted by the hologram.

Let $V_{ip}(\bar{x}, Z_1, t)$ represent the analytic signal distribution of the reconstructed wavefront downstream of the hologram due to an illuminating wavefront $A_i\ e^{j(\omega t + kZ_1)}$, then,

$$V_{ip}(\bar{x}, Z_1, t) = \chi_p\ A_i\ e^{j(\omega t + kZ_1)}$$

$$= A_i\ e^{j(\omega t + kZ_1)} \left\{ K|A_R|^2 T \right.$$

$$+ KT \left| \iint_{\bar{\xi},\ Z} \frac{jk\ A(\bar{\xi},\ Z)}{2\pi r(\bar{\xi},\ \bar{x},\ Z)}\ X \right.$$

$$\left. e^{j[kr(\bar{\xi},\ \bar{x},\ Z)\ +\ \theta(\bar{\xi},\ Z)\ -\ kZ_1]} d\bar{\xi}\ dZ \right|^2$$

$$+ KA_R T \iint_{\bar{\xi},\ Z} \frac{jk\ |G_{mR}(o)|}{2\pi r(\bar{\xi},\ \bar{x},\ Z)}\ X$$

$$e^{j[\omega\tau\ +\ \theta(\bar{\xi},\ Z)]} A(\bar{\xi},\ Z) d\bar{\xi}\ dZ$$

$$- KA_R T \iint_{\bar{\xi},\ Z} \frac{jk\ |G_{mR}(o)|}{2\pi r(\bar{\xi},\ \bar{x},\ Z)}\ X$$

$$\left. e^{-j[\omega\tau\ +\ \theta(\bar{\xi},\ Z)]} A(\bar{\xi},\ Z) d\bar{\xi}\ dZ \right\} \qquad (2\text{-}27)$$

Considering now just a single term from equation 2-27, in particular the third term, where we have

$$V'_{ip}(\bar{x},\ Z_1,\ t) = A_i A_R KT \iiint_{\bar{\xi},\ Z} \frac{jk\ A(\bar{\xi},\ Z)\ |G_{mR}(o)|}{2\pi r(\bar{\xi},\ \bar{x},\ Z)}\ X$$

$$e^{j[\omega t + kZ_1 + \omega\tau + \theta(\xi,\ Z)]} d\bar{\xi}\ dZ. \qquad (2\text{-}28)$$

Recalling that

$$\tau = (k/\omega)[r(\bar{\xi},\ \bar{x},\ Z) - Z_1]$$

yields for equation 2-28,

$$V'_{ip}(\bar{x},\ Z_1,\ t) = A_i A_R KT \iiint_{\bar{\xi},\ Z} \left\{ \frac{jk\ |G_{mR}(o)|\ A(\bar{\xi},\ Z)}{2\pi r(\bar{\xi},\ \bar{x},\ Z)}\ X \right.$$

$$\left. e^{j[\omega t + kr(\bar{\xi},\ \bar{x},\ Z) + \theta(\bar{\xi},\ Z)]} \right\} d\bar{\xi}\ dZ \qquad (2\text{-}29)$$

which represents a partial expression for the reconstructed image wavefront just behind and downstream of the hologram. The original object wavefront in the hologram plane (equation 2-15) was

$$V_{obj} = \iiint_{\bar{\xi},\ Z} \frac{jk\ A(\bar{\xi},\ Z)}{2\pi r(\bar{\xi},\ \bar{x},\ Z)}\ e^{j[\omega t + kr(\bar{\xi},\ \bar{x},\ Z) + \theta(\bar{\xi},\ Z)]} d\bar{\xi}\ dZ \qquad (2\text{-}30)$$

which, except for an amplitude difference due to the reconstructing wavefront amplitude and the hologram processing, differs from the reconstructed wavefront only by the multiplier $|G_{mR}(o)|$. As a consequence of the recorded radiation being quasi-monochromatic, the quantity $|G_{mR}(o)|$ is essentially a function of the object point m because the magnitude of the coherence varies very little over distances, $r(\bar{\xi},\ \bar{x},\ Z)$ from object to recording plane for each object point providing the distance variation is small compared to the coherence length of the radiation. Then equation 2-29 represents a wave, identical to the original object wave, except that the amplitude of the radiation from each image point m' is now proportional to the absolute value of the modified complex degree of coherence that existed between the radiation leaving the object point m and the reference beam during recording. In terms of the radiance of the reconstructed image, the above result can be stated concisely as,

$$R(m') = a\ R_o(m)\ |G_{mR}(o)|^2 \qquad (2\text{-}31)$$

which relates the radiance of the reconstructed image point m' to that of the object point m through the modified complex degree of coherence. The constant a is to account for the processing and dimensional quantities. Then, to an observer, a clear, undistorted image of the object is visible with the radiance of the image shaded by $|G_{mR}(o)|$. This result, fundamental to the holographic process and its application to holographic interferometry, forms the foundation of the study to be presented.

REFERENCES

1. E. Leith and J. Upatnieks, J. Opt. Soc. Am., 52, 1123 (1962)

2. M. Lurie, Effects of Partial Coherence on Holography, Doctoral Thesis, Newark College of Engineering, (1967)

3. J.B. De Velis and G.O. Reynolds, Theory and Applications of Holography, Addison-Wesley Publishing Company, 7 (1967)

4. M. Lurie, J. Opt. Soc. Am., 56, 1369 (1966)

5. M. Born and E. Wolf, Principles of Optics, third edition, Pergamon Press, N.Y., 499 (1965)

6. J.B. De Velis and G.O. Reynolds, op. cit., 17

7. M.J. Beran and G.B. Parrent Jr., Theory of Partial Coherence, Prentice-Hall Inc., 28 (1965)

8. M.J. Beran and G.B. Parrent Jr., Ibid., 38

9. M. Born and E. Wolf, op. cit., 500

10. Y.W. Lee, Statistical Theory of Communication, John Wiley and Sons, Inc., 58 (1960)

11. M. Born and E. Wolf, op. cit., 501

12. M. Born and E. Wolf, op. cit., 502

13. M.J. Beran and G.B. Parrent Jr., op. cit., 45

14. M. Born and E. Wolf, op. cit., 500

15. J.M. Stone, Radiation and Optics, McGraw Hill Book Company, 299 (1963)

16. J.B. De Velis and G.O. Reynolds, op. cit., 20

17. M. Born and E. Wolf, op. cit., 264

18. M. Born and E. Wolf, op. cit., 507

19. M. Born and E. Wolf, op. cit., 507

19A. M. Born and E. Wolf, op. cit., 453

20. J.B. De Velis and G.O. Reynolds, op. cit., 30

21. M. Lurie, op. cit., 36

22. Grant R. Fowles, Introduction to Modern Optics, Holt, Rinehart and Winston, Inc., 144 (1968)

23. E. Leith and J. Upatnieks, J. Opt. Soc. Am., 54, 1295 (1964)

24. J.B. De Velis and G.O. Reynolds, op. cit., 28

25. M.J. Beran and G.B. Parrent Jr., op. cit., 39

26. J.B. De Velis and G.O. Reynolds, op. cit., 29

27. M.J. Beran and G.B. Parrent Jr., op. cit., 41

28. E.L. O'Neill, Introduction to Statistical Optics, Addison-Wesley Publishing Company, 36 (1963)

29. M. Born and E. Wolf, op. cit., 455

30. M. Zambuto and M. Lurie, Applied Optics, 9, 2066 (1966)

CHAPTER III

HOLOGRAPHY WITH EITHER FILM OR OBJECT MOTION

In the development of holography, small motions, which resulted in distorted reconstructed images, continually plagued holographers. Eventually, it was realized that the hologram's sensitivity to motion could be used to measure these small displacements and deformations with a high degree of precision. This realization prompted a great deal of research in the study of holographic interferometry, particularly concerning the techniques of measurement. Subsequent developments indicated two useful measurement procedures which are referred to as "time average" holography[1] and "double exposure" holography.[2] Essentially, in the time average holographic method the object is in motion with respect to the recording plane during the exposure of the hologram. Double exposure holography, which can be shown to be a special case of time average holography[3], entails exposing the hologram at two different times during the object's motion. The duration of the individual hologram exposure is such that the object's displacement during each exposure is negligible, but, the amount of object motion between the individual hologram exposures may or may not be significant depending on the law of motion under consideration.

*Other clarifications of methods of holographic interferometry (such as real time, stroboscopic etc.) can be shown to be special cases of the above).

When viewing the reconstructed image resulting from the holographic interferometric study of an object in motion, one perceives alternate light and dark regions apparently superposed on the object image. These light and dark regions are referred to as fringes. When properly interpreted, the fringe shape and spacing yields quantitative information concerning the object motion that took place during the hologram recording.

Our discussion will present a general expression, initially obtained by M. Zambuto and M. Lurie[4], which describes the effects of object motion during the recording of a hologram on the holographic process. This will be accomplished by computing a "modified complex degree of coherence", i.e., the characteristic function, for an object in motion with respect to a fixed film plate. This result will then be extended to include the effect of film motion with respect to a fixed object on holography. The latter computation, which is a new result, is of particular interest for the study of simultaneous film and object motion. Also, the discussion indicates a unique method of simulating complicated optical path disturbances on holography which is the subject of a later chapter.

3.1 Holography with a Moving Object

The radiance of each point of a reconstructed holographic image depends on the degree of coherence existing between the reference beam and the radiation diffused by the object during the formation of a hologram.[5,6] This result, which is fundamental to the holographic process, was demonstrated in the previous chapter. We will now apply this concept to determining the effect, on the reconstructed holographic image, of having the object in motion during the recording of a hologram.

We shall assume that both the illuminating and reference sources are completely coherent. Additionally, we assume that the object motion is such that the reference and "object" waves satisfy the quasi-monochromatic conditions, then, the radiance of the reconstructed image point is,[7,8]

$$R(m') = R(m)\,|G_{mR}(o)|^2 \qquad (3\text{-}1)$$

where R(m) is a quantity which is proportional to the radiance of the object m during recording, varies from object point to object point, and depends on the conditions existing during the formation of the hologram and the film processing.[9] The quantity $G_{mR}(o)$ is the complex degree of spatial coherence existing between the reference

beam and the radiation diffused by m during the recording of the hologram. Immediately obvious is that reduced coherence during the formation stage of a hologram will result in a darker reconstructed image of the object point m. As a consequence of the object experiencing motion during the recording of a hologram, such a reduction of coherence can result because the object radiation is shifted in frequency by virtue of the Doppler effect.

Consider a plane wave monochromatic reference beam represented in the recording plane by,

$$V_R(t) = A_R\, e^{j\omega t} = A_R\, e^{j \int_0^t \omega d\tau}. \qquad (3\text{-}2)$$

The object, which is presumed to be in motion during the recording of the hologram, rediffuses light from a monochromatic illuminating source of constant amplitude completely coherent with the reference source. The rediffused radiation will be shifted in frequency with respect to the illuminating source due to the Doppler effect. This radiation can be represented in the film plane as,

$$V_m(t) = A_m\, e^{j \int_0^t \omega_m'(\tau) d\tau} \qquad (3\text{-}3)$$

where $\omega_m'(\tau)$ is the instantaneous frequency of the light reaching the hologram plate from the point m.

We shall further assume that during the recording of the hologram, A_R and A_m, the amplitudes of the reference and object radiation, remain constant with respect to time. Then, during the hologram exposure,

$$I_R = A_R^2 \text{ and } I_m = A_m^2.$$

It now follows that the modified complex degree of coherence is,

$$G_{mR}(o) = \langle V_m(t) V_R^*(t) \rangle / (I_m I_R)^{1/2} \qquad (3\text{-}4)$$

where the pointed brackets indicate the time average previously defined by equation 2-22; and, it is understood that the time average extends only over the exposure time T of the hologram. Equation 3-4 can now be written as,

$$G_{mR}(o) = \frac{1}{T} \int_0^T \exp\{j \int_0^t [\omega_m'(\tau) - \omega] d\tau\} dt \qquad (3\text{-}5)$$

which is a basic expression for our discussion.

To determine the instantaneous frequency, $\omega_m'(t)$ of light rediffused from the moving object at the hologram plane, consider figure 3-1. For an infinitesimal displacement, dx_m, of the object point m, there is a corresponding change in phase generated at the hologram plate due to the change in optical path created by the object motion. This change in phase is,

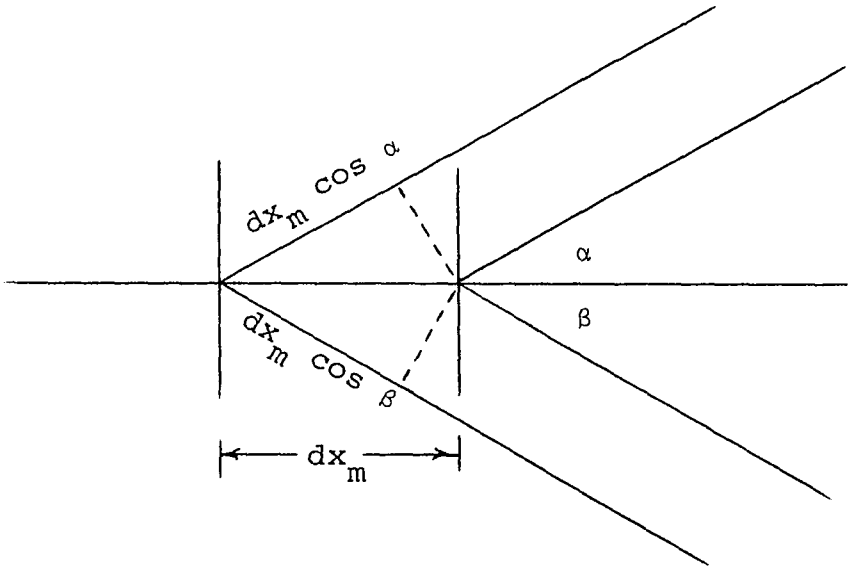

Figure 3-1

Geometry for the calculation of the Doppler Shift associated with an object displacement

$$d\phi_m = (\frac{2\pi}{\lambda})\ dS_m = (\frac{2\pi}{\lambda})\ dx_m\ (\cos\ \alpha + \cos\ \beta) \qquad (3\text{-}6)$$

where we assume that the object motion magnitude is so small that the ray paths remain parallel before and after the motion.

The corresponding instantaneous frequency associated with this change in phase is

$$\omega_m'(t) = \omega + d\phi_m/dt$$

$$= \omega + (\frac{2\pi}{\lambda})(\frac{dx_m}{dt})(\cos\ \alpha + \cos\ \beta). \qquad (3\text{-}7)$$

The modified complex degree of coherence for this instantaneous frequency is,

$$G_{mR}(o) = \frac{1}{T}\int_0^T \exp\{j(\frac{2\pi}{\lambda})x_m(t)[\cos\ \alpha + \cos\ \beta]\}dt \qquad (3\text{-}8)$$

where $x_m(t)$ is the x component of the law of motion for the point m on the object. For our purposes, α and β will be assumed to equal zero (these angles are often controlled experimental quantities) with no loss in generality. This assumption results in a simplified expression for equation 3-8 which is

$$G_{mR}(o) = \frac{1}{T}\int_0^T e^{j\frac{4\pi}{\lambda}x_m(t)}dt. \qquad (3\text{-}9)$$

Equation 3-9 then is an expression which relates the law of motion of any point of the object during the recording of a hologram with the pertinent modified complex degree of coherence. Then, the effects on the reconstructed image of a hologram with a known object law of motion can be computed using equations 3-1 and 3-9.

3.2 An Example of Step Object Motion

Consider the situation of step object motion during the exposure of a hologram. Let the law of motion be that depicted in figure 3-2 which indicates no object motion for the first half of the hologram exposure and an object displacement of an amount D for the second half of the exposure.

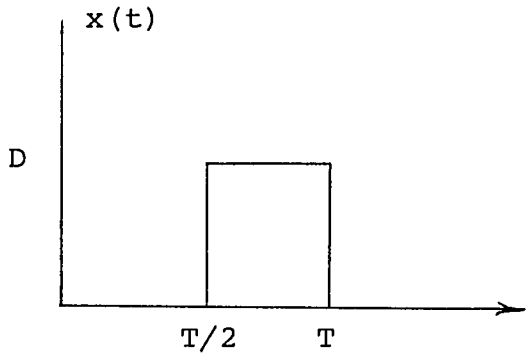

Figure 3-2

A step law of motion

The associated modified complex degree of coherence is

$$G_{mR}(o) = \frac{1}{T}\int_{0}^{T/2} e^{j\frac{4\pi}{\lambda}(o)}\, dt + \frac{1}{T}\int_{T/2}^{T} e^{j\frac{4\pi}{\lambda}D}\, dt$$

$$= \frac{1}{2}\,(1 + e^{j\frac{4\pi}{\lambda}D}) \qquad (3\text{-}10)$$

The characteristic function, $G_{mR}(T)$ introduced in Chapter I, is the quantity which directly affects the image brightness and,

$$G_{mR}(T) = |G_{mR}(o)|^2 = \frac{1}{2}\,[1 + \cos\,(\tfrac{4\pi}{\lambda}D)]. \qquad (3\text{-}11)$$

A sketch of equation 3-11 can be found in figure 3-4a. Essentially, the sketch indicates that whenever the object motion magnitude is such as to cause $G_{mR}(T)$ to be zero, a dark fringe will occur in the reconstructed holographic image.

Accompanying the graph in figure 3-4a is a photograph of the reconstructed virtual image of a hologram taken of an object whose step motion was introduced as an object rotation through a small angle θ about the point F causing all points on the object to have the same law of motion (see figure 3-3). The magnitude of each object point displacement now increases with increasing distance from the axis of rotation (fulcrum). This technique of introducing

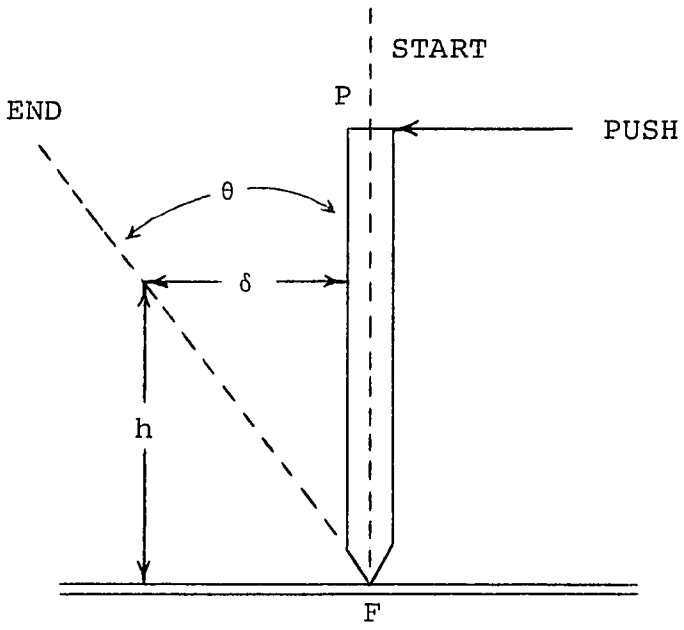

Figure 3-3

Technique for the generation of the motion

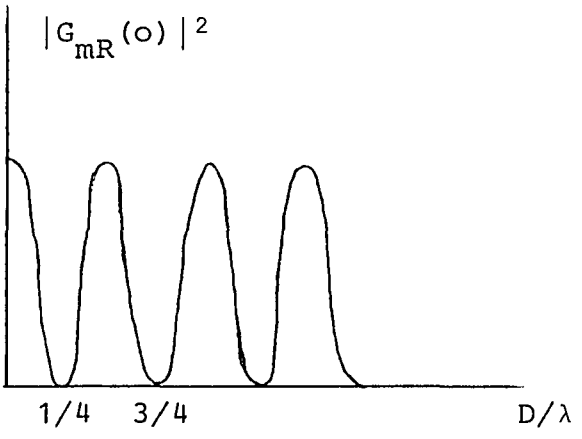

Figure 3-4a

The modified complex degree of coherence for step object motion

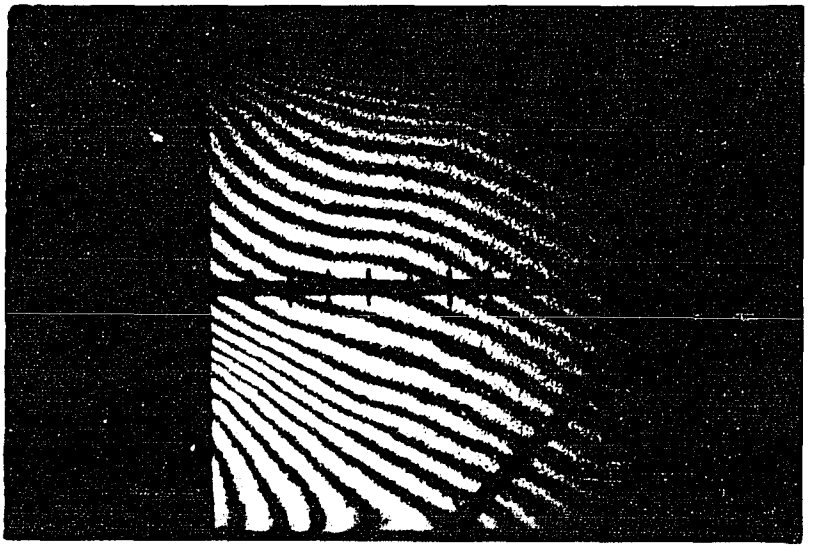

Figure 3-4b

Photograph of the reconstructed image with step object motion

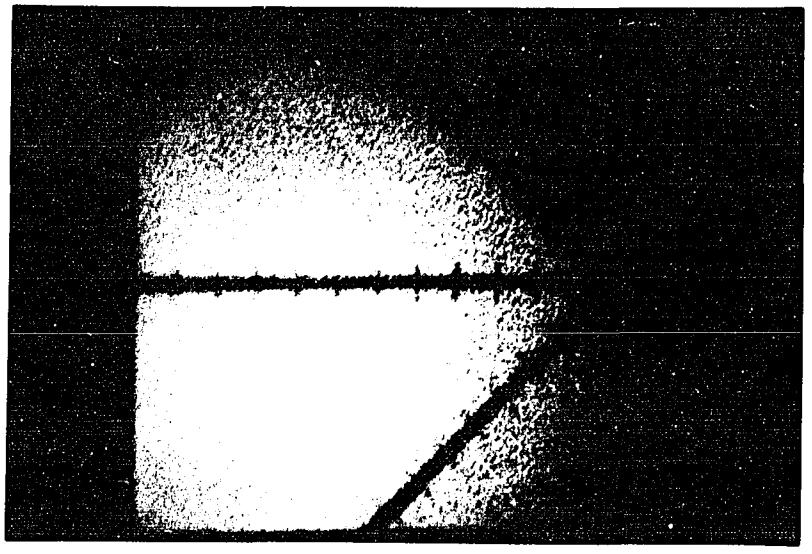

Figure 3-4c

Photograph of the reconstructed image of the object used for experimentation

the object motion, originally suggested by Lurie[10], results in the recording of a whole range of displacements simultaneously with a single hologram exposure rather than just a single measurement. The predictable fringes, corresponding to the zeros of equation 3-11, are readily observable in the photograph of the reconstructed image of the object presented in figure 3-4b. As a reference, a photograph of the reconstructed virtual image of the object with no motion is also presented in figure 3-4c.

The sketch of $|G_{mR}(o)|^2$ implies that the fringes occur at multiples of $D/\lambda = 0.25$. From the recording geometry, the displacement of the object during the recording of the hologram is easily calculated using the measured fringe spacing from the hologram. A sample calculation of this type is presented in chapter VII.

3.3 Holography with a Moving Film Plate

The previous analysis concerning object motion during the exposure of a hologram will now be extended to consider a new topic, that of film motion with respect to a stable object during the recording process. The approach to the analysis of this situation will parallel the analysis of object motion. The apparent doppler shifted frequency of the radiation diffused by an object point will be computed for one point in the film plane and one point on the object.

This will be accomplished by determining the phase variation at a point on the recording medium for an infinitesimal change in film position. Then, the modified complex degree of coherence will be computed using the relationships between phase variation and instantaneous frequency.

The geometry presented in figure 3-5 is typical for a split beam hologram configuration. For an infinitesimal displacement, dx, of the recording plane along the CC' axis, the change in optical path difference between the point in the recording plane on the CC' axis and points P_R (a point source reference beam in the plane of the object) and P_m (a point on the object) is

$$dS_{mR} = (P'P_R - P'P_m) - (PP_R - PP_m)$$

$$= dx\ (\cos \beta' - \cos \alpha'). \qquad (3\text{-}12)$$

For α' and β' small, i.e., α' and β' less than five degrees (implying the distance from the center axis to the points P_R and P_m are small compared to the object-recording plane distance), the path length change becomes,

$$dS_{mR} \approx dx\ (\alpha'^2 - \beta'^2)/2! \qquad (3\text{-}13)$$

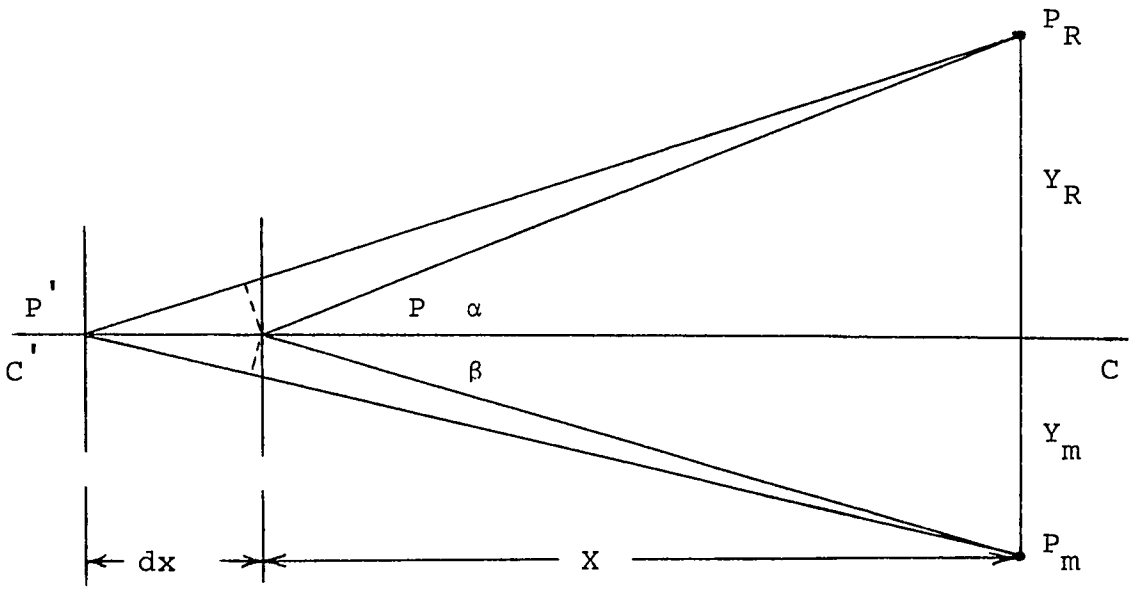

Figure 3-5

Geometry used to calculate the Doppler Shift due to a film displacement

The corresponding phase variation is

$$d\phi_{mR} = \frac{2\pi}{\lambda} dS_{mR}$$

$$= \frac{2\pi}{\lambda} \frac{dx}{2!} \frac{Y_R^2 - Y_m^2}{(X + x)^2} \qquad (3\text{-}14)$$

where X is the object-film distance at the beginning of the motion and X + x is the object-film distance at time t. Letting $x' = x/X$ results in the complex degree of coherence becoming,

$$G_{mR}(o) = \frac{1}{T} \int_0^T e^{j\phi_{mR}} dt$$

$$= \frac{1}{T} \int_0^T \{e^{j \int_0^{x'} \frac{2\pi}{2!\lambda X} (Y_R^2 - Y_m^2) \frac{dx'}{(1 + x')^2}}\} dt. \qquad (3\text{-}15)$$

Consider for the present just the integral in the exponent of equation 3-15; letting $u = 1 + x'$ yields,

$$\int_0^{x'} \frac{dx'}{(1 + x')^2} = \int_1^{1 + x'} \frac{du}{u^2} = \frac{x'}{1 + x'} . \qquad (3\text{-}16)$$

For most experimental conditions, $x' \leq 0.01$ implying that

$$\int_0^x \frac{dx'}{(1 + x')^2} \approx x'(1 - x') \tag{3-17}$$

The modified complex degree of coherence then becomes,

$$G_{mR}(o) = \frac{1}{T} \int_0^T e^{j\{\frac{\pi}{\lambda} \frac{Y_R^2 - Y_m^2}{X} x'(1 - x')\}} dt$$

$$= \frac{1}{T} \int_0^T \exp j\{\frac{2\pi}{\lambda} Kx(t)[1 - \frac{x(t)}{X}]\} dt \tag{3-18}$$

where $x(t)$ is the x component of the law of motion of the film and $K = Y_R^2 - Y_m^2/2X^2$, a constant dependent on the recording geometry.

Observe that for film motion, more than just the manner of the displacement is required for the computation of the modified complex degree of coherence. Cognizance of the object-film, reference source-object point distances and the film point under consideration are also necessary. As an example, consider that the object and reference distances are equal for a given point on the film, i.e., $Y_R = Y_m$. Then, the constant K would be identically equal to zero no matter what the film displacement was during the hologram recording for this particular film point. Consequently, the effect of the film motion on the

reconstructed hologram image would be as if no motion had occurred during the hologram exposure*. Notice that this is an image reconstructed from just that one point on the hologram. Knowledge of the recording geometry then plays an important role in the interpretation of film motion effects on the reconstructed image of a hologram.

3.4 An Example of Step Film Motion

The step motion of figure 3-2 with the displacement D along the CC' axis defined in figure 3-5 is applied to the film during the recording of a hologram. The modified complex degree of coherence is computed as,

$$G_{mR}(o) = \frac{1}{T}\left\{ \int_0^{T/2} e^{j(o)}dt + \int_{T/2}^{T} e^{j\frac{2\pi}{\lambda} K(D - D^2/X)}dt \right\}$$

$$= \frac{1}{2}\left\{1 + e^{j\frac{2\pi}{\lambda} KD}\ e^{-j\frac{2\pi}{\lambda} KD^2/X}\right\}. \qquad (3\text{-}19)$$

The characteristic function is

$$G_{mR}(T) = |G_{mR}(o)|^2$$

$$= \frac{1}{2}\left\{ 1 + \cos\left[\frac{2\pi}{\lambda} KD'\right] \right\}$$

*here we have assumed that the film displacement was such that the recorded radiation remained quasi-monochromatic and the small angle assumptions remained valid.

with

$$D' = D(1 - D/X)$$

and

$$K = (Y_R^2 - Y_m^2)/2X^2 \qquad (3\text{-}20)$$

Figure 3-6 is a photograph of the reconstructed image of an object taken from the center of the hologram with step film motion applied during recording of the hologram. The method of application of the displacement was also a rotation of the film through a small angle which was previously explained for object motion. This technique results in the recording of a complete range of displacements for the film motion with all film points having the same law of motion but different magnitudes. The details of the computation relating fringe spacing to the film displacement are discussed in chapter VII. The characteristic fringes indicating the zeros of equation 3-19 are clearly visible giving qualitative proof to the discussion.

At this point, it is instructive to indicate more on the dependence of the hologram geometry for interpretation of the fringe spacing and shape. We have already indicated the dependence on the reference and object point distance from the central axis, but we must now consider the point on the film that we are using to reconstruct the holographic image. For an arbitrary point on the film, not on the central axis, Y_F, the constant K becomes

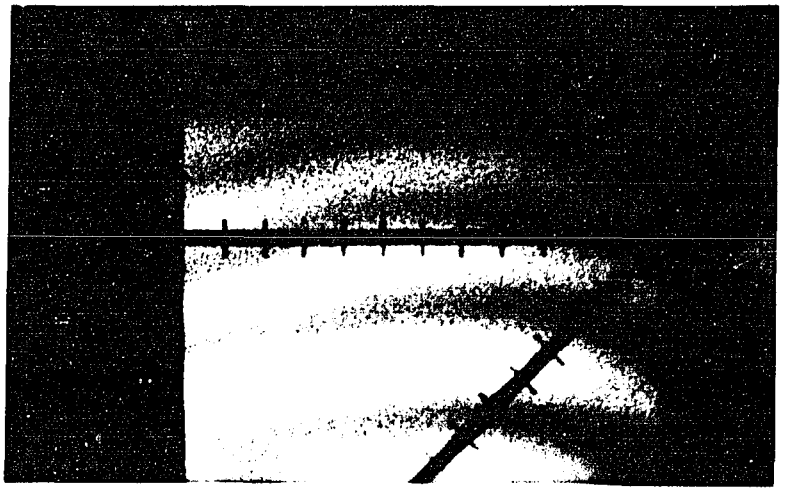

Figure 3-6

Photograph of the reconstructed image of an object taken with step film motion

$$K = (Y_R + Y_F)^2 - (Y_m - Y_F)^2/2X^2$$

$$= [(Y_R^2 - Y_m^2) + 2Y_F(Y_R + Y_m)]/2X^2 \qquad (3\text{-}21)$$

Observe now that even if $Y_R = Y_m$, for Y_F non zero there will be evidence of a fringe pattern for film motion. Actually, with a displacement in Y_F to the point,

$$Y_R^2 - Y_m^2 = -2Y_F(Y_R + Y_m)$$

or

$$Y_F = \frac{Y_m - Y_R}{2} \qquad (3\text{-}22)$$

we will again observe the condition of no fringe pattern for a film motion.

To continue, if instead of a rotation of the film to introduce the step film motion, a single linear displacement was used for the whole film plate, then we should expect to see a series of dark curved or straight line fringes in the reconstructed holographic image (see chapter 6). The apparent shape of the fringe will depend on the reconstruction process, and, most likely for small objects will appear as straight lines. The fringe spacing will be in accordance with equations 3-21 and 3-20. Observe again that these fringes will vary for different points of the

film plate used to reconstruct the image. To observe the variation one will have to use different small sections of the hologram plate for the image reconstruction process.

Lastly, in this discussion, we have assumed that the dimensions Y_R, Y_m, Y_F are all such that during the recording of the hologram, the radiation recorded was indeed quasi-monochromatic. Additionally, it must be remembered that the size of the film and of the object are limited, for we are considering only those ray paths that form small angles with respect to the point on the film under consideration. This requires that the film and object size be limited according to the following conditions,

$$(Y_R + Y_F) << X;\ (Y_R - Y_m) << X$$

and

$$(Z_m - Z_F) << X.$$

Several direct consequences of the film motion concept are of particular interest. The study of simultaneous film and object motion, i.e., the case in which both film and object are in motion with respect to the reference source during the hologram exposure can be investigated. An analysis of this situation has direct application to the fringe interpretation problem encountered in holographic interferometric non-destructive testing.

Applications to the study of optical path changes due to small variations in the medium separating the object and recording planes is a natural extension of the computation. Both of these concepts (simultaneous motion and optical path perturbation) will be the subjects of further consideration in the following chapters.

REFERENCES

1. R.L. Powell and K.A. Stetson, J. Opt. Soc. Am., 55, 1593 (1965)

2. L.O. Heflinger, R.F. Wuerker, and R.F. Brooks, J. Appl. Phys., 37, 642 (1966)

3. M. Zambuto and M. Lurie, Applied Optics, 9, 2066 (1966)

4. Ibid. (2066)

5. M. Lurie, J. Opt. Soc. Am., 56, 1369 (1966)

6. M. Zambuto and M. Lurie, op. cit., 2066

7. M. Lurie, Effects of Partial Coherence on Holography, Doctoral Thesis, Newark College of Engineering, (1967)

8. M. Lurie, J. Opt. Soc. Am., 56, 1369 (1966)

9. M. Zambuto and M. Lurie, op. cit., 1369

10. M. Lurie, Doctoral Thesis, (1967)

CHAPTER IV

THE INTERPRETATION OF TURBULENCE EFFECTS ON HOLOGRAPHY AS A RANDOM FILM MOTION

The study of wave propagation through non-homogeneous media has in the past been of special interest to astronomers who wish to know how much the earth's atmosphere disturbs the light from distant sources before reaching the collecting optics of a telescope.[1,2,3] Today there is increased interest in optical communication and remote sensing of pollution through the atmosphere. The significance of work investigating the effects of turbulence both on the resolution and range of optical systems and on the techniques for improving optical system resolution has become greatly enhanced.

In search of determining the effects of atmospheric turbulence on light propagation, researchers at Stanford University reported the results of an interesting experiment. Goodman et. al.[4] were investigating the effect of inserting a random phase perturbing object in the optical path of an imaging system. Specifically, they were considering both a holographic type imaging system as well as a conventional photographic system. Their work showed that when the random medium is a thin, stationary, phase-perturbing

plate (e.g., a piece of shower or ground glass) located near the hologram recording plane for the entire exposure time, the method of wavefront reconstruction resulted in much better image resolution than has been obtained, under identical circumstances, with conventional imaging systems.

This experimental result prompted Gaskill to further consider the holographic process when the recording and object planes of a holographic experiment are separated by an extended random medium during recording. Gaskill applied conventional methods of turbulence analysis, reported by many researchers working on the problems associated with conventional imaging through turbulent media.[6,7] He concluded that when the exposure time of the hologram recording was long compared to the characteristic fluctuations of the medium separating the object and film, the randomness of the wavefronts tends to reduce the radiance of the reconstructed image.[8] Additionally, for image points with sufficient radiance to be observed, no effect on the resolution of the image can be discerned.

In this chapter the analysis of the effects on the holographic process of a random medium interposed between the object and recording planes during recording will be discussed using a novel approach. The computation of the effects of randomness of the medium will be related to the effects on a reconstructed image ensuing from the variation

of the complex degree of coherence for a hologram with film motion during recording. It will be shown that this technique results in identical conclusions to those arrived at by Gaskill using conventional turbulence analysis. Additionally, this approach suggests some interesting prospects concerning the simulation of turbulence effects in the controlled environment of a laboratory, as well as a means of measuring atmospheric turbulence parameters.

4.1 Representation of the Change of Refractive Index in the Medium Separating Object and Film in Terms of Film Motion

The effects of film motion during recording on the holographic process have already been discussed in chapter III. The complex degree of coherence for film motion during the recording of a hologram for conditions of quasi-monochromatic light and α', β' small was determined to be

$$G_{mR}(o) = \frac{1}{T}\int_0^T e^{j\frac{2\pi}{\lambda}K\hat{x}(t)}dt$$

$$K = (Y_R^2 - Y_m^2)/2X^2$$

$$\hat{x}(t) = x(t)[1 - x(t)/X]. \qquad (4\text{-}1)$$

The geometry of the holographic process relating to equation 4-1 is depicted in figure 4-1 with X the distance from the film to the object prior to the film motion and x(t) the law of motion of the film supposed along the x axis. The quantity Y_R is the distance from the CC' axis to the point source reference beam P_R, and Y_m is the distance from the centerline to the object point P_m. Additionally, the discussion concerning the effect of partial coherence on holography indicated that the radiance of an image point m' in the reconstructed holographic image is

$$R(m') = R_o(m) \; |G_{mR}(o)|^2 \qquad (4\text{-}2)$$

where $R_o(m)$ is dependent on the characteristics of the reconstructing process, the film processing and the radiance of the object point m. $G_{mR}(o)$ is the modified complex degree of coherence which existed between the radiation reaching the film plate from the object and from the reference source during the formation of the hologram and the point on the film chosen for the reconstruction of the hologram is on the CC' axis. Then, the computation of the effect of film motion on a reconstructed holographic image was effected by combining equations 4-1 and 4-2.

Implied in equation 4-1 but not explicitly stated is an assumption of constant refractive index (value unity) of the medium separating the object and recording planes during the

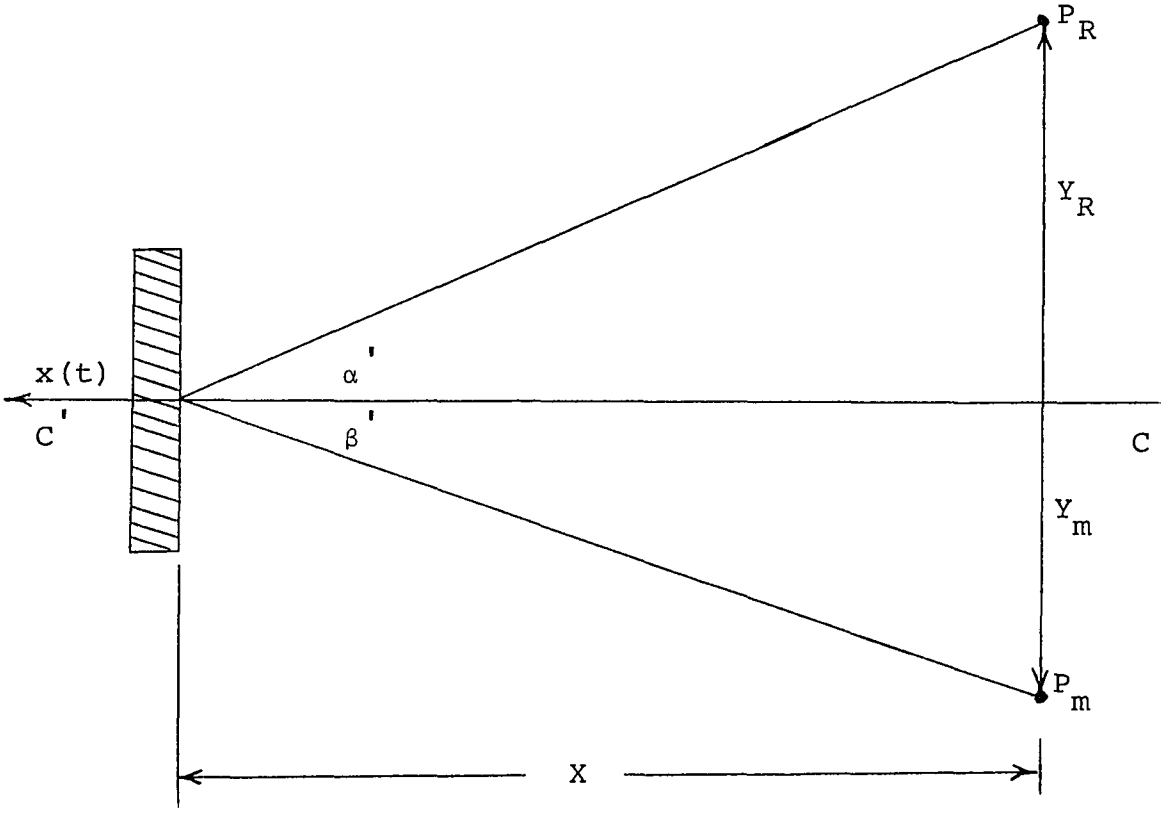

Figure 4-1

Geometry for the computation of the effect of film motion on holography

hologram recording. This restriction will now be reconsidered in order that the effects on holography of a refractive index perturbation (e.g., atmospheric turbulence or the interposing, during exposure, of a piece of optical glass) of part or all of the medium separating the film and object-reference source planes during recording can be determined.

In general, when considering the effects of wave propagation through regions of turbulence, the specific refractive index variations contained in the turbulent volume are of irregular shape and extent. This complex situation is very difficult to analyze. As a first step in the study of turbulence effects on holography in order to gain insight into the problems encountered, the situation depicted in figure 4-2 will be considered. Here both the object and film remain stationary with respect to the reference source during the hologram exposure. Interposed between the film and both the object and the reference source at a time subsequent to the start of the hologram exposure and prior to the end of the exposure is a region (enclosed by the dotted line) of refractive index N_2 different from N_1 of the rest of the medium. As a matter of convenience for this analysis N_1 will be assumed as unity, so that N_2 will indicate the ratio N_2/N_1.

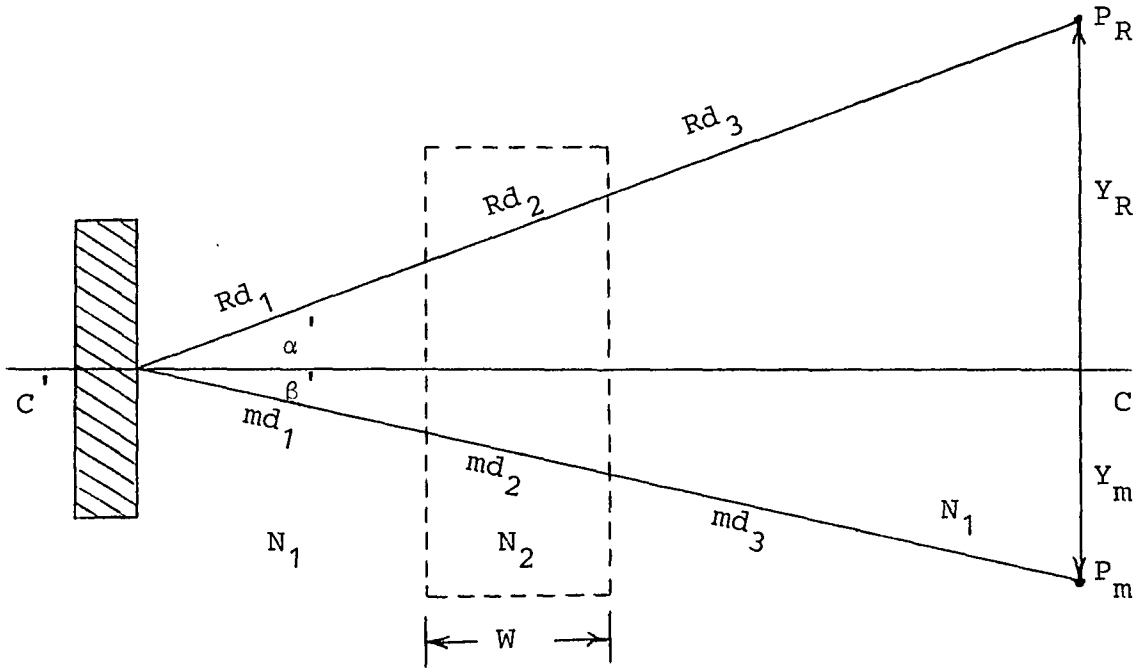

Figure 4-2

Geometric configuration for consideration of refractive index changes of the medium separating the object and film

The phase variations across the film plate due to this interposing of a change in refractive index during the hologram exposure will be calculated under the assumptions that,

a) the refractive index slab is a regular rectangle in shape with its opposing surfaces parallel to each other at all times

b) the slab has a constant refractive index and is homogeneous and isotropic in its optical properties

c) the slab remains parallel to the film plane at all times

d) the reference source is a point source in the plane of the object and this plane (object-reference) is parallel to the film plane

e) the magnitudes of the distances from the system centerline to the reference and object points are small compared to the object-film distance so that only paraxial ray paths are considered and the slab thickness must be thin with respect to the object-film distance

The importance of these assumptions becomes apparent by considering figure 4-3 where a typical slab of refractive index N_2 different from the surrounding medium of refractive index

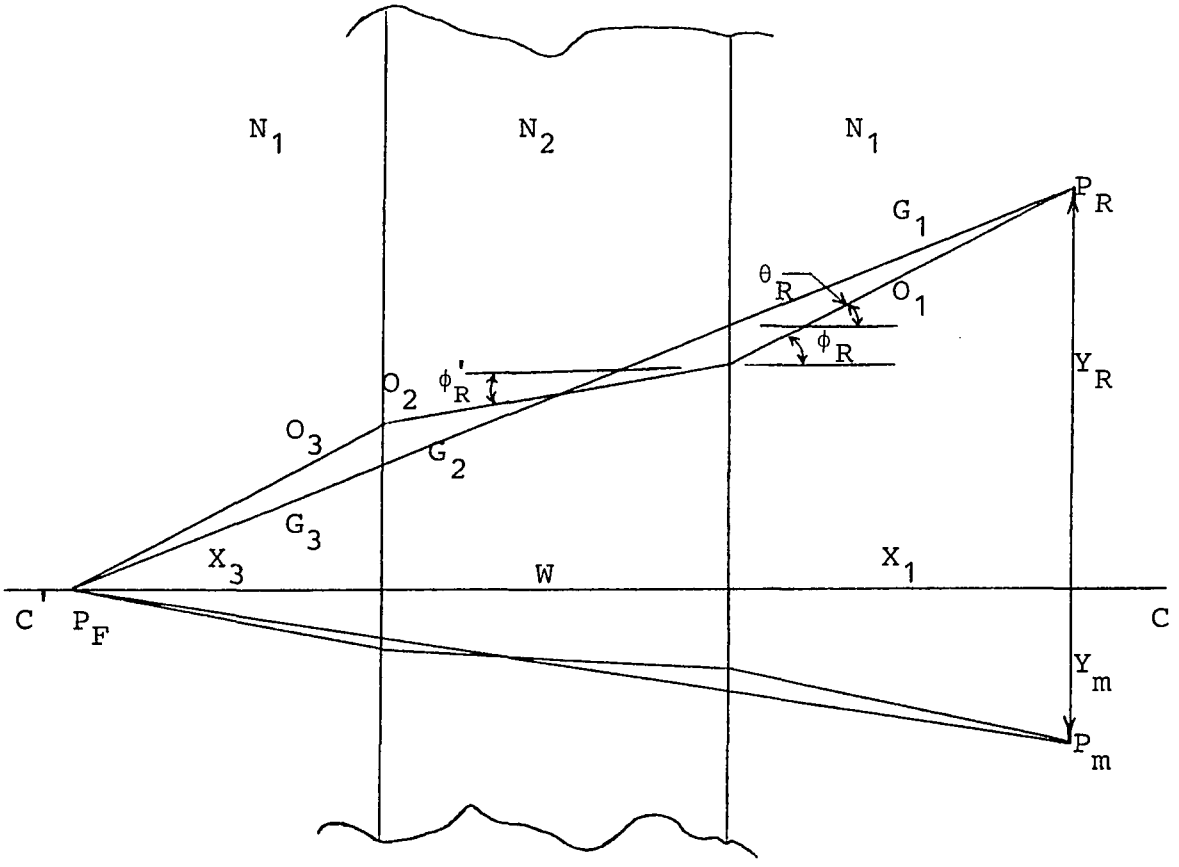

Figure 4-3

Comparison of the difference in refracted and unrefracted geometric path for an optical system which includes a slab of thickness W.

N_1 is illustrated. When a ray travels from one medium to another it undergoes refraction which results in a change in ray direction. The magnitude of the change in ray direction is a function of the two refractive indices, the angle of incidence of the ray (angle θ), and shape of the slab. The assumptions as stated are intended to preclude conditions which require consideration of a dynamically moving film point in the film plane due to varying angles of refraction during recording. The dynamics referred to can result from N_2 changing during the exposure, the angle of incidence at the refractive index slab varying due to a slab tilt with respect to the film or the opposing sides of the slab becoming non-parallel causing varying slab boundaries. The conditions will be shown to be negligible under the stated assumptions as the discussion develops.

The computation of the complex degree of coherence for a single change in refractive index during the hologram exposure (the equivalent of a step film motion) requires finding the variation ΔS_{mR} generated in the optical path by the refractive index perturbation. With reference to figure 4-2, the difference between the optical paths from P_R (the point source reference beam position) to a film point, and from P_m (an object point) to the same point on the film plane (here considered to be on the CC' axis)

with the refractive index perturbation (the dashed region of figure 4-2) is, to a first approximation

$$S_{mR} = N_1Rd_1 + N_2Rd_2 + N_1Rd_3$$

$$- N_1md_1 - N_2md_2 - N_1md_3 \qquad (4\text{-}3)$$

The refractive index of the slab, N_2, can be decomposed in terms of the free space index, $N_1 = 1.0$ and a small variational component Δn,

$$N_2 = N_1 + \Delta n$$

$$= 1.0 + \Delta n \qquad (4\text{-}4)$$

where Δn is the normalized difference between the refractive indices of the interposed slab and that of free space.[9] The optical path difference becomes, when equation 4-4 is substituted into equation 4-3,

$$S_{mR} = N_1 \{ Rd_1 + Rd_3 - md_1 - md_3 \}$$

$$+ (N_1 + \Delta n) \{ Rd_2 - md_2 \} \qquad (4\text{-}5)$$

$$= N_1 \{ (Rd_1 + Rd_2 + Rd_3) - (md_1 + md_2 + md_3) \}$$

$$+ \Delta n \{ Rd_2 - md_2 \} \qquad (4\text{-}6)$$

The first bracket of equation 4-6 encloses terms which represent the optical path difference for a uniform refractive index of N_1 of the entire medium separating the object and film plane. The change in optical path difference due to the interposing of the refractive index perturbation is then

$$dS_{mR} = \Delta n \{ Rd_2 - md_2 \}$$

$$= \Delta n \, \Delta d \qquad (4\text{-}7)$$

where Δd is the geometric path difference inside the perturbing region.

In order to reach a simple approximate expression for Δd consider figure 4-3. The indicated slab has a refractive index of N_2 while the surrounding medium has an index of N_1. Two ray paths from the reference source to the film point are indicated. One path, represented by $G_1 + G_2 + G_3$, is the unrefracted geometric path from P_R to P_F and the refracted geometric path from P_R to P_F with an interposed slab is given by $0_1 + 0_2 + 0_3$. Indicated in figure 4-3 but not expanded in detail are the ray paths for the refracted and unrefracted paths from an object point P_m to the same film point P_F. For the moment we will consider in detail only the paths from P_R to P_F.

The width of the slab indicated in figure 4-3 is W. The angle of incidence for the geometric ray path is θ_R. The angle of incidence for the refracted ray path is ϕ_R and ϕ_R' is the angle of refraction for the refracted ray path in the interposed slab.

The angle of incidence and the angle of refraction are related by Snell's law as,[10]

$$N_1 \sin \phi = N_2 \sin \phi' . \qquad (4\text{-}8)$$

We have assumed that the rays are paraxial, i.e., they will form angles of less than six degrees with respect to the CC' axis, hence, we can replace the sin by its angle in radians, resulting in,

$$N_1 \phi \approx N_2 \phi' . \qquad (4\text{-}9)$$

Consider now the difference ΔL between the unrefracted and the refracted geometric paths from the reference point P_R to the film point P_F. Note as this is a difference between two geometric paths, it is not the quantity Δd, which we require in 4-7, but, it will give insight into the phenomenon and eventually permit us to adopt a convenient simplifying assumption in computing Δd. The difference in the geometric paths is,

$$\Delta L = (O_1 + O_2 + O_3) - (G_1 + G_2 + G_3)$$

$$= (O_1 - G_1) + (O_2 - G_2) + (O_3 - G_3) \qquad (4\text{-}10)$$

From figure 4-3 we have the following relationships,

$$O_1 = X_1/\cos\,\phi \approx X_1(1 + \phi^2/2!)$$

$$O_2 = W/\cos\,\phi' \approx W(1 + \phi'^2/2!)$$

$$O_3 = X_3/\cos\,\phi \approx X_3(1 + \phi^2/2!)$$

$$G_1 = X_1/\cos\,\theta \approx X_1(1 + \theta^2/2!)$$

$$G_2 = W/\cos\,\theta \approx W(1 + \theta^2/2!)$$

$$G_3 = X_3/\cos\,\theta \approx X_3(1 + \theta^2/2!) \qquad (4\text{-}11)$$

where the approximate form assumes that the angles are less than or equal to 0.1 radians (the paraxial approximation). Now, the difference in paths becomes

$$\Delta L \approx \frac{X_1}{2}(\phi^2 - \theta^2) + \frac{X_2}{2}(\phi^2 - \theta^2) + \frac{W}{2}(\phi'^2 - \theta^2). \qquad (4\text{-}12)$$

Again, making use of the small angle approximation to replace the tan by its angle in radians, we have from figure 4-3 that

$$\theta(W + X_1 + X_3) = \phi(X_1 + X_3) + \phi' W \qquad (4\text{-}13)$$

and from equation 4-4 with $\Delta n < 1$ we have that

$$\phi' = (N_1/N_2)\ \phi \approx \phi(1 - \Delta n/N_1) \qquad (4\text{-}14)$$

Now, equation 4-13 becomes

$$\theta(W + X_1 + X_3) = \phi(W + X_1 + X_3 - W\Delta n/N_1). \qquad (4\text{-}15)$$

Using equation 4-15, we can compute the quantity $\phi^2 - \theta^2$ as

$$\phi^2 - \theta^2 = \phi^2 \left[\frac{2W}{W + X_1 + X_3}\ \frac{\Delta n}{N_1} - \frac{W^2\ \Delta n^2}{(W + X_1 + X_3)^2\ N_1^2}\right]$$

$$\approx \phi^2\ \frac{2W}{W + X_1 + X_3}\ \frac{\Delta n}{N_1} \qquad (4\text{-}16)$$

Then, the expression for ΔL is found by substituting equations 4-16 and 4-14 into equation 4-12, resulting in,

$$\Delta L = \frac{1}{2}\ (\phi^2 - \theta^2)(X_1 + X_2) + \frac{W}{2}\left[\phi^2\left(1 - \frac{\Delta n}{N_1}\right)^2 - \theta^2\right]$$

$$\approx \frac{1}{2}\ \phi^2\ \left(\frac{\Delta n}{N_1}\right)(2W) + \frac{W}{2}\ \phi^2\ \left[\left(\frac{\Delta n}{N_1}\right)^2 - 2\ \frac{\Delta n}{N_1}\right], \qquad (4\text{-}17)$$

and finally

$$\Delta L \approx \frac{1}{2}\ W\phi^2\ \left(\frac{\Delta n}{N_1}\right)^2 \qquad (4\text{-}18)$$

which represents an expression for the geometrical path difference between the unrefracted and refracted ray paths for an interposed slab.

An expression identical in form to equation 4-18 will give the geometrical path difference from the object point P_m to the same film point giving, as the total difference between the unrefracted and refracted geometric paths lengths

$$\Delta L_t = \frac{W}{2} \left(\frac{\Delta n}{N_1}\right)^2 (\phi_R^2 - \phi_m^2) \qquad (4\text{-}19)$$

where ϕ_R is the angle formed between the refracted ray path from the reference point and the CC' axis and ϕ_m is the angle formed between the refracted ray path from the object point and the CC' axis.

For typical experimental conditions, ϕ_R and ϕ_m are both less than 0.1 radians. As an example, consider $\phi_R \approx 1.5$ degrees and $\phi_m \approx 1.0$ degrees, then equation 4-19 becomes

$$\Delta L_t = W\left(\frac{\Delta n}{N_1}\right)^2 (1.9 \times 10^{-4}) \qquad (4\text{-}20)$$

For the conditions of atmospheric turbulence, the typical values of $\Delta n/N_1$ are on the order of 10^{-4}. This gives a path difference of

$$\Delta L_t = W(1.9 \times 10^{-12}) \qquad (4\text{-}21)$$

which implies that approximating the geometric path length of the refracted ray by that of the unrefracted ray is a reasonable approximation for narrow slabs.

As a second example, to indicate the limitations of the approximation, consider the slab to be a piece of optical glass. Here $\Delta n/N_1 \approx 0.5$. Notice that under these conditions the approximation of equation 4-14 becomes invalid, but, to the first order of magnitude we can assume that

$$\Delta L_t = W(0.475 \times 10^{-4}). \qquad (4\text{-}22)$$

For a typical piece of optical plate, the width is approximately one centimeter giving

$$\Delta L_t = 0.475 \times 10^{-6} \text{ m}$$

$$= 0.475 \ \mu\text{m} \qquad (4\text{-}23)$$

which is on the order of a wavelength of light. This makes the approximation a rather poor choice for computation. Under experimental conditions, the geometrical path length of the refracted ray will have to be computed. The optical path length must then be computed from this if the analysis of the perturbation introduced is to be valid.

Essentially then, for small angles of incidence, small slab thickness and no tilt of the slab with respect to the film plane, the unrefracted geometric path can be considered a good approximation to the actual geometric ray path in the slab with the error in approximation given by equation 4-19.

For an infinitesimal region of refractive index N_2 of thickness dW, Δd becomes

$$\Delta d \approx dW(1/\cos \alpha' - 1/\cos \beta') \qquad (4\text{-}24)$$

where α' and β' are angles defined in figure 4-2. For paraxial rays (implying an object-reference separation small compared to the object-film separation) find that

$$\Delta d = dW\left(\frac{\alpha'^2 - \beta'^2}{2!}\right). \qquad (4\text{-}25)$$

Employing the procedures and approximations discussed in chapter III to compute the effects of film motion, results in the following expression for the change in optical path due to the interposing of a refractive index perturbation,

$$dS_{mR} = \Delta n dW \left\{\frac{Y_R^2 - Y_m^2}{(X + \Delta nW)^2}\right\} \qquad (4\text{-}26)$$

and

$$\int_0^W \frac{Y_R^2 - Y_m^2}{2X^2} \frac{\Delta n dW}{\left(1 + \frac{\Delta nW}{X}\right)^2} = \frac{Y_R^2 - Y_m^2}{2X} \int_1^{1 + \frac{\Delta nW}{X}} \frac{d\mu}{\mu^2}$$

$$= \frac{Y_R^2 - Y_m^2}{2X^2} \frac{\Delta nW}{1 + \frac{\Delta nW}{X}}$$

$$\approx K\Delta nW(1 - \Delta nW/X) \qquad (4\text{-}27)$$

for

$$\frac{\Delta nW}{X} << 1.$$

The modified complex degree of coherence is equal to

$$G_{mR}(o) \approx \frac{1}{T} \int_0^T e^{j\frac{2\pi}{\lambda}\hat{x}(t)}\, dt$$

$$\hat{x}(t) = K\Delta nW(1 - \Delta nW/X)$$

$$K = (Y_R^2 - Y_m^2)/2X^2 \qquad (4\text{-}28)$$

where ΔnW is the equivalent in magnitude of a step displacement of the film plane.

The expression for the modified complex degree of coherence is identical in form to that obtained for film motion in chapter III. This implies that the appearance of a reconstructed holographic image of an object taken with

a step refractive index change interposed between the film and the object-reference source during the hologram exposure will be identical to that of the reconstructed image of the object taken with a step mechanical film displacement of magnitude ΔnW.

4.2 The Complex Degree of Coherence for a Slab of Randomly Varying Refractive Index

The computation of the complex degree of coherence when the magnitude of the refractive index of the slab (see figure 4-2) is random during the hologram exposure will now be considered. The model and results of section 4.1 will be used in this discussion but the slab generating the refractive index perturbation is now supposed to be a random phase screen. It should be recognized that this is not a limitation for this discussion as it has been shown[12] that a large or extended turbulent region can be decomposed into small thin homogeneous and isotropic regions as is proposed here with no loss of generality. When, in fact, the situation is an extended region of turbulence, it must be remembered that each of the individual phase screens must remain parallel to the film plane so that a paraxial ray will remain paraxial after passing through the many regions.

Continuing, the phase screen will be considered to represent a region of laminar turbulence which is statistically homogeneous and isotropic with respect to directions parallel to the film plane. The temporal variations of the turbulence will be assumed to be a stationary stochastic process with characteristic fluctuation times which vary much more slowly than the incident light field and very much faster than the exposure time of the hologram. Additionally, the geometry of the hologram recording, the width of the slab and the magnitude of the refractive index perturbation shall be such that paraxial conditions prevail and paraxial rays remain essentially paraxial when passing through the perturbed refractive index region. Lastly, all of the assumptions concerning the slab itself and the slab's relationship to the film plane made in section 4.1 will be supposed to hold for this discussion.

Consider figure 4-2 where N_2 is again assumed in two parts, a random time variable of mean zero and a constant of value unity, i.e.,

$$N_2 = 1 + \delta n$$

and

$$\overline{\delta n} = 0. \qquad (4\text{-}29)$$

During the exposure of the hologram, the slab will remain geometrically fixed in position relative to the reference source with the magnitude of the refractive index changing between different successive time intervals. The slab itself will be assumed very thin so that the second order term in $\hat{x}(t)$, $K(\Delta nW)^2/X$ is small compared to unity and can be neglected.

The corresponding complex degree of coherence becomes,

$$G_{mR}(o) \approx \frac{1}{T} \int_0^T e^{j\frac{2\pi}{\lambda} K' \delta n} \, dt$$

$$K' = KW = (Y_R^2 - Y_m^2)W/2X \qquad (4\text{-}30)$$

where W is the thickness of the slab (phase screen), Y_R and Y_m are the distances from the optical axis to the reference source and the object point respectively, and X the distance from the object to the film.

To evaluate the integral for $G_{mR}(o)$, basic assumptions concerning the nature of the refractive index variation must be introduced. The assumptions invoked herein are those generally employed by researchers studying the effects of turbulent refractive indices on the propagation of light.[13]

The random function δn will be assumed to have stationary first increments.* The characteristic fluctuations of the variation of refractive index about its mean value are short compared to the hologram exposure implying that during a hologram exposure, a great many different changes occur in the optical path length. This makes it reasonable now to consider the ensemble average of $G_{mR}(o)$ to perform our computation. Then equation 4-30 becomes,

$$\langle G_{mR}(o)\rangle = \left\langle \frac{1}{T}\int_0^T e^{j\frac{2\pi}{\lambda}K'\delta n}\,dt \right\rangle$$

$$= \frac{1}{T}\int_0^T \langle e^{j\frac{2\pi}{\lambda}K'\delta n}\rangle\,dt \qquad (4\text{-}31)$$

where K' is assumed to have a fixed value for the ensemble of fluctuations. Invoking the principle of ergodicity results in,

$$\langle G_{mR}(o)\rangle = \langle e^{j\frac{2\pi}{\lambda}K'\delta n}\rangle . \qquad (4\text{-}32)$$

If the distribution of the random variable δn is assumed gaussian, locally homogeneous and locally isotropic in directions parallel to the film plane, the average in equation 4-26 is well known to researchers working on descriptions of turbulence effects on light propagation. Equation 4-32 becomes[14]

*refer to appendix II for a discussion of the meaning of these terms

$$\langle G_{mR}(o)\rangle = e^{-\frac{1}{2}\left(\frac{2\pi}{\lambda}\right)^2 K'^2 \langle \delta n^2\rangle}$$

$$= e^{-\frac{1}{2}\left(\frac{2\pi}{\lambda}\right)^2 D(0;\ r)} \qquad (4\text{-}33)$$

where $D(0;\ r)$ is the wave structure function for the random process δn with r representing the separation of the points P_R and P_m in the object plane. Recalling equation 4-2, the radiance of the reconstructed image point m' under conditions of randomly varying index of refraction during recording is,

$$R(m') = R_o(m)\ e^{-\left(\frac{2\pi}{\lambda}\right)^2 D(0;\ r)}. \qquad (4\text{-}34)$$

Equation 4-34 indicates that the radiance of the reconstructed image point will be shaded by the quantity $e^{-\left(\frac{2\pi}{\lambda}\right)^2 D(0;\ r)}$ but no loss of image resolution will occur. This conclusion was reached by Gaskill analytically (using a totally different technique) and Goodman et. al. experimentally. It is of importance because here the concept of a random film motion was used to obtain results equivalent to those concerning turbulence effects using conventional analysis. This technique opens a new avenue of interpretation and experimental evaluation of turbulence effects. Now, a flexible and relatively inexpensive simulation technique is available for studying and classifying different types of turbulence in the laboratory under controlled conditions.

4.3 Measurement of the Wave Structure Function by Means of a Hologram

In the previous section, the distribution of the radiance of the reconstructed image of a hologram taken with a random refractive index variation of the medium separating the object-reference plane and the film plane was shown to be dependent on the wave structure function, $D(0; r)$, of the medium. This suggests a rather interesting technique for the determination of the constants[15] which are normally associated with the structure function for atmospheric turbulence using holography.

Figure 4-4 indicates an experimental setup which is proposed for this measurement. The object of this hologram will be a painted piece of diffusing (ground) glass and the reference beam will be formed as a point source in the plane of the object. The object itself will be such that a means of easily identifying point separation on the object with respect to the reference beam can be made accurately. This will require a grid type object with equidistant lines of known separation and position from the reference source.

Removed from the object-reference beam plane will be the film used to record the hologram. The distance between the film and object planes will depend on the type of

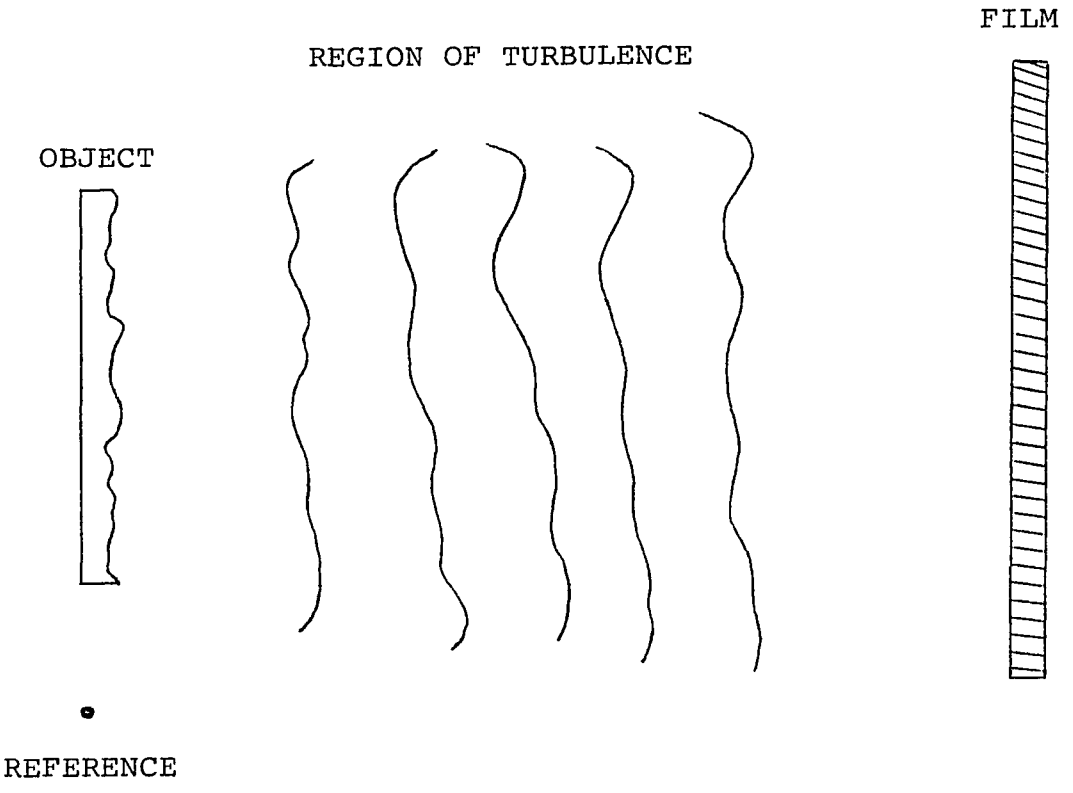

Figure 4-4

An experimental geometry for the measurement of atmospheric turbulence effects

atmospheric turbulence which is to be measured (long or short path) but, to be consistent with other reported measurements, the separation should be at least one kilometer.

The bases employed to support the film and the object-reference source must be made very stable. Any motion in these support structures will tend to reduce the radiance of the reconstructed holographic images. For best results, the two supports should be as stable with respect to each other as if they were part of the same rigid optical bench. This will require a feedback control system which links the two structures and can sense a relative position error between them. One possible means of achieving the sensor sensitivity would be to use a laser beam of light with an angle sensitive receiver. The receiver, which would be designed similarly to a radar monopulse type antenna, would then give an error indication when the angle between the laser beam and the receiver was different from zero.

The hologram which results from an exposure just described will then have a radiance distribution according to equation 4-34. Upon reconstruction, the image brightness would fall as distances from the reference beam increase. The reduction in image brightness will be in accordance with the magnitude of the structure function for the object-reference beam separation.

Measurements of the image radiance versus object point-reference beam position as measured from the reconstructed holographic image can then be used to determine the shape and turbulence constants associated with the structure function for atmospheric turbulence. The technique for the measurement of the effects of atmospheric turbulence will give a multitude of data with which to determine the form and shape of the structure function. In addition, the data is recorded on a single exposure which reduces the chance of experimental error. This is in contrast to the usual techniques of interferometric measurements which are generally used to gather the data.

It must be indicated that although the experiment described is basically straightforward, there are many difficulties which must be overcome before useful data can be obtained, the most critical difficulty, of course, being the relative stabilization of the two platforms, which is followed by the less critical problems of obtaining sufficient laser power and film sensitivity to ensure proper exposure of the recording medium. When these problems can be overcome, useful data can then be obtained in a relatively short period of time with a high degree of accuracy.

The apparently very large distance between object and film plane can of course be achieved by folding the optical path by means of a mirror system (parallel mirrors in the turbulent medium or analogous optical system).

REFERENCES

1. D.L. Fried, J. Opt. Soc. Am., 56, 1372 (1966)

2. G.O. Reynolds and T.J. Skinner, J. Opt. Soc. Am., 54, 1302 (1964)

3. H. Hodara, Proc. IEEE, 54, 368 (1966)

4. J.W. Goodman, W.H. Huntly Jr., D.W. Jackson, and M. Lehmann, Appl. Phys. Letters, 8, 311 (1966)

5. R.J. Collier and K.S. Pennington, Applied Optics, 6, 1091 (1967)

6. V.I. Tatarski, Wave Propagation in a Turbulent Medium, McGraw-Hill Book Company, (1961)

7. R.E. Hufnagel and N.R. Stanley, J. Opt. Soc. Am., 54, 52 (1964)

8. J.D. Gaskill, J. Opt. Soc. Am., 58, 600 (1968)

9. H. Hodara, op. cit., 368

10. J.M. Stone, Radiation and Optics, McGraw-Hill Book Company, 223 (1963)

11. H. Hodara, op. cit., 368

12. W.P. Brown Jr., J. Opt. Soc. Am., 57, 1539 (1967)

13. R.E. Hufnagel and N.R. Stanley, op. cit., 52

14. G.R. Heidbreder, J. Opt. Soc. Am., 57, 1477 (1967)

15. V.I. Tatarski, op. cit.

CHAPTER V

5.1 Simultaneous Film and Object Motion

Figure 5-1 indicates a situation where both the object and film have experienced a displacement relative to the reference source. The film moves a distance x_F from point P to P' along the system centerline CC'. Simultaneously the object moves a distance x_o from P_m to P_m', with the direction of the object motion remaining parallel to the system centerline CC' at all times. The monochromatic point source reference is located a distance X from the film and a distance Y_R from the system centerline CC'. The object point under consideration, P_m, is located a distance Y_m from the system centerline. The illumination of the object is accomplished by directing the reference source radiation using two fixed mirrors M_1 and M_2, where mirror M_2 is located a distance D from the object measured parallel to CC'; and a distance Y_D from the object point P_m measured in a plane parallel to the film plane. Lastly, the object is located a distance X from the film plane as measured along the system centerline CC'.

To determine the effect of the simultaneous motion of the film and object on the reconstructed holographic image, the change in optical paths due to the simultaneous displacement of both the object and film will be computed. Consider that during a hologram exposure, a point on the film plate,

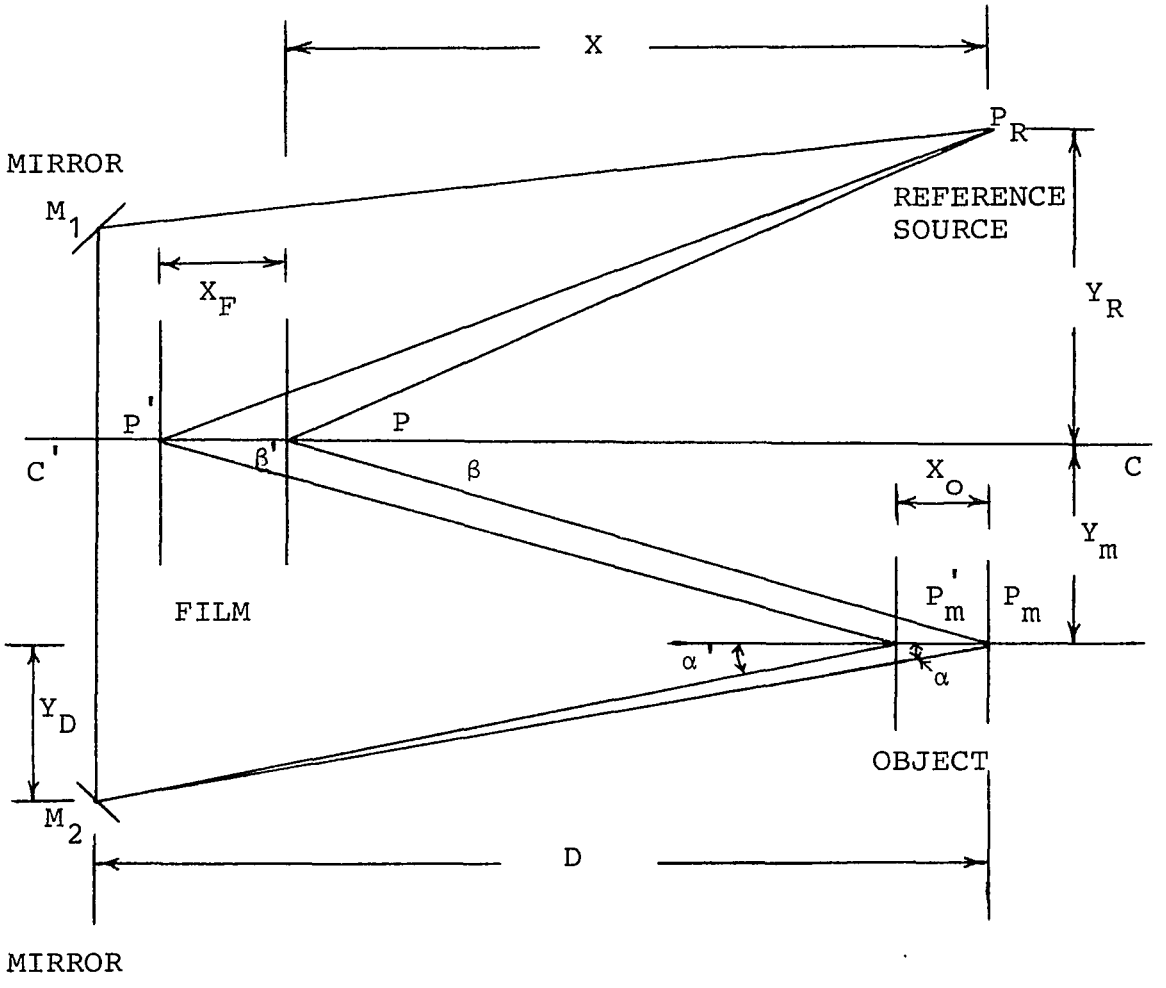

Figure 5-1

Geometric configuration for the computation of the change in optical path due to a simultaneous change in both film and object position.

P, is displaced to position P' and a point on the object, P_m, is displaced to P_m'. Prior to this displacement, the difference between the optical path from the reference source, P_R, to a point on the film P; and the optical path from the reference source to the object point P_m and then to the same point P on the film is,

$$\Delta = P_R P - (PP_m + P_m M_2 + M_2 M_1 + M_1 P_R). \qquad (5\text{-}1)$$

When both the film and the object have experienced a displacement to positions P' and P_m', where we assume that the direction of the displacements are parallel to the system centerline, the new difference in optical path becomes,

$$\Delta' = P_R P' - (P'P_m' + P_m' M_2 + M_2 M_1 + M_1 P_R). \qquad (5\text{-}2)$$

For the sake of clarity in figure 5-1, the displacement of the film was drawn in a manner as to cause an increase in optical path. The displacement of the object is drawn in a manner as to cause a reduction in optical path. Later in this development, a sign convention for object and film motion will be chosen using these facts.

Determining the effects of this dual motion on the reconstructed image of a hologram requires computing the change in the relative phase between reference and object

wave at the film plate due to the simultaneous motion of the film and object. This change in phase, due directly to the change in the optical path difference of formulas 5-1 and 5-2, will then be used to compute the modified complex degree of coherence which, as already shown in chapter three, is used to compute these effects on the reconstructed holographic image.

The change in optical path difference, δ is

$$\delta \equiv \Delta - \Delta' \tag{5-3}$$

$$\delta = P_R P - P_R P' - (P P_m + P_m M_2 + M_2 M_1 + M_1 P_R)$$

$$+ (P' P_m' + P_m' M_2 + M_2 M_1 + M_1 P_R). \tag{5-4}$$

Combining and rearranging terms yields,

$$\delta = (P_R P - P P_m) - (P_R P' - P' P_m') + (P_m' M_2 - P_m M_2). \tag{5-5}$$

Consideration of figure 5-1 indicates the following relationships can be written for the optical paths (here we are assuming a uniform index of refraction)

$$P_R P = [X^2 + Y_R^2]^{1/2} = X[1 + Y_R^2/X^2]^{1/2}$$

$$PP_m = [X^2 + Y_m^2]^{1/2} = X[1 + Y_m^2/X^2]^{1/2}$$

$$P_R P' = [(X + x_F)^2 + Y_R^2]^{1/2} = (X + x_F)[1 + Y_R^2/(X + x_F)^2]^{1/2}$$

$$P'P_m' = [(X + x_F - x_o)^2 + Y_m^2]^{1/2}$$

$$= (X + x_F - x_o)[1 + Y_m^2/(X + x_F - x_o)^2]^{1/2}$$

$$P_m M_2 = [D^2 + Y_D^2]^{1/2} = D[1 + Y_D^2/D^2]^{1/2}$$

$$P_m' M_2 = [(D - x_o)^2 + Y_D^2]^{1/2} = (D - x_o)[1 + Y_D^2/(D - x_o)^2]^{1/2}.$$

(5-6)

For this presentation, the distances of either the object (Y_m) or the reference source (Y_R) from the centerline of the holographic system (CC') are assumed very much smaller than the distance from the object-reference plane to the film plane (X). These distances are experimentally controlled quantities indicating that here we will be considering those rays which form small angles with respect to the CC' direction. Consequently, the statements that

$$Y_R/X << 1$$

$$Y_m/X << 1 \qquad (5\text{-}7)$$

and

$$Y_D/D << 1$$

imply that

$$Y_R^2/X^2 << 1$$

$$Y_m^2/X^2 << 1 \qquad (5\text{-}8)$$

and

$$Y_D^2/D^2 << 1$$

resulting in equations 5-6 becoming

$$P_RP \approx X[1 + Y_R^2/2X^2]$$

$$PP_m \approx X[1 + Y_m^2/2X^2]$$

$$P_RP' \approx (X + x_F)[1 + Y_R^2/2(X + x_F)^2]$$

$$P'P_m' \approx (X + x_F - x_o)[1 + Y_m^2/2(X + x_F - x_o)^2]$$

$$P_mM_2 \approx D[1 + Y_D^2/2D^2]$$

$$P_m'M_2 \approx (D - x_o)[1 + Y_D^2/2(D - x_o)^2] \qquad (5\text{-}9)$$

In the interest of clarity the individual optical path differences indicated in equation 5-5 will be considered initially, then the complete path difference computed. The quantity $P_RP - PP_m$, in light of equations 5-9 becomes,

$$P_RP - PP_m = X[1 + Y_R^2/2X^2] - X[1 + Y_m^2/2X^2]$$

$$= (Y_R^2 - Y_m^2)/2X \ . \qquad (5\text{-}10)$$

The quantity $P_RP' - P'P_m'$ is,

$$P_RP' - P'P_m' = (X + x_F)[1 + Y_R^2/2(X + x_F)^2]$$

$$- (X + x_F - x_o)[1 + Y_m^2/2(X + x_F - x_o)^2]$$

$$= Y_R^2/2(X + x_F) + x_o$$

$$- Y_m^2/2(X + x_F)[1 - x_o/(X + x_F)]. \qquad (5\text{-}11)$$

Now, realizing that $x_o/(X + x_F)$ is very small compared to unity, we have that

$$P_RP' - P'P_m' = Y_R^2/2(X + x_F) + x_o$$

$$- [Y_m^2/2(X + x_F)][1 + x_o/(X + x_F)]$$

$$= \frac{Y_R^2 - Y_m^2}{2(X + x_F)} + x_o\left\{1 - \frac{Y_m^2}{2(X + x_F)^2}\right\} \qquad (5\text{-}12)$$

Continuing, the quantity $P_m'M_2 - P_mM_2$ is

$$P_m'M_2 - P_mM_2 = (D - x_o)[1 + Y_D^2/2(D - x_o)^2]$$

$$- D[1 + Y_D^2/2D^2]$$

$$= - x_o + Y_D^2/2(D - x_o) - Y_D^2/2D$$

$$= - x_o[1 - Y_D^2/2D^2] \qquad (5\text{-}13)$$

Returning to figure 5-1, observe that the quantity $Y_m/(X + x_F)$ is equal to the tan β'. Considering the previous assumption that $Y_m/(X + x_F)$ is very small implies that,

$$\frac{Y_m}{(X + x_F)} = \tan \beta' \approx \beta' \qquad (5\text{-}14)$$

where β' is the angle in radians (less than six degrees to be a good approximation). Here, the usual small angle approximation of replacing the tan function by its angle in radians has been used, and for β' small the approximation is valid for this situation. Incorporation of equation 5-14 into equation 5-12 yields,

$$P_RP' - P'P_m' = \frac{Y_R^2 - Y_m^2}{2(X + x_F)} + x_o\left\{1 - \frac{\beta'^2}{2!}\right\}. \qquad (5\text{-}15)$$

Following the same reasoning and realizing that Y_D/D is very small, gives that

$$\frac{Y_D}{D} = \tan \alpha \approx \alpha \tag{5-16}$$

then equation 5-13 can be written as

$$P_m'M_2 - P_mM_2 = - x_o[1 - \alpha^2/2!]. \tag{5-17}$$

The series expansion for the cosine function is,

$$\cos x = 1 - \frac{x^2}{2!} + \frac{x^4}{4!} - \frac{x^6}{6!} + ... \tag{5-18}$$

which when coupled with the small angle approximation (i.e., the angle less than or equal to six degrees) implies that

$$x \leq 0.1047 \text{ radians} \tag{5-19}$$

implying that the cosine function can be approximated by

$$\cos x \approx 1 - x^2/2! \tag{5-20}$$

with a peak error of $x^4/4! = 5 \times 10^{-6}$. Now, incorporation of equation 5-20 into equation 5-15 and 5-17 yields,

$$P_RP' - P'P_m' = \frac{Y_R^2 - Y_m^2}{2(X + x_F)} + x_o \cos \beta' \tag{5-21}$$

and

$$P_m'M_2 - P_mM_2 = - x_o \cos \alpha. \qquad (5\text{-}22)$$

Now, the computation of the complete change in optical path is, recalling equation 5-5,

$$\delta = (P_RP - PP_m) - (P_RP' - P'P_m') + (P_m'M_2 - P_mM_2)$$

which is,

$$\delta \approx \frac{Y_R^2 - Y_m^2}{2X} - \frac{Y_R^2 - Y_m^2}{2(X + x_F)} - x_o \cos \beta' - x_o \cos \alpha$$

$$= \frac{Y_R^2 - Y_m^2}{2} \left[\frac{1}{X} + \frac{1}{X + x_F}\right] - x_o[\cos \alpha + \cos \beta']$$

$$= \frac{Y_R^2 - Y_m^2}{2} \left[\frac{x_F}{X(X + x_F)}\right] - x_o[\cos \alpha + \cos \beta'] \qquad (5\text{-}23)$$

Letting $x' \equiv x_F/X$ equation 5-23 becomes

$$\delta = \frac{Y_R^2 - Y_m^2}{2X} \left[\frac{x'}{(1 + x')}\right] - x_o[\cos \alpha + \cos \beta'] \qquad (5\text{-}24)$$

Recalling that the quantity x' is small,

$$x' \equiv x_F/X << 1 \qquad (5\text{-}25)$$

gives for the change in optical path,

$$\delta \approx \frac{Y_R^2 - Y_m^2}{2X} [x'(1 - x')] - x_o(\cos \alpha + \cos \beta'). \qquad (5\text{-}26)$$

The change in phase in the hologram plane due to the simultaneous motion of the film and the object which results in the change of optical path δ is

$$\phi_{mR} = \frac{2\pi}{\lambda} \delta \qquad (5\text{-}27)$$

which gives a complex degree of coherence equal to (see chapter III)

$$G_{mR}(o) = \frac{1}{T} \int_0^T e^{j\phi_{mR}} dt$$

$$= \frac{1}{T} \int_0^T e^{j\frac{2\pi}{\lambda}} \{ \frac{Y_R^2 - Y_m^2}{2X} [x'(1 - x')]$$

$$- x_o(\cos \alpha + \cos \beta') \}_{dt} \qquad (5\text{-}28)$$

Comparing equation 5-28 with equation 3-18 of chapter three for the complex degree of coherence for just film motion and with equation 3-8 of chapter three for the complex degree of coherence for object motion, the similarities can be immediately distinguished. The first bracketed term in the exponential of equation 5-28 is identical to that for film motion. Recall also that in both cases the change

in film position with respect to the reference source was such as to cause an increase in optical path of the holographic system. Thus, we shall define the following:

$$F(t) \equiv \frac{Y_R^2 - Y_m^2}{2X} [x'(1 - x')] \qquad (5\text{-}29)$$

We shall call F(t) the modified film motion function.

Continuing, the second term in the exponent of equation 5-28 is essentially identical to that for film motion except for the change in sign and the angle β'. In the original derivation of the film motion effect in chapter three, an assumption was made that during the exposure of the hologram the angles α and β do not change significantly. For this derivation concerning simultaneous motion, this is equivalent to the statement that $\cos \beta' \approx \cos \beta$. For the system discussed here, this approximation is valid when x_F/X is very small. We have already assumed that $x_F/X << 1$, consequently we can assume that $\cos \beta' \approx \cos \beta$.

Lastly, as was mentioned earlier, for the sake of figure clarity, the object was displaced in a manner as to cause a decrease in optical path with respect to the reference source. Thus, adopting a sign convention that motions along CC' causing increases in optical path with respect to the reference source are positive and motions causing decreases in optical path are negative, we can define, for the object motion,

$$O(t) \equiv x_o(\cos \alpha + \cos \beta). \tag{5-30}$$

where x_o is measured along the CC' axis.

For the situation of simultaneous object and film motion, we now have

$$G_{mR}(o) = \frac{1}{T} \int_0^T e^{j\frac{2\pi}{\lambda}} [F(t) + O(t)]_{dt} \tag{5-31}$$

which represents the complex degree of coherence for the situation of simultaneous film and object motion. As has been shown in previous chapters, this is used to compute the effects of the simultaneous motions on the reconstructed holographic image.

Several interesting examples of simultaneous motion will now be discussed which indicate the application of expression 5-31.

5.2 Simultaneous Object and Film Step Motion

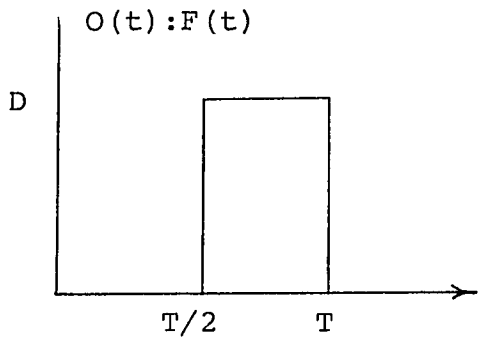

Figure 5-2

Law of motion for the computation of simultaneous film and object motion

Assume as a law of motion for O(t) and F(t) the step function depicted in figure 5-2. The law indicates no motion existing for the first half of the exposure, and both the film and the object perturbed to cause a step displacement of D_O and D_F respectively* for the seocnd half of the exposure.

The modified complex degree of coherence can now be computed as

$$G_{mR}(o) = \frac{1}{T}\int_0^{T/2} e^{j\frac{2\pi}{\lambda}[0 + 0]}dt$$

$$+ \frac{1}{T}\int_{T/2}^{T} e^{j\frac{2\pi}{\lambda}[D_O + D_F]}dt$$

$$= \frac{1}{2}\{ 1 + e^{j\frac{2\pi}{\lambda}[D_O + D_F]} \} \qquad (5\text{-}32)$$

The determination of the effect on the reconstructed image of the hologram requires computing the absolute value square of $G_{mR}(o)$, then,

*It should be pointed out that D_O and D_F are the magnitudes of O(t) and F(t). To determine the actual film or object displacement, equation 5-30 and 5-29 must be used. Notice that both X_F and X_O will still be steps, but of different amplitude. Also, because of the $Y_R^2 - Y_m^2$ dependence of D_F, for a step motion of the film, the amplitude will change along the Y axis of the film.

$$|G_{mR}(o)|^2 = \frac{1}{4}\{\ 1 + e^{j\frac{2\pi}{\lambda}[D_O + D_F]}\ \}\{\ 1 + e^{-j\frac{2\pi}{\lambda}[D_O + D_F]}\ \}$$

$$= \frac{1}{2}\{\ 1 + \cos\frac{2\pi}{\lambda}(D_O + D_F)\ \} \qquad (5\text{-}33)$$

The reconstructed image then will have a regular pattern of dark bands (fringes) located at the zeros of equation 5-33, i.e., the fringe location will be in accordance with

$$D_O + D_F = \frac{n\lambda}{2} \text{ for n odd.} \qquad (5\text{-}34)$$

5.3 Simultaneous Staircase Film and Object Motion

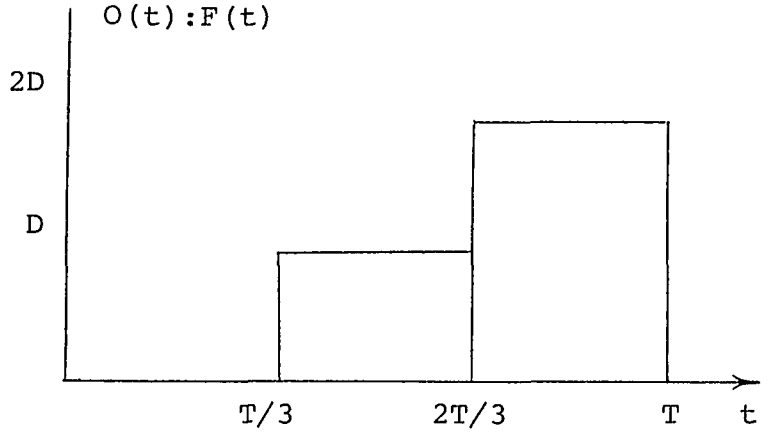

Figure 5-3

The law of motion for the computation of simultaneous film and object staircase motion

Consider now a law of motion for O(t) and F(t) to be the staircase function of figure 5-3. Here, no motion exists for the initial one third of the exposure; a step of D_O and D_F occur for the second third of the exposure; and the final third of the exposure is a step of $2D_O$ and $2D_F$.

The modified complex degree of coherence is computed as,

$$G_{mR}(o) = \frac{1}{T}\int_0^{T/3} e^{j\frac{2\pi}{\lambda}[0 + 0]}dt$$

$$+ \frac{1}{T}\int_{T/3}^{2T/3} e^{j\frac{2\pi}{\lambda}[D_O + D_F]}dt$$

$$+ \frac{1}{T}\int_{2T/3}^{T} e^{j\frac{2\pi}{\lambda}[2D_O + 2D_F]}dt$$

$$G_{mR}(o) = \{ 1 + e^{j\frac{2\pi}{\lambda}[D_O + D_F]}$$

$$+ e^{j\frac{2\pi}{\lambda}[2D_O + 2D_F]} \}. \qquad (5\text{-}35)$$

The corresponding absolute value square of the modified complex degree of coherence is

$$|G_{mR}(o)|^2 = \frac{1}{9}\{1 + e^{j\frac{2\pi}{\lambda}(D_O + D_F)} + e^{j\frac{2\pi}{\lambda}2(D_O + D_F)}\} X$$

$$\{1 + e^{-j\frac{2\pi}{\lambda}(D_O + D_F)} + e^{-j\frac{2\pi}{\lambda}2(D_O + D_F)}\}$$

$$= \frac{1}{9}\{3 + 4\cos\frac{2\pi}{\lambda}(D_O + D_F)$$

$$+ 2\cos\frac{2\pi}{\lambda}2(D_O + D_F)\} \qquad (5\text{-}36)$$

Employing the double angle trigonometric identity,

$$\cos\frac{2\pi}{\lambda}2(D_O + D_F) \equiv 2\cos^2[\frac{2\pi}{\lambda}(D_O + D_F)] - 1 \qquad (5\text{-}37)$$

results in equation 5-36 becoming

$$|G_{mR}(o)|^2 = \frac{1}{9}\{1 + 4\cos\frac{2\pi}{\lambda}(D_O + D_F)$$

$$+ 4\cos^2\frac{2\pi}{\lambda}(D_O + D_F)\}$$

$$|G_{mR}(o)|^2 = \frac{1}{9}\{1 + 2\cos\frac{2\pi}{\lambda}(D_O + D_F)\}^2 \qquad (5\text{-}38)$$

The reconstructed holographic image will then have fringes located at the zeros of equation 5-38, i.e., the fringe location will be in accordance with

$$(D_O + D_F) = \lambda(\frac{1}{3} + n)$$

n an integer

$$(D_O + D_F) = \lambda(\frac{2}{3} + n) \qquad (5\text{-}39)$$

5.4 Simultaneous Staircase Object and Step Film Motion

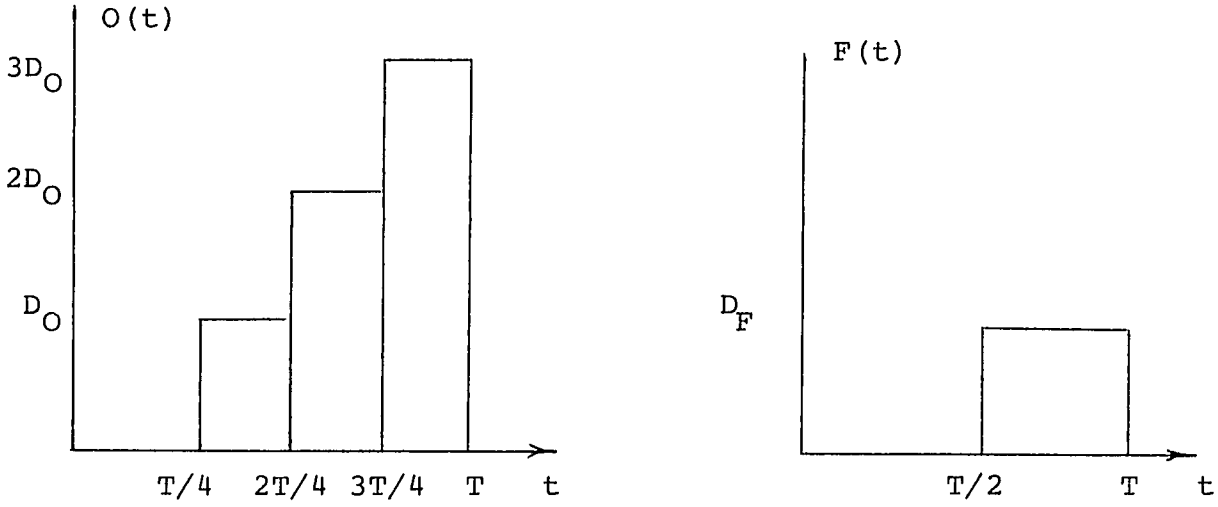

Figure 5-4

The laws of motion for simultaneous staircase object and step film motion

Consider the laws of motion depicted in figure 5-4 where during the hologram exposure, the object experiences a staircase motion (no motion for the initial quarter of the exposure, a single step of D_O for the second quarter, $2D_O$ for the third quarter and $3D_O$ for the fourth quarter) and the film simultaneously experiences no motion during

the first half of the exposure and a step of D_F for the second half of the exposure.

The modified complex degree of coherence for this situation is,

$$G_{mR}(o) = \frac{1}{T}\int_0^{T/4} e^{j\frac{2\pi}{\lambda}(0+0)}dt + \frac{1}{T}\int_{T/4}^{2T/4} e^{j\frac{2\pi}{\lambda}(D_O+0)}dt + \frac{1}{T}\int_{2T/4}^{3T/4} e^{j\frac{2\pi}{\lambda}(2D_O+D_F)}dt + \frac{1}{T}\int_{3T/4}^{T} e^{j\frac{2\pi}{\lambda}(3D_O+D_F)}dt$$

$$= \frac{1}{4}\{\,1 + e^{j\frac{2\pi}{\lambda}D_O}\,\}\{\,1 + e^{j\frac{2\pi}{\lambda}D_F}\,e^{j\frac{2\pi}{\lambda}2D_O}\,\}. \qquad (5\text{-}40)$$

The absolute value square of the modified complex degree of coherence is

$$|G_{mR}(o)|^2 = \frac{1}{16}\{\,1 + e^{j\frac{2\pi}{\lambda}D_O}\,\}\{\,1 + e^{j\frac{2\pi}{\lambda}D_F}\,e^{j\frac{2\pi}{\lambda}2D_O}\,\} \times \{\,1 + e^{-j\frac{2\pi}{\lambda}D_O}\,\}\{\,1 + e^{-j\frac{2\pi}{\lambda}D_F}\,e^{-j\frac{2\pi}{\lambda}2D_O}\,\}$$

$$= \frac{1}{8}\{\,1 + \cos\frac{2\pi}{\lambda}D_O\,\}\{\,1 + \cos\frac{2\pi}{\lambda}(D_F + 2D_O)\,\}. \qquad (5\text{-}41)$$

Observe from equations 5-41 that the effect on the reconstructed holographic image is as if two step motions had been applied to the system. The image will then have a regular fringe pattern with the fringes located at the zeros of equation 5-41, i.e., the fringe locations will be in accordance with

$$D_O = \frac{n\lambda}{2}$$

n an odd integer

$$D_F + 2D_O = \frac{n\lambda}{2} \qquad (5\text{-}42)$$

5.5 Simultaneous, Non-Synchronous, Step Film and Object Motion

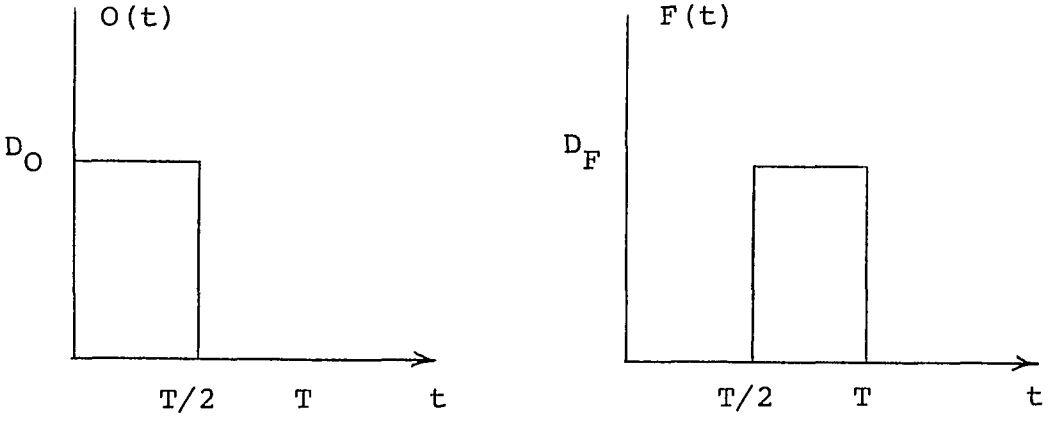

Figure 5-5

Laws of motion for simultaneous, non-synchronous film and object motion

As the last example, consider the laws of motion depicted in figure 5-5 where for the first half of the exposure the object experiences a step displacement of D_O and the film has no displacement. For the second half of the exposure, the object experiences no displacement, but the film experiences a step of D_F. The situation is that both the film and the object laws of motion are step functions, but the functions occur asynchronously during the exposure time.

The modified complex degree of coherence is

$$G_{mR}(o) = \frac{1}{T}\int_0^{T/2} e^{j\frac{2\pi}{\lambda}(D_O + 0)}dt + \frac{1}{T}\int_{T/2}^{T} e^{j\frac{2\pi}{\lambda}(0 + D_F)}dt$$

$$= \frac{1}{2}\left\{ e^{j\frac{2\pi}{\lambda}D_O} + e^{j\frac{2\pi}{\lambda}D_F} \right\} \qquad (5\text{-}43)$$

The corresponding absolute value square is

$$|G_{mR}(o)|^2 = \frac{1}{4}\left\{ e^{j\frac{2\pi}{\lambda}D_O} + e^{j\frac{2\pi}{\lambda}D_F} \right\} X \left\{ e^{-j\frac{2\pi}{\lambda}D_O} + e^{-j\frac{2\pi}{\lambda}D_F} \right\}$$

$$= \frac{1}{2}\left\{ 1 + \cos\frac{2\pi}{\lambda}(D_O - D_F) \right\} \qquad (5\text{-}44)$$

Then, the effect on the holographic reconstructed image is a regular fringe pattern, the fringes located at the zeros of equation 5-44, i.e., the fringe locations are in accordance with

$$(D_O - D_F) = \frac{n\lambda}{2} \quad n \text{ an odd integer} \tag{5-45}$$

Observe that for this situation, the effect on the image is the same as if the two motions were synchronous, but of opposite sign.

5.6 Simultaneous Film and Object Motion - An Approximate For Complex Motions

The two motions defined previously, O(t) and F(t), are assumed to occur simultaneously during the exposure of a hologram; O(t) representing the modified law of motion of the object and F(t) the modified law of motion for the film. The modified complex degree of coherence,

$$G_{mR}(o) = \frac{1}{T}\int_0^T e^{j\frac{2\pi}{\lambda}[O(t) + F(t)]}dt \tag{5-46}$$

for all but the most elementary classes of motion is exceedingly difficult to evaluate. Expansion of the integrand in series form yields for equation 5-46,

$$G_{mR}(o) = \frac{1}{T}\int_0^T \{ 1 + j\frac{2\pi}{\lambda} [O(t) + F(t)]$$

$$+ \frac{1}{2!} j^2 (\frac{2\pi}{\lambda})^2 [O(t) + F(t)]^2$$

$$+ \frac{1}{3!} j^3 (\frac{2\pi}{\lambda})^3 [O(t) + F(t)]^3$$

$$+ \ldots \} dt \qquad (5\text{-}47)$$

$$G_{mR}(o) = \frac{1}{T}\int_0^T \{ 1 + j(\frac{2\pi}{\lambda}) [O(t) + F(t)]$$

$$+ \frac{1}{2!} j^2 (\frac{2\pi}{\lambda})^2 [O(t)^2 + F(t)^2]$$

$$+ \frac{1}{2!} j^2 (\frac{2\pi}{\lambda})^2 [2\ O(t)\ F(t)]$$

$$+ \frac{1}{3!} j^3 (\frac{2\pi}{\lambda})^3 [O(t)^3]$$

$$+ \frac{1}{3!} j^3 (\frac{2\pi}{\lambda})^3 F(t)^3 [1 + 3\frac{O(t)}{F(t)} + 3\frac{O(t)^2}{F(t)^2}]$$

$$+ \frac{1}{4!} j^4 (\frac{2\pi}{\lambda})^4 [O(t)^4 + F(t)^4]$$

$$+ \frac{1}{4!} j^4 (\frac{2\pi}{\lambda})^4 [6\ O(t)^2\ F(t)^2]$$

$$+ \frac{1}{5!} j^5 \left(\frac{2\pi}{\lambda}\right)^5 [O(t)^5]$$

$$+ \frac{1}{5!} j^5 \left(\frac{2\pi}{\lambda}\right)^5 F(t)^5 \left[1 + 5 \frac{O(t)}{F(t)} + 10 \frac{O(t)^2}{F(t)^2}\right.$$

$$\left. + 10 \frac{O(t)^3}{F(t)^3} + 5 \frac{O(t)^4}{F(t)^4}\right]$$

$$+ \ldots . \} \, dt \qquad (5\text{-}48)$$

If the film motion is very much larger than the object motion, i.e.,

$$O(t)/F(t) << 1 \qquad (5\text{-}49)$$

and additionally the ratio of object to film motion magnitude is such that

$$O(t)/F(t) << 1/n \qquad (5\text{-}50)$$

where n is the largest term of the series expansion that is necessary to accurately describe the exponential functions, equation 5-48 can then be approximated by

$$G_{mR}(o) \quad \frac{1}{T} \int_0^T \{ 1 + j\left(\frac{2\pi}{\lambda}\right) O(t) + \frac{1}{2!} j^2 \left(\frac{2\pi}{\lambda}\right)^2 O(t)^2 + \ldots$$

$$+ j\left(\frac{2\pi}{\lambda}\right) F(t) + \frac{1}{2!} j^2 \left(\frac{2\pi}{\lambda}\right)^2 F(t)^2 + \ldots$$

$$+ \frac{1}{2!} j^2 \left(\frac{2\pi}{\lambda}\right)^2 [2\, O(t)\, F(t)]$$

$$+ \frac{1}{4!} j^2 \left(\frac{2\pi}{\lambda}\right)^4 [6\, O(t)^2\, F(t)^2]$$

$$+ \ldots\ldots \} \, dt$$

$$G_{mR}(o) = \frac{1}{T} \int_0^T \{ e^{j\frac{2\pi}{\lambda} O(t)} + e^{j\frac{2\pi}{\lambda} F(t)}$$

$$+ \sum_{p=0}^{\infty} j^{2p} \left(\frac{1}{p!}\right)^2 \left[\frac{2\pi}{\lambda} O(t)\right]^p \left[\frac{2\pi}{\lambda} F(t)\right]^p$$

$$- 2 \} \, dt \qquad (5\text{-}51)$$

The modified complex degrees of coherence for O(t) and F(t) acting alone are

$$G_{FmR}(o) = \frac{1}{T} \int_0^T e^{j\frac{2\pi}{\lambda} F(t)} dt$$

$$G_{OmR}(o) = \frac{1}{T} \int_0^T e^{j\frac{2\pi}{\lambda} O(t)} dt \qquad (5\text{-}52)$$

The series expansion in equation 5-51 can be represented in closed form by

$$\sum_{p=0}^{\infty} j^{2p} (1/p!)^2 \left[\frac{2\pi}{\lambda} O(t)\right]^p \left[\frac{2\pi}{\lambda} F(t)\right]^p$$

$$= J_o \{ 2 \left(\frac{2\pi}{\lambda}\right) \sqrt{O(t)\, F(t)} \}. \qquad (5\text{-}53)$$

In equations 5-52, $G_{FmR}(o)$ represents the degree of coherence for a moving film plate and $G_{OmR}(o)$ represents the degree of coherence for a moving object, and in equation 5-53, $J_o(x)$ is a zero order Bessel function. Then, equation 5-51 can be rewritten as,

$$G_{mR}(o) = G_{OmR}(o) + G_{FmR}(o) - 2 + \frac{1}{T}\int_0^T J_o \left\{ \frac{4\pi}{\lambda} \sqrt{O(t)\ F(t)} \right\} dt. \qquad (5\text{-}54)$$

Equation 5-54 represents a simplified method for computation of more complex simultaneous motion effects for the condition of modified object motion smaller than the modified film motion. This approximation can be useful to indicate the general trend of effects of the simultaneous motion that one might expect.

In addition to the ratio of object to film motion magnitude small, a further assumption concerning the motion magnitudes can be made, i.e., if

$$\frac{4\pi}{\lambda} [O(t)\ F(t)]^{1/2} << 1 \qquad (5\text{-}55)$$

then

$$J_o \left\{ \frac{4\pi}{\lambda} [O(t)\ F(t)]^{1/2} \right\} \approx 1 - \frac{1}{4} \left(\frac{4\pi}{\lambda}\right)^2 O(t)\ F(t). \qquad (5\text{-}56)$$

Equation 5-54 becomes, under these conditions,

$$G_{mR}(o) \quad G_{OmR}(o) + G_{FmR}(o) - 2$$

$$+ \frac{1}{T} \int_0^T \{ 1 - (\frac{2\pi}{\lambda})^2 O(t) F(t) \} dt$$

$$G_{OmR}(o) + G_{FmR}(o) - 1 - R_{OF}(o) \qquad (5\text{-}57)$$

where $R_{OF}(o)$ is the correlation of the modified object and modified film laws of motion, i.e.

$$R_{OF} = \frac{1}{T} \int_0^T (\frac{2\pi}{\lambda}) O(t) F(t) dt. \qquad (5\text{-}58)$$

Then for these conditions, the modified complex degree of coherence is equal to the modified complex degrees of coherence of the object and film motion acting independently reduced by the correlation of the two motions minus unity.

The application of equation 5-57 occurs when very precise measurements of small object motions or distortions (e.g. 0.05λ) are required in the presence of film plate drift due to air motion or thermal distortion of the film or film holder. Now, the individual motions satisfy the conditions of 5-55 and 5-50 making equation 5-57 useful for the extraction of the object motion from the measurement of

the simultaneous motions of film and object that was recorded. This technique for the separation of motion effects will then allow the accurate computation of the film motions as if acting alone, even though the measurements available are corrupted by film motion during the recording of the hologram.

CHAPTER VI

THE EFFECT OF FILM MOTION DURING RECORDING ON THE RECONSTRUCTED IMAGE OF A HOLOGRAM FOR THE CASE OF THE OBJECT AND FILM POINTS OFF THE HORIZONTAL PLANE CONTAINING THE REFERENCE SOURCE

The discussions presented concerning the effects of film motion on holography have considered the special case in which the film point, object point and reference source are all in the same horizontal plane. In this chapter, we will consider the situation of having both the film and object points located off the horizontal plane which contains the reference source. This analysis will be useful for the interpretation of the observed fringe spacing in the reconstructed image of a hologram taken with film motion during the exposure. Lastly, the discussion of simultaneous film and object motion will also be extended to consider film and object points located in horizontal planes that are different from each other and from the horizontal plane containing the reference source. This result will also serve to aid in interpreting observed fringe patterns in reconstructed holographic images taken with simultaneous film and object motion.

6.1 The Effect of Film Motion During Recording when the Object and Film Points are not in the Same Horizontal Plane Containing the Reference Source

Figure 6-1 depicts the case in which the film experiences a displacement relative to the reference source during the recording of a hologram. A cartesian coordinate system is indicated in which the x axis forms the system central axis, and the y, z axes define a vertical plane perpendicular to the x axis containing both the monochromatic point reference source and the object point. This plane will be termed the object plane. The x, y axes form the horizontal plane which also contains the reference source located a distance Y_R from the x axis. The film plane is parallel to the object plane, located a distance X from the object plane, and is perpendicular to the x axis. The film point P_F is located in the film plane, a distance Z_F above the x axis. The object point, P_m, is located in the object plane a distance Y_m from the x axis and Z_m above the horizontal plane.

During the recording of the hologram, the film point P_F under consideration is displaced from position P_F (X, o, Z_F) to position P_F' (X + x_F, o, Z_F) in a direction parallel to the x axis.

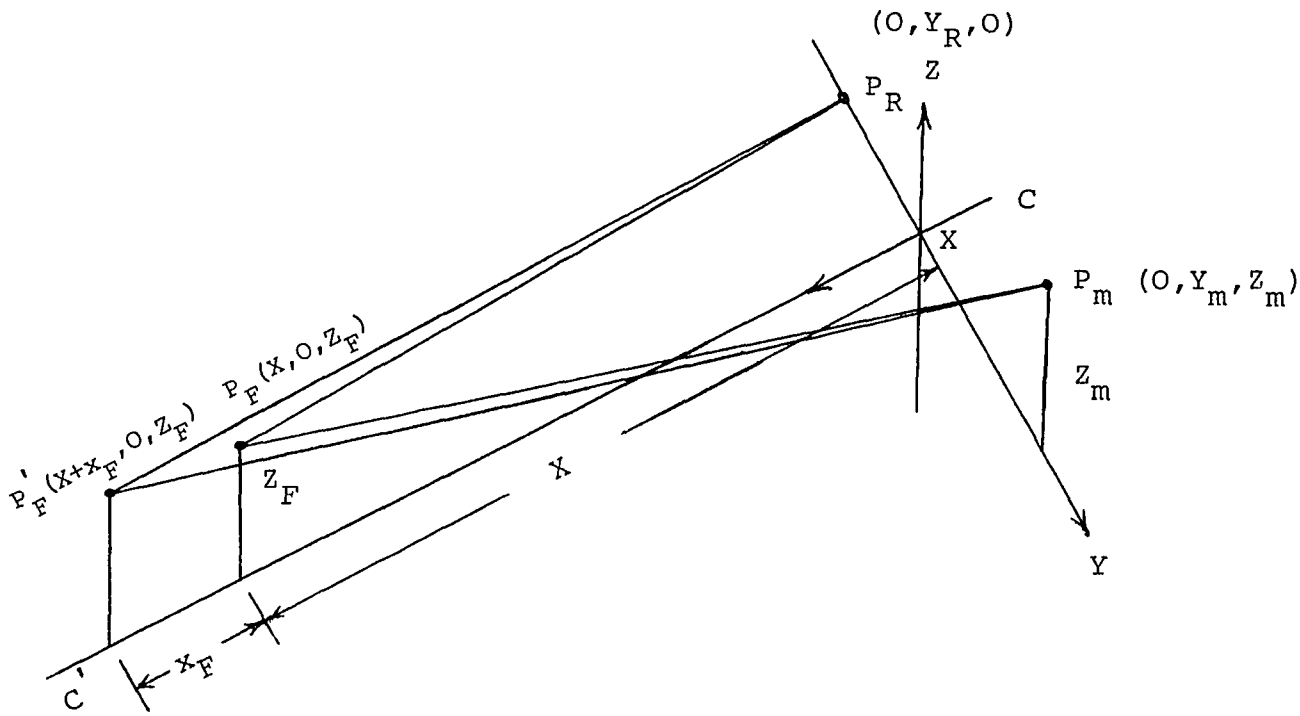

Figure 6-1

Geometry for film motion with both the object and film points removed from the X,Y plane containing the reference source

To determine the effect of this film motion on the reconstructed holographic image, the change in optical path due to the film motion will be computed to determine the variation in phase at the film point. As was done previously, this change in phase will then be used to compute the modified complex degree of coherence. As has already been indicated in Chapter III, the modified complex degree of coherence can then be used to compute the motion effects on the reconstructed holographic image.

Consider now that during a hologram exposure, the point P on the film is displaced to position P' (a displacement of x_F in the direction of the x axis). Prior to this displacement, the difference between the optical path from the reference source P_R to the film point P; and the optical path from the object point P_m to the film point P is,

$$\Delta = P_R P_F - P_m P_F. \tag{6-1}$$

When the film point experienced a displacement to position P, where we assume that the direction of the displacement is parallel to the x axis, the new difference in optical path becomes

$$\Delta' = P_R P_F' - P_m P_F' \tag{6-2}$$

The change in optical path difference, δ, is

$$\delta = \Delta - \Delta'$$

$$= (P_R P_F - P_m P_F) - (P_R P_F' - P_m P_F'). \qquad (6\text{-}3)$$

Considering figure 6-1, the following relationships can be written (here we are assuming a uniform index of refraction),

$$P_R P_F = [X^2 + Y_R^2 + Z_F^2]^{1/2} = X\left\{1 + (Y_R^2 + Z_F^2)/X^2\right\}^{1/2}$$

$$P_m P_F = [X^2 + Y_m^2 + (Z_m - Z_F)^2]^{1/2}$$

$$= X\left\{1 + [Y_m^2 + (Z_m - Z_F)^2]/X^2\right\}^{1/2}$$

$$P_R P_F' = [(X + x_F)^2 + Y_R^2 + Z_F^2]^{1/2}$$

$$= (X + x_F)\left\{1 + (Y_R^2 + Z_F^2)/(X + x_F)^2\right\}^{1/2}$$

$$P_m P_F' = [(X + x_F)^2 + Y_m^2 + (Z_m - Z_F)^2]^{1/2}$$

$$= (X + x_F)\left\{1 + [Y_m^2 + (Z_m - Z_F)^2]/(X + x_F)^2\right\}^{1/2} \qquad (6\text{-}4)$$

For this discussion, we shall assume that the paraxial approximation is valid, i.e., we shall be considering only those rays which form small angles with respect to the CC' axis. Consequently, we have that,

$$Y_R/X << 1 \qquad Z_m/X << 1$$

$$Y_m/X << 1 \qquad Z_F/X << 1$$

and

$$(Z_m - Z_F)/X << 1. \tag{6-5}$$

We can then imply from equations 6-5 that

$$Y_R^2/X^2 << 1$$

$$Y_m^2/X^2 << 1$$

$$Z_m^2/X^2 << 1$$

$$Z_F^2/X^2 << 1$$

and

$$\frac{(Z_m - Z_F)^2}{X^2} << 1 \tag{6-6}$$

which results in equations 6-4 becoming,

$$P_R\, P_F \approx X \left\{ 1 + (Y_R^2 + Z_F^2)/2X^2 \right\}$$

$$P_m\, P_F \approx X \quad 1 + [Y_m^2 + (Z_m - Z_F)^2]/2X^2$$

$$P_R P_F' \approx (X + x_F)\left\{1 + (Y_R^2 + Z_F^2)/2(X + x_F)^2\right\}$$

$$P_m P_F' \approx (X + x_F)\left\{1 + [Y_m^2 + (Z_m - Z_F)^2]/2(X + x_F)^2\right\} . \quad (6\text{-}7)$$

Equation 6-1 now becomes,

$$\Delta = X\left\{1 + (Y_R^2 + Z_F^2)/2X^2\right\} - X\left\{1 + [Y_m^2 + (Z_m - Z_F)^2]/2X^2\right\}$$

$$= \frac{Y_R^2 - Y_m^2 + Z_F^2 - (Z_m - Z_F)^2}{2X} \quad (6\text{-}8)$$

and equation 6-2 is

$$\Delta' = (X + x_F)\left\{1 + (Y_R^2 + Z_F^2)/2(X + x_F)^2\right\} - (X + x_F)\left\{1 + [Y_m^2 + (Z_m - Z_F)^2]/2(X + x_F)^2\right\}$$

$$= \frac{Y_R^2 - Y_m^2 + Z_F^2 - (Z_m - Z_F)^2}{2(X + x_F)} \quad (6\text{-}9)$$

The variation in optical path difference, δ, becomes,

$$\delta = \frac{Y_R^2 - Y_m^2 + Z_F^2 - (Z_m^2 - Z_F)^2}{2}\left[\frac{1}{X} - \frac{1}{X + x_F}\right]$$

$$= \frac{Y_R^2 - Y_m^2 + Z_F^2 - (Z_m - Z_F)^2}{2X^2}\left[\frac{x_F}{1 + x_F/X}\right] \quad (6\text{-}10)$$

which, for $x_F/X << 1$ becomes

$$\delta \approx \left\{ \frac{Y_R^2 - Y_m^2 + Z_F^2 - (Z_m^2 - Z_F^2)}{2X^2} \right\} x_F (1 - \frac{x_F}{X}). \qquad (6\text{-}11)$$

Then, the modified complex degree of coherence can now be written as

$$G_{mR}(0) = \frac{1}{T} \int_0^T e^{j \frac{2\pi}{\lambda} K x_F(t)[1 - x_F(t)/X]} dt$$

$$K = \frac{Y_R^2 - Y_m^2 + Z_m(2Z_F - Z_m)}{2X^2} . \qquad (6\text{-}12)$$

Notice that for the motion considered, i.e., a displacement occurring in the x direction, K is a constant for a particular film and object point. Then, for Y_R and Z_F fixed, the value of K will vary on the Y_m, Z_m plane as

$$K = \frac{-Y_m^2 - Z_m^2 + 2Z_F Z_m + Y_R^2}{2X^2}. \qquad (6\text{-}13)$$

Observe that K is a constant over contours for which

$$Y_m^2 + Z_m^2 - 2Z_F Z_m = \text{constant}. \qquad (6\text{-}14)$$

Equation 6-13 represents a family of concentric circles. Further, for the case of $K \equiv 0$, we have that

$$Y_m^2 + Z_m^2 - 2Z_F Z_m = Y_R^2 \qquad (6\text{-}15)$$

which represents a circle that is centered at $(0, Z_F)$ and passes through the point Y_R in the y_m, z_m plane. The contour for which $K \equiv 0$ represents a curve of constant brightness which is insensitive to the magnitude of the film motion. The family of bright circles is defined by

$$K\, x_F(t) \left[1 - \frac{x_F(t)}{X} \right] = n\lambda \qquad (6\text{-}16)$$

and these curves will be circles centered at $(Z_F, 0)$ downstream of the point P_F (in actuality a "very small" region of the film around P_F) with a radius equal to $\sqrt{Z_F^2 + Y_R^2}$. When viewing the reconstructed holographic image, one would see a family of concentric circles of constant brightness across the image of the object when the magnitude of the film motion was a step.

6.2 The Effects on a Reconstructed Holographic Image of Simultaneous Film and Object Motion During Recording when the Film and Object Points are Located off of the Horizontal Plane Containing the Reference Source

Figure 6-2 indicates an experimental condition in which both the object and film simultaneously experience a displacement relative to the reference source. Again the cartesian coordinate system is shown with the x axis forming the system central axis. The y, z axes define a vertical plane perpendicular to the x axis which contains

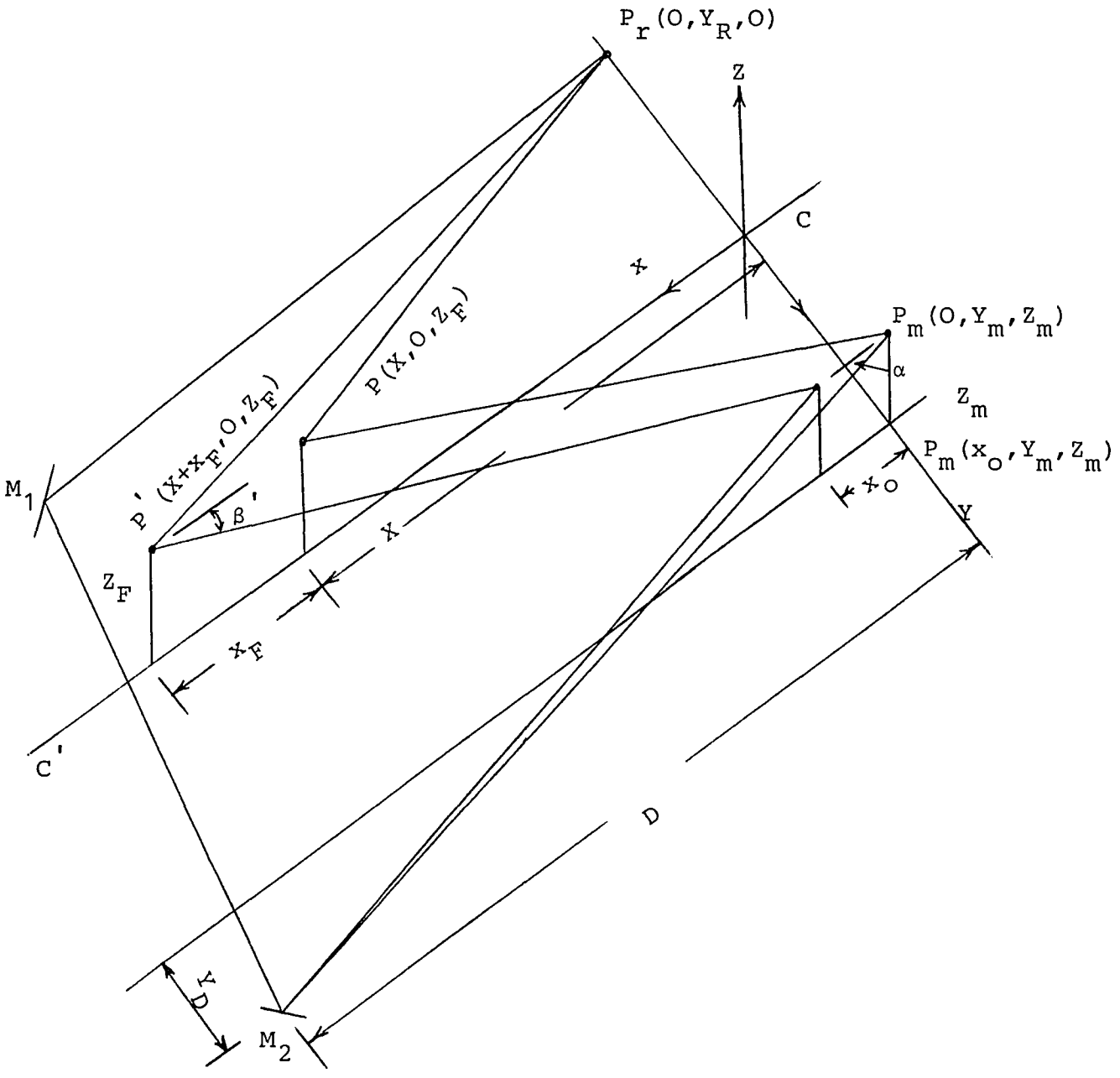

Figure 6-2

Geometry for simultaneous film and object motion for film and object points not in the plane of the reference source

the monochromatic point reference source and initially the object point under consideration. This plane will be termed the object plane. The reference, P_r, is located on the y axis at a distance Y_R from the x axis. The film plane is located at distance X from the object plane and is parallel to it. The film point P_F is located in the film plane a distance Z_F above the x axis. The object point P_m is in the object plane located a distance Z_m above the horizontal plane and a distance y_m from the x axis.

The illumination of the object is accomplished by directing the reference source radiation using two fixed mirrors M_1 and M_2. Mirror M_2 is located a distance D from the object measured parallel to the x axis, and a distance Y_D from the object point P_m measured parallel to the y axis.

During the recording of the hologram, the film moves a distance x_F from P_F (X, o, Z_F) to P_F' (X + x_F, o, Z_F) parallel to the x axis. Simultaneously, the object moves a distance x_o from P_m (o, Y_m, Z_m) to P_m' (x_o, Y_m, Z_m) also in a direction parallel to the x axis.

To determine the effect of the simultaneous motion of the film and object on the reconstructed holographic image, the change in optical path due to the simultaneous displacement of both the object and film will be computed. Prior to this displacement, the difference between the

optical path from the reference source, P_R, to a point on the film P_F, and the optical path from the reference source to the object point P_m and then to the same film point P_F is,

$$\Delta = P_R P_F - (P_F P_m + P_m M_2 + M_2 M_1 + M_1 P_R). \qquad (6\text{-}17)$$

When both the film and the object have experienced a displacement to positions P_F' and P_m', where we assume that the direction of the displacements are parallel to the system centerline, the new difference in optical path becomes

$$\Delta' = P_R P_F' - (P_F' P_m' + P_m' M_2 + M_2 M_1 + M_1 P_R). \qquad (6\text{-}18)$$

The change in optical path difference, δ, which will ultimately be used to compute the change in relative phase between the reference and object wave at the film plate is,

$$\begin{aligned}\delta &= \Delta - \Delta' \\ &= P_R P_F - P_R P_F' - (P_F P_m + P_m M_2 + M_2 M_1 + M_1 P_R) \\ &\qquad + (P_F' P_m' + P_m' M_2 + M_2 M_1 + M_1 P_R) \\ &= (P_R P_F - P_F P_m) - (P_R P_F' - P_F' P_m') + (P_m' M_2 - P_m M_2).\end{aligned} \qquad (6\text{-}19)$$

From figure 6-1, the following relationships can be written for the optical path (assuming a uniform index of refraction)

$$P_R P_F = [X^2 + Y_R^2 + Z_F^2]^{1/2} = X[1 + (Y_R^2 + Z_F^2)/X^2]^{1/2}$$

$$P_F P_m = [X^2 + Y_m^2 + (Z_m - Z_F)^2]^{1/2}$$

$$= X\left\{1 + [Y_m^2 + (Z_m - Z_F)^2]/X^2\right\}^{1/2}$$

$$P_R P_F' = [(X + x_F) + Y_R^2 + Z_F^2]^{1/2}$$

$$= (X + x_F)\left\{1 + [Y_R^2 + Z_F^2]/(X + x_F)^2\right\}^{1/2}$$

$$P_F' P_m' = [(X + x_F - x_o)^2 + Y_m^2 + (Z_m - Z_F)^2]^{1/2}$$

$$= (X + x_F - x_o)\left\{1 + [Y_m^2 + (Z_m - Z_F)^2]/(X + x_F - x_o)^2\right\}^{1/2}$$

$$P_m M_2 = [D^2 + Y_D^2 + Z_m^2]^{1/2} = D\,[1 + (Y_D^2 + Z_m^2)/D^2]^{1/2}$$

$$P_m' M_2 = [(D - x_o)^2 + Y_D^2 + Z_m^2]^{1/2}$$

$$= (D - x_o)\,[1 + (Y_D^2 + Z_m^2)/(D - x_o)^2]^{1/2} \qquad (6\text{-}20)$$

For this presentation, we will assume that paraxial conditions exist, i.e.,

$$Y_R/X << 1$$

$$Y_m/X << 1$$

$$Y_D/X << 1$$

$$Z_m/X << 1$$

$$Z_F/X << 1$$

$$(Z_m - Z_F)X << 1$$

$$Z_m/D << 1 \qquad (6\text{-}21)$$

This implies that

$$Y_R^2/X^2 << 1$$

$$Y_m^2/X^2 << 1$$

$$Y_D^2/X^2 << 1$$

$$Z_m^2/X^2 << 1$$

$$Z_F^2/X^2 << 1$$

$$(Z_m - Z_F)^2/X^2 << 1$$

$$Z_m^2/D^2 << 1 \qquad (6\text{-}22)$$

resulting in equations 6-20 becoming

$$P_R\,P_F \approx X[1 + (Y_R^2 + Z_F^2)/2X^2]$$

$$P_F\,P_m \approx X\left\{1 + [Y_m^2 + (Z_m - Z_F)^2]/2X^2\right\}$$

$$P_R\,P_F' \approx (X + x_F)\left\{1 + [Y_R^2 + Z_F^2]/2(X + x_F)^2\right\}$$

$$P_F'\,P_m' \approx (X + x_F - x_o)\left\{1 + [Y_m^2 + (Z_m - Z_F)^2]/2(X + x_F - x_o)^2\right\}$$

$$P_m\,M_2 \approx D[1 + (Y_D^2 + Z_m^2)/2D^2]$$

$$P_m'\,M_2 \approx (D - x_o)[1 + (Y_D^2 + Z_m^2)/2(D - x_o)^2]. \qquad (6\text{-}23)$$

Consider now the quantity $P_RP_F - P_FP_m$,

$$P_R\,P_F - P_F\,P_m = X\left\{1 + (Y_R^2 + Z_F^2)/2X^2\right\} - X\left\{1 + [Y_m^2 + (Z_m - Z_F)^2]/2X^2\right\}$$

$$= \frac{Y_R^2 - Y_m^2 + Z_F^2 - (Z_m - Z_F)^2}{2X} \qquad (6\text{-}24)$$

and the quantity $P_R P_F' - P_F' P_m'$ becomes

$$P_R P_F' - P_F' P_m' = (X + x_F)\left\{1 + [Y_R^2 + Z_F^2]/2(X + x_F)^2\right\} - (X + x_F - x_o)\left\{1 + [Y_m^2 + (Z_m - Z_F)^2]/ 2(X + x_F - x_o)^2\right\}$$

$$= x_o + \frac{Y_R^2 + Z_F^2}{2(X + x_F)} - \frac{Y_m^2 + (Z_m - Z_F)^2}{2(X + x_F)[1 - x_o/(X + x_F)]} \quad . \qquad (6\text{-}25)$$

Realizing that $x_o/(X + x_F)$ is very small compared to unity gives

$$P_R P_F' - P_F' P_m' = \frac{Y_R^2 + Z_F^2}{2(X + x_F)} + x_o - \frac{Y_m^2 + (Z_m - Z_F)^2}{2(X + x_F)}\left\{1 + \frac{x_o}{(X + x_F)}\right\}$$

$$= \frac{Y_R^2 - Y_m^2 + Z_F^2 - (Z_m - Z_F)^2}{2(X + x_F)} + x_o\left\{1 - \frac{Y_m^2 + (Z_m - Z_F)^2}{2(X + x_F)^2}\right\}. \qquad (6\text{-}26)$$

Continuing, the quantity $P_m' M_2 - P_m M_2$ is

$$P_m' M_2 - P_m M_2 = (D - x_o) \left\{ 1 + \frac{Y_D^2 + Z_m^2}{2(D - x_o)^2} \right\}$$

$$- D \left\{ 1 + \frac{Y_D^2 + Z_m^2}{2D^2} \right\}$$

$$= - x_o + \frac{Y_D^2 + Z_m^2}{2(D - x_o)} - \frac{Y_D^2 + Z_m^2}{2D}$$

$$\approx - x_o \left\{ 1 - \frac{Y_D^2 + Z_m^2}{2D^2} \right\}. \qquad (6\text{-}27)$$

Referring to figure 6-2, observe that $Y_m/(X + x_F)$ is equal to $\tan \beta'$ which for β small (implying $Y_m/(X + x_F)$ is small) gives

$$Y_m/(X + x_F) = \tan \beta' = \beta' \qquad (6\text{-}28)$$

where β' (see fig. 6-2) is the angle in radians (less than six degrees to be a good approximation). Incorporation of equation 6-28 into 6-26 yields

$$P_R P_F' - P_F' P_m' = \frac{Y_R^2 - Y_m^2 + Z_F^2 - (Z_m - Z_F)^2}{2(X + x_F)}$$

$$+ x_o \left[1 - \beta'^2/2! \right]$$

$$- x_o \frac{(Z_m - Z_F)^2}{2(X + x_F)^2} \qquad (6\text{-}29)$$

Following the same line of reasoning we have that Y_D/D is small giving

$$Y_D/D = \tan \alpha \approx \alpha \tag{6-30}$$

(see fig. 6-2) and,

$$P_m' M_2 - P_m M_2 = - x_o \left[1 - \frac{Y_D^2}{2D^2}\right] - x_o \frac{Z_m^2}{2D^2} . \tag{6-31}$$

But the cosine function can be approximated by

$$\cos x \approx 1 - x^2/2! \tag{6-32}$$

with a peak error of 5×10^{-6} assuming small angles (see also Chapter V, equations 5-17 through 5-20). Then incorporation of equation 6-28 into equation 6-31 and 6-29 gives

$$P_R P_F' - P_F' P_m' = \frac{Y_R^2 - Y_m^2 + Z_F^2 - (Z_m - Z_F)^2}{2(X + x_F)}$$

$$+ x_o \cos \beta' - x_o \frac{(Z_m - Z_F)^2}{2(X + x_F)^2} \tag{6-33}$$

and

$$P_m' M_2 - P_m M_2 = - x_o \cos \alpha - \frac{x_o Z_m^2}{2D^2} . \tag{6-34}$$

Now, the complete change in optical path is,

$$\delta = (P_R P - P P_m) - (P_R P_F' - P_F' P_m') + (P_m' M_2 - P_m M_2)$$

$$= \frac{Y_R^2 - Y_m^2 + Z_F^2 - (Z_m - Z_F)^2}{2X}$$

$$- \left\{ \frac{Y_R^2 - Y_m^2 + Z_F^2 - (Z_m - Z_F)^2}{2(X + x_F)} + x_o \cos \beta \right.$$

$$\left. - \frac{x_o (Z_m - Z_F)^2}{2(X + x_F)^2} \right\}$$

$$+ \left\{ - x_o \cos \alpha - \frac{x_o Z_m^2}{2D^2} \right\}$$

$$= \frac{Y_R^2 - Y_m^2 + Z_F^2 - (Z_m - Z_F)^2}{2X} \left\{ \frac{x_F}{X + x_F} \right\}$$

$$- x_o (\cos \beta' + \cos \alpha)$$

$$- x_o \left\{ \frac{Z_m^2}{2D^2} + \frac{(Z_m - Z_F)^2}{(X + x_F)^2} \right\}$$

Then, the complex degree of coherence for the case of simultaneous motion with object and film points not in the plane containing the reference source is

$$G_{mR}(0) = \frac{1}{T}\int_0^T e^{j\frac{2\pi}{\lambda}\phi}\,dt$$

$$= \frac{1}{T}\int_0^T e^{j\frac{2\pi}{\lambda}[\hat{x}_o(t) + \hat{x}_F(t)]}\,dt \qquad (6\text{-}35)$$

where

$$\hat{x}_o(t) = -x_o(t)(\cos\beta' + \cos\alpha)$$

$$- x_o(t)[Z_m^2/2D^2 + (Z_m - Z_F)^2/(X + x_F)^2]$$

$$x_F(t) = \frac{Y_R^2 - Y_m^2 + Z_F^2 - (Z_m - Z_F)^2}{2X^2}\left\{x_F(t)\left[1 - \frac{x_F(t)}{X}\right]\right\}$$

Observe that for the motion considered, the quantity

$$\frac{Y_R^2 - Y_m^2 + Z_F^2 - (Z_m - Z_F)^2}{2X^2}$$

is a constant for a particular film and object point. Then

$$K = \frac{Y_R^2 - Y_m^2 + Z_F^2 - Z_m^2 + 2Z_mZ_F - Z_F^2}{2X^2}$$

$$= \frac{Y_R^2 - Y_m^2 - Z_m^2 + 2Z_mZ_F}{2X^2}$$

is identical to the constant K found in the previous section (equation 6-13). This implies that for a constant film displacement, the reconstructed holographic image will contain contours of constant brightness centered in front of the film point P_F used to reconstruct the hologram image. This then indicates a result equivalent to the case of film motion alone.

CHAPTER VII

EXPERIMENTAL RESULTS

7.1 A Description of the Equipment Utilized for the Experimentation

An experimental verification of the theory presented in chapters III and IV will now be presented. The geometry employed for the experimentation is shown in figure 7-1. The object for the holograms was constructed of a 4.72 inch square piece of cardboard. The cardboard was marked in a manner to indicate reference points useful for the measurement of distance on the object when viewing the reconstructed holographic image (see chapter III, figure 3-4c).

The film was mounted in a standard photographic glass plate holder which was secured to a section of I beam to increase the positional stability of the film on the holographic table.

The location of the film was 39.25 inches from the object. The film and the object were positioned parallel to each other to an accuracy of about 0.125 inches. The horizontal centerline of the film was placed at the same height above the holographic table as the horizontal centerline of the object.

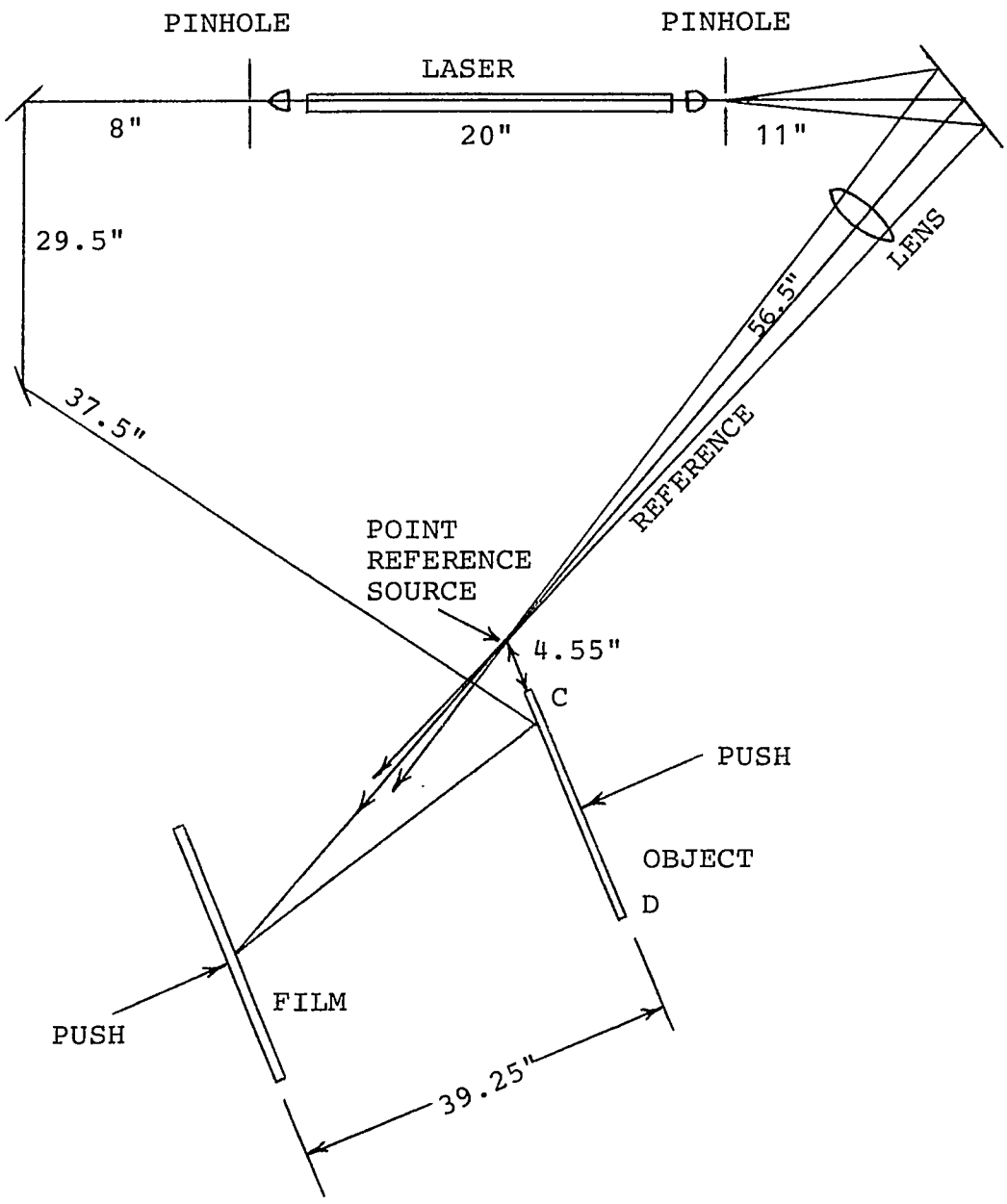

Figure 7-1

The experiment geometry for the holograms discussed in Chapter VII

The reference beam was obtained from the light output at the "back" end of the laser. A lens was used to focus the light to a point in the object plane, thus forming the point source reference required. The direction of the reference beam was adjusted with particular care by the first surface mirror so that a uniform distribution of illumination was obtained over the entire film. The position of the point source in the object plane was 4.55 inches from the edge of the object.

Figure 7-1 also indicates the usual other basic equipment needed to take good quality holograms. At each end of the laser is the usual lens-pinhole combination which forms a spatial filter. The mirrors indicated are first surface mirrors and are used to direct the beams of light for the reference source and to illuminate the object.

For this experimentation, it was required that both the object and film be displaced during the exposure of the hologram. The push referred to in figure 7-1 was accomplished by using a micrometer fastened to a second I beam. The I beam and consequently the micrometer were positioned behind either the film holder or the object to produce the displacement. The point of contact between the micrometer and either the object or film was located

along the vertical axis of the object or film. To maintain a positive contact between the micrometer and the displaced surface, elastic bands were used. The elastic bands were installed so as to encircle the micrometer head and the displaced surface, but not be visible in the reconstructed image of the hologram. The action of the elastic bands was to reduce backlash and ensure repeatability in the displacement values from experiment to experiment.

Lastly, the maximum angles formed by the object and reference beams were checked to ensure that the small angle assumption associated with the paraxial condition was met. Referring to figure 7-1, the angle, at the film, between the reference beam and light coming from one edge of the object (point C) is 6.61 degrees; for the outer edge of the object (point D) the angle is 13.26 degrees. Although 13 degrees is somewhat larger than strictly required by the small angle approximation, the error introduced is only 1.8 percent in the approximations involving the small angle assumptions.

7.2 The Computation of Fringe Spacing for Object Motion

Figure 7-2 indicates the technique of displacement used for the experimentation. The object rotates through an angle θ due to the displacement from the micrometer.

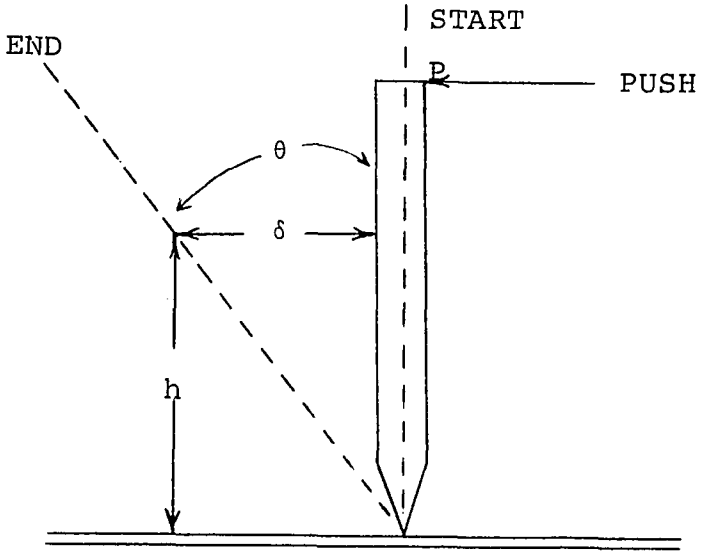

Figure 7-2

Manner of motion for the experimentation

For a typical point of the object a height h above the fulcrum, the linear displacement of the point, δ, is to a first approximation, for θ small,

$$\delta = h\ \theta, \tag{7-1}$$

for θ in radians. Equation 7-1 indicates that a displacement of magnitude D at point P of figure 7-2 results in a wide range of displacements across the object with magnitudes varying from zero to D. The magnitude of the object displacement for a given point then depends on the distance from the fulcrum to the point under consideration.

For a step law of motion of the object during the exposure of the hologram, the modified complex degree of coherence was found to be (see chapter III),

$$|G_{mR}(o)|^2 = \frac{1}{2}\ (1 + \cos \frac{4\pi}{\lambda}\ \delta) \tag{7-2}$$

where, for each object point, δ is the magnitude of the step displacement given by 7-1. The radiance of each point of the reconstructed image will be shaded by $|G_{mR}(o)|^2$. When the displacement is applied in the manner just described, the reconstructed holographic image for the step law of motion will exhibit a fringe pattern across the object. The location of the fringes will correspond to the zeros of equation 7-2. Hence, the fringes will occur when

$$\frac{4\pi}{\lambda}\,\delta = n\pi$$

$$\delta = n\lambda/4 \qquad (7\text{-}3)$$

for n an odd integer.

The difference in distance between two points on two different extinction fringes, $\Delta\delta$, is

$$\Delta\delta = \delta_a - \delta_b$$

$$= (n_a - n_b)\lambda/4 \qquad (7\text{-}4)$$

where the n's are odd integers. For adjacent fringes, $n_a - n_b = 2$ and

$$\Delta\delta = \lambda/2. \qquad (7\text{-}5)$$

From figure 7-2 and equation 7-1 we determine then,

$$\Delta\delta = \Delta h\theta \qquad (7\text{-}6)$$

where Δh is the linear distance between fringes as measured on the object. Consequently, we can determine the angle of rotation by

$$\theta = \Delta\delta/\Delta h$$

$$= \lambda/2\Delta h \qquad (7\text{-}7)$$

which relates the angular rotation of the object to the distance between any two adjacent fringes as measured on the reconstructed holographic image of the object.

7.3 Object Motion

The effect of object motion on holography was discussed in chapter III and again in the previous section. A conventional photograph of the reconstructed virtual image of a hologram taken with step object motion is presented in figure 7-3.

For the experiment conducted, a step displacement of 2×10^{-4} inches was applied to the object at a height of 4.55 inches from the objects axis of rotation. This displacement, which corresponds to an object angle of rotation equal to 4.4×10^{-5} radians, was applied at the beginning of the second half of the hologram exposure time. During the first half, no displacement was applied to the object.

For an angle of rotation equal to 44 microradians, the computed fringe spacing is 0.283 inches using equation 7-5 and a light wavelength of 24.91×10^{-6} inches. Measurement of the fringe spacing from the reconstructed holographic image indicates an average value of 0.276 inches. The measurements from the hologram were taken on the vertical centerline of the hologram where the

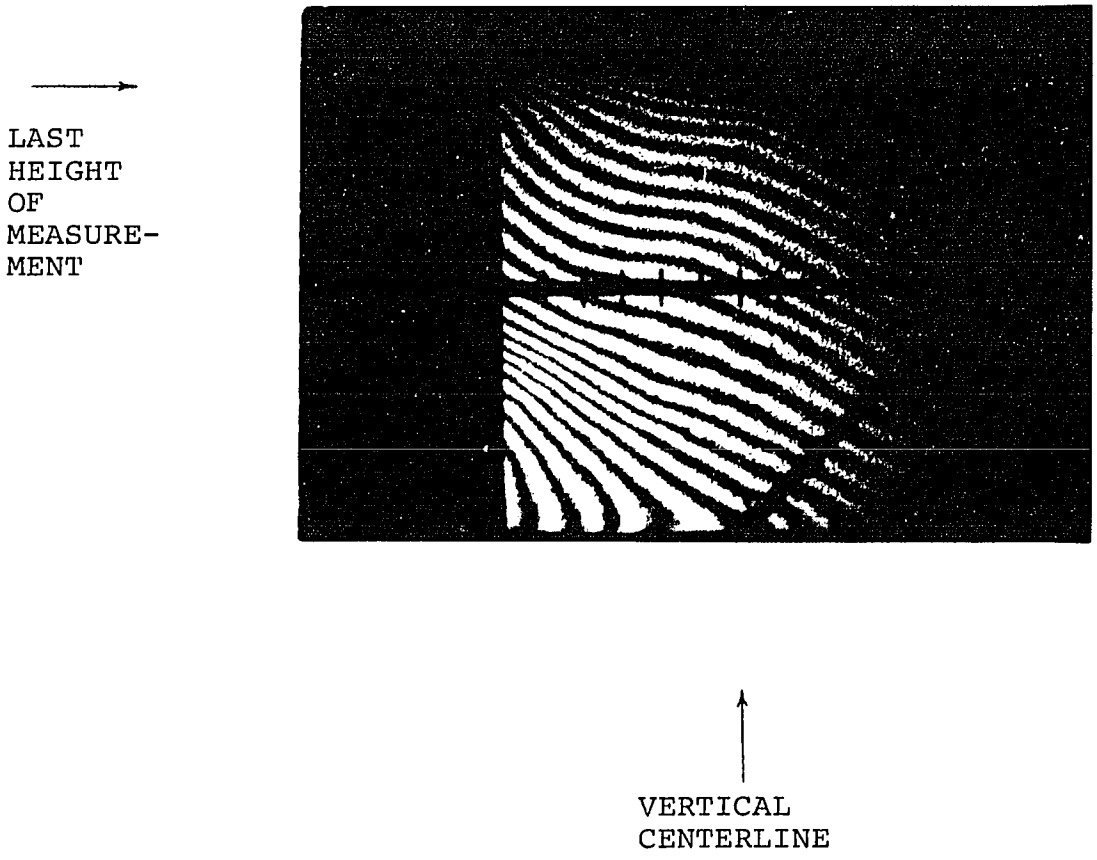

Figure 7-3

Photograph of the reconstructed holographic image of an object with step motion

TABLE 7-I

Fringe Position (predicted)	Fringe Position (measured)
0 (reference)	0 (reference)
0.283	0.286
0.566	0.565
0.844	0.876
1.132	1.145
1.415	1.410
1.698	1.675
1.981	1.961
2.274	2.247
2.554	2.533
2.840	2.809
3.123	3.073
3.406	3.327
3.689	3.608

Average Measured Spacing	0.276
Standard Deviation	0.015
Predicted Fringe Spacing	0.283

micrometer displacement occurred. The intersection of the first fringe and the bottom of the hologram was taken as the measurement reference.

Mention has already been made of the hologram's sensitivity to small distortions and displacements. This fact is evident in the experimental result presented. Notice that not every point at a given height of the object experienced the same magnitude of displacement during the hologram exposure. All points did follow the same law of motion. The deviation of the shape of the fringes from the expected straight parallel lines is due to the distortion of the object during the motion.

This distortion is most probably due to the elastic bands exerting the restraining force necessary to eliminate backlash between the film holder and the micrometer head. To reduce experimental error, care was taken to use data from the center section of the object where the actual displacement force was applied. Also, the data was restricted as indicated in figure 7-3 to only part of the vertical centerline. The last point of measurement is indicated. The motion above this indicated point also exhibits a good deal of object distortion along this vertical line in the vicinity of the actual mechanical push of

the object. This push occurred below the region constrained by the elastic bands causing a barrel type of distortion in the object motion.

7.4 The Computation of Fringe Spacing for Film Motion

Figure 7-2 again indicates the technique employed to displace the film for this experiment. The film is caused to rotate through an angle θ due to the displacement of the micrometer. For a given height h above the axis of rotation, the linear displacement of the film point, δ, is, to a first approximation, for θ small,

$$\delta = h\ \theta. \tag{7-8}$$

Equation 7-8 again indicates that a displacement of magnitude D at point P of figure 7-2 results in a wide range of displacement across the object with the magnitudes varying from zero to D. The magnitude of the film displacement for a given point on the film then depends on the distance from the axis of rotation to the point under consideration.

For a step law of motion of the film during the exposure of the hologram, the absolute value square of the modified complex degree of coherence is found to be (see chapters III equation 3-18 and VI equation 6-12 in which $Y_F = 0$)

$$|G_{mR}(o)|^2 = \frac{1}{2}\{1 + \cos\frac{2\pi}{\lambda} kD'\}$$

$$D' = \delta(1 - \delta/X)$$

$$k = [(Y_R - Y_F)^2 - (Y_m - Y_F)^2 + Z_m(2Z_F - Z_m)]/2X^2$$

(7-9)

where for each film point, δ is the magnitude of the step displacement given by equation 7-1, Y_F is the y position of that film point and Z_F is the z position of the film point in the film plane. Y_R and Y_m are the distances from the reference source and the object point to the system axis, and X is the distance from the film to the object.

The reconstructed holographic image will exhibit a fringe pattern across the object with the location of the fringes in accordance with the zeros of equation 7-9. Hence, the fringes will occur when

$$\frac{2\pi}{\lambda} kD' = n\pi \qquad (7\text{-}10)$$

for n an odd integer. This implies that the fringe location is found from,

$$Z_m^2 - 2Z_mZ_F + (Y_R - Y_F)^2 - (Y_m - Y_F)^2 - n\lambda X/D = 0$$

or

$$Z_m = Z_F \left\{ 1 \pm \sqrt{1 + \frac{1}{Z_F^2} (Y_R - Y_F)^2 - \frac{1}{Z_F^2} (Y_m - Y_F)^2 - \frac{n\lambda X}{D' Z_F^2}} \right.$$

(7-11)

Then for a given point on the film (defining Y_F, Z_F, D') the fringe location on the object can be determined as a function of Y_R and Y_m.

7.5 Film Motion

A conventional photograph of the reconstructed virtual image of a hologram taken with step object motion is presented in figure 7-4.

For the experiment conducted, the displacement of the film holder was 1.0×10^{-2} inches applied during the second half of the hologram exposure. The point of application of the displacement was the top of the film holder located 9.625 inches from the point of film rotation. The point on the film under consideration has $Z_F = -2.0$ inches and $Y_F = 2.0$ inches. This point is actually the center of a circular region of the hologram that was used to reconstruct the object image. The circular region was that corresponding to the size of the input lens aperture of the camera (about 1/2 inch in diameter) used to photograph the reconstructed image. This corresponds to a displacement

of the film equal to 7 x 10^{-3} inches. With Y_R = -4.55 inches, the location of the fringes is computed for 3 values of Y_m = ,

a) Y_m = o (right edge of the object)

$$Z_m = -2 \{ 1 \pm \sqrt{1.63 + 1.37n} \} \quad (7\text{-}12)$$

b) Y_m = 4.72 (left side of the object)

$$Z_m = -2 \{ 1 \pm \sqrt{0.78 + 1.37n} \} \quad (7\text{-}13)$$

and

c) Y_m = 2.0 (near center of the object)

$$Z_m = -2 \{ 1 \pm \sqrt{2.63 + 1.37n} \} . \quad (7\text{-}14)$$

Table 7-II contains the predicted and the measured fringe positions referenced to the bottom edge of the object.

7.6 Simultaneous Film and Object Step Motion

A modification of the procedure described for film and object motion alone was employed for the experimentation with simultaneous film and object motion. Now, a piece of optical glass was interposed in the path between the object and the film, in very close proximity to the

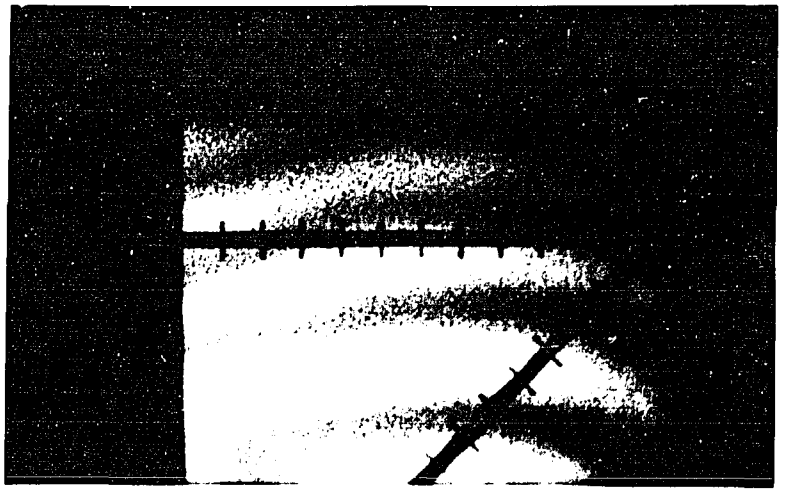

Figure 7-4

Photograph of the reconstructed image of a hologram with step film motion

TABLE 7-II

Fringe Position (predicted)	Fringe Position (measured)	
$Y_m = 0$		
.15	.15	
1.46	1.37	
2.51	2.32	Peak Error = 7.7%
3.39	3.13	
4.16	3.86	
$Y_m = 4.72$		
-.38	0 (off the object)	
1.726	1.71	
2.826	2.99	Peak Error = 5.8%
3.746	3.95	
4.546	4.78	
$Y_m = 2.0$		
.694	.694	
1.886	1.794	
2.854	2.764	Peak Error = 7.7%
3.684	3.584	
4.434	4.274	

film. The glass was introduced to simulate a film step motion. This technique was employed in lieu of using a micrometer to displace the film. The glass introduces a large equivalent film motion* without the associated mechanical problems of bending and twisting of the film holder.

More importantly, the use of optical glass to produce the film motion enabled the simultaneous recording of two holograms at the same time. Since the physical size of the glass and the glass holder chosen for the experimentation was such as to cover only the lower half of the film, two separate holograms could be recorded simultaneously. For the section of the film not covered by the glass, the recorded hologram would not experience film motion. The section of the film that is covered by the glass will essentially experience a film motion due to the interposing of a change in refractive index during the exposure time.

Achieving the desired laws of motion for the experiments concerning simultaneous motion required the placement and removal of the glass during the hologram exposure. This will, of course, have the risk of introducing

*a discussion of the relationship between a change in refractive index (the interposing of the optical glass) and film motion can be found in chapter IV.

extraneous table motions into the experiment if great care is not exercised. To reduce the possibility of table distortions and vibrations occurring during the exposure time, the interval between the action, i.e., the placement or removal of glass, and the exposure was sufficiently long to ensure that no deleterious effects would occur. Typically, for the holograms concerning simultaneous motion, this time span was three-quarters of an hour.

The calculation of the modified complex degree of coherence for simultaneous object and film step motion was considered in chapter V. The absolute value square of the modified complex degree of coherence was found to be

$$|G_{mR}(o)|^2 = \frac{1}{2}\left[1 + \cos\frac{2\pi}{\lambda}(D_o + D_F)\right] \qquad (7\text{-}15)$$

where D_o is the magnitude of the object step displacement and D_F is the equivalent film motion step displacement. Then, for a film displacement of δ, the equivalent film motion D_F is given by

$$D_F = k\,\delta(1 - \delta/X)$$

$$k = [(Y_R - Y_F)^2 - (Y_m - Y_F)^2 + Z_m(2Z_F - Z_m)]/2X^2$$

For the conditions of motion considered (both object and film motion in the direction of the x axis) this quantity is a constant. If the film step motion is very much larger than the object step motion, equation 7-15 becomes

$$|G_{mR}(o)|^2 = \frac{1}{2}\left[1 + \cos\frac{2\pi}{\lambda} D_F(1 + D_o/D_F)\right]$$

$$\frac{1}{2}\left[1 + \cos\frac{2\pi}{\lambda} D_F\right] \qquad (7\text{-}16)$$

for $D_o/D_F << 1$.

The implication of equation 7-16 is that the hologram with the larger film motion will show no sign of the smaller object motion.

Experimentally, the optical glass introduces a very large film motion. The piece of glass used was 0.254 inches thick. This corresponds to an optical path of 5400 wavelengths. The fringe pattern that results from a motion this large is spaced so closely as to not be discernible. Then, the resulting holographic image will tend to appear darker overall, but have no apparent fringe pattern.

Figure 7-5 is a photograph of the reconstructed image of such a hologram. The recording procedure was to expose the film with no motion introduced for one half of the normal exposure. For the second half of the exposure, the

object was displaced by using the micrometer and the glass was placed in front of the lower half of the film. This results in the two simultaneous recordings previously discussed. One hologram, the upper section of the film, will be a record of step object motion. The other hologram, the lower section of the film, will be a record of the simultaneous object and film motion.

In figure 7-5, the results are quite evident. The upper hologram, which is of the object motion, shows the characteristic regular fringe pattern. The lower hologram, which is of the simultaneous motion, has no discernible fringe pattern. Notice, however, that the "crosshair" markings are still quite clearly visible indicating that the hologram has not been obliterated.

As a check on the use of the zero order approximation employed, a second hologram was taken. Here, two simultaneous object motions (no film motion) were recorded to show the effect of having a large and small motion simultaneously occurring. The smaller motion was introduced with a micrometer and the larger motion was introduced using the optical glass. The recording procedure was to expose the film for half the exposure time and then introduce the two motions for the second half of the exposure interval.

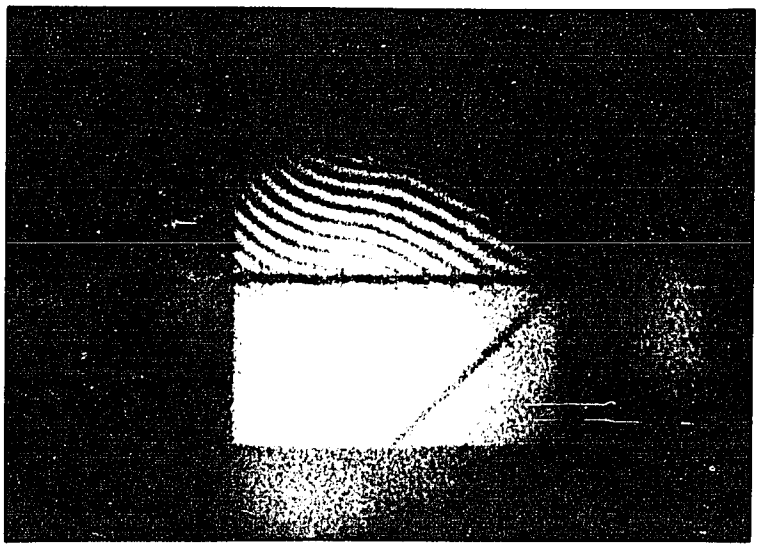

Figure 7-5

Photograph of the reconstructed image of simultaneous holograms for object and object plus film step motion

Figure 7-6 contains a photograph of the reconstructed holographic image of an object taken with simultaneous large and small step object motion. Figure 7-6A contains a sketch indicating the regions of interest. There are three regions that clearly show the effects of the different motions. Notice that the outline of the glass holder is very clear. The region above the glass (the glass holder shadow indicates the boundary) has the characteristic fringe pattern associated with the step motion applied to the object. Notice also that a small region in the lower left of the object, just below the glass, is also visible with the fringe pattern. This is a region of open space between the glass and the glass holder giving a view of the object with just one object motion alone during the hologram recording. The region of the object covered by the glass has no discernible fringe pattern because the fringe spacing is so close together as to be unresolvable by the observer. Notice here that the "crosshairs" of the object are clearly visible. The third region is essentially that part of the object which is in the shadow of the glass holder. This region of the object, as far as the hologram is concerned, was exposed to the film for only half the exposure time and hence shows no motion effects. Notice, however, that the crosshairs are visible, just very much darker than in the rest of the hologram.

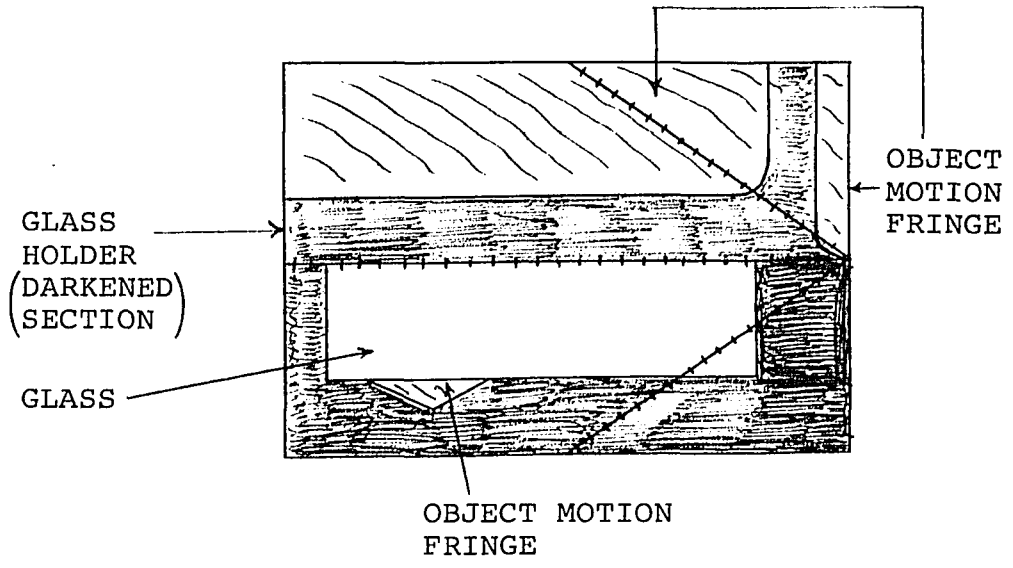

Figure 7-6A - Sketch indicating regions of interest of the photograph in figure 7-6

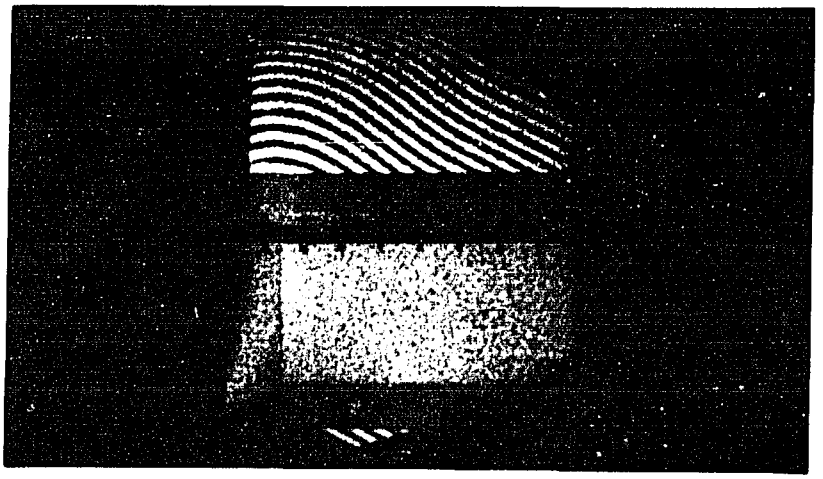

Figure 7-6

Photograph of the reconstructed image of a hologram with simultaneous large and small object motion

7.7 Simultaneous Film and Object Staircase Motion

The technique for recording this hologram was identical to that for the simultaneous step motion hologram. Here, there was no object motion for the first one third of the exposure time, followed by a displacement of 0.25×10^{-3} inches for the second third, and an additional 0.25×10^{-3} inch displacement for the last third of the exposure. The film motion was again simulated using optical glass. For the first third of the exposure no glass was placed in front of the film, followed by a single piece of glass for the second third and two pieces of glass for the final third of the exposure.

The absolute value square of the modified complex degree of coherence for this simultaneous staircase motion is found to be (see chapter V equation 5-38)

$$|G_{mR}(o)|^2 = \frac{1}{9}\left[1 + 2\cos\frac{2\pi}{\lambda}(D_o + D_F)\right]^2 \qquad (7\text{-}17)$$

where D_F is the equivalent perturbation of the film (see definition of D_F in section 7.6) due to the interposing of the optical glass and D_o is the magnitude of the displacement applied to the object. For $D_F >> D_o$ we have that

$$|G_{mR}(o)|^2 = \frac{1}{9}\left[1 + 2\cos\frac{2\pi}{\lambda} D_F(1 + D_o/D_F)\right]^2$$

$$\frac{1}{9}\left[1 + 2\cos\frac{2\pi}{\lambda} D_F\right]^2 \qquad (7\text{-}18)$$

which implies that the effect of the small object motion will again not be observable in the reconstructed holographic image.

Figure 7-7 is a photograph of the reconstructed holographic image of two simultaneous holograms. The upper reconstruction is of the object motion alone. The lower image is of the simultaneous object and film motion. Notice that for the simultaneous motion there is no observable fringe pattern and the crosshairs are clearly visible.

7.8 Simultaneous Step Film and Staircase Object Motion

The recording of this hologram was similar to the others described concerning simultaneous object and film motion effects. The film law of motion was a step function with no glass interposed between the film and object during the first half of the exposure, and a single piece of glass interposed during the second half of the exposure. The object law of motion was a staircase function which consisted of no motion for the first quarter of the exposure, followed by three equal increases of 0.17×10^{-3} inches in each of the following three quarters of the exposure time.

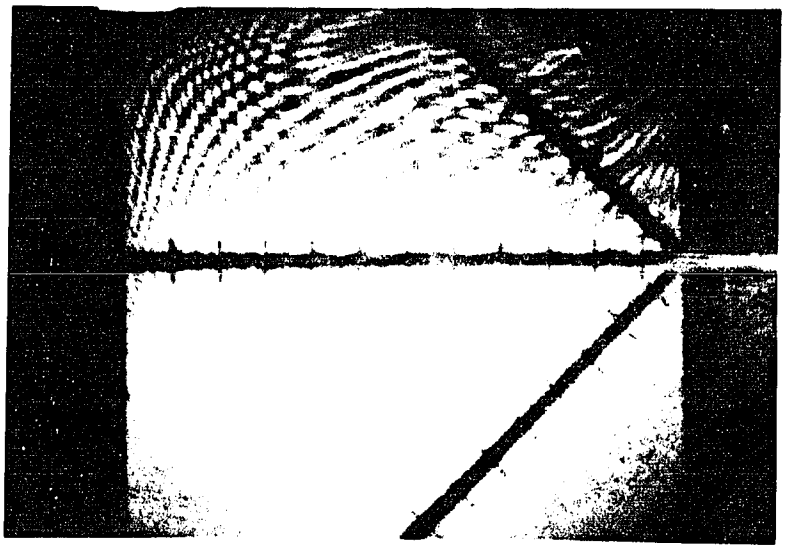

Figure 7-7

Photograph of the reconstructed image of holograms of staircase object and simultaneous staircase object and film motion

For this simultaneous motion, the absolute value square of the modified complex degree of coherence was found to be (see chapter V equation 5-41)

$$|G_{mR}(o)|^2 = \frac{1}{8}\left(1 + \cos\frac{2\pi}{\lambda} D_o\right)\left\{1 + \cos\frac{2\pi}{\lambda}(D_F + 2D_o)\right\}. \tag{7-19}$$

where D_o is the object motion magnitude and D_F is the equivalent film motion magnitude.

For the case of object motion much smaller than the film motion, we have that

$$|G_{mR}(o)|^2 = \frac{1}{8}\left(1 + \cos\frac{2\pi}{\lambda} D_o\right)\left(1 + \cos\frac{2\pi}{\lambda} D_F\right). \tag{7-20}$$

When D_F is very large, the effect on the reconstructed image for the simultaneous motions is to observe a fringe distribution due to the object motion only. Fringes attributable to the film motion would again be unobservable due to the large equivalent motion introduced by the optical glass. Then for the simultaneous motion, the fringe pattern should appear as that for step motion with the fringe spacing satisfying

$$D = n\lambda/2 \text{ for } n \text{ odd}. \tag{7-21}$$

For just object motion alone, the absolute value square of the modified complex degree of coherence is

$$|G_{mR}(o)|^2 = \frac{1}{4}\left(1 + \cos\frac{2\pi}{\lambda} D_1\right)\left(1 + \cos\frac{2\pi}{\lambda} 2D_1\right) \qquad (7\text{-}22)$$

indicating that the fringe pattern will satisfy the two relationships, i.e.,

$$D_1 = n\lambda/2 \text{ and } D_1 = n\lambda/4 \text{ for } n \text{ odd.} \qquad (7\text{-}23)$$

This implies that the fringe distribution will be at $D_1 = \lambda/4$, $2\lambda/4$, $3\lambda/4$, $5\lambda/4$, $6\lambda/4$, $7\lambda/4$, $9\lambda/4$, $10\lambda/4$, $11\lambda/4$ etc. which is to say that the fringes will occur in groupings of three.

Figure 7-8 contains the conventional photograph of the reconstructed holographic image of the simultaneous type holograms that have been presented. The upper section of the object indicates the object motion alone while the lower section is of the simultaneous film and object motions. Notice that the object motion alone image appears as a very complex fringe pattern due to the distortions introduced by the elastic bands. The lower section represents the simultaneous film and object motion. Notice that the basic fringe shape is that of step motion. Again, the shape of the fringes indicates the distortion of the object during the recording of the hologram.

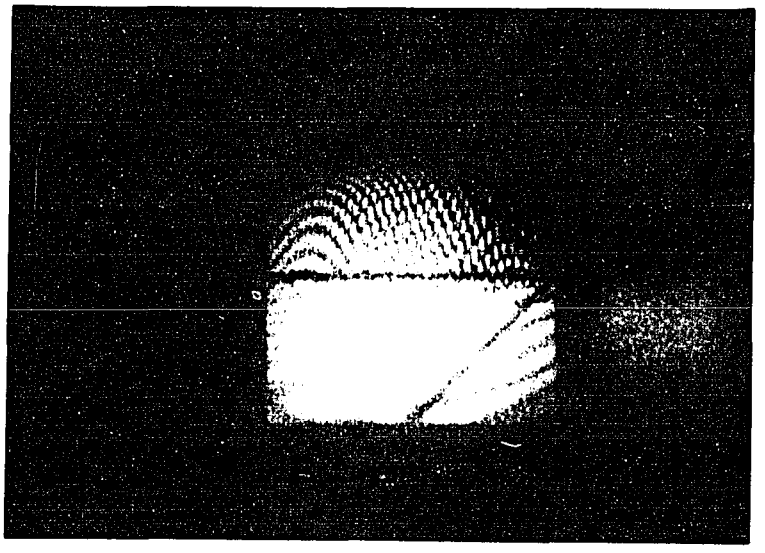

Figure 7-8

Conventional photograph of the reconstructed image of a hologram taken with simultaneous staircase object and step film motion

This experiment was repeated with a different object in an attempt to obtain better data. The results of the second experiment are shown in figure 7-9a and 7-9b. The object motion alone (figure 7-9b) is now clearly visible as groupings of three fringes as predicted. The simultaneous film and object motion (figure 7-9a) appears as if only step motion were presented, again as predicted. It is instructive to indicate that even with this improved object, a small distortion is evident in the object motion indicated by the lack of parallelism of the fringes across the object.

Table 7-III contains the measured and predicted values of fringe spacing for both the object motion alone and simultaneous object and film motion. It is readily seen that the agreement between measured and predicted fringe positions is quite good.

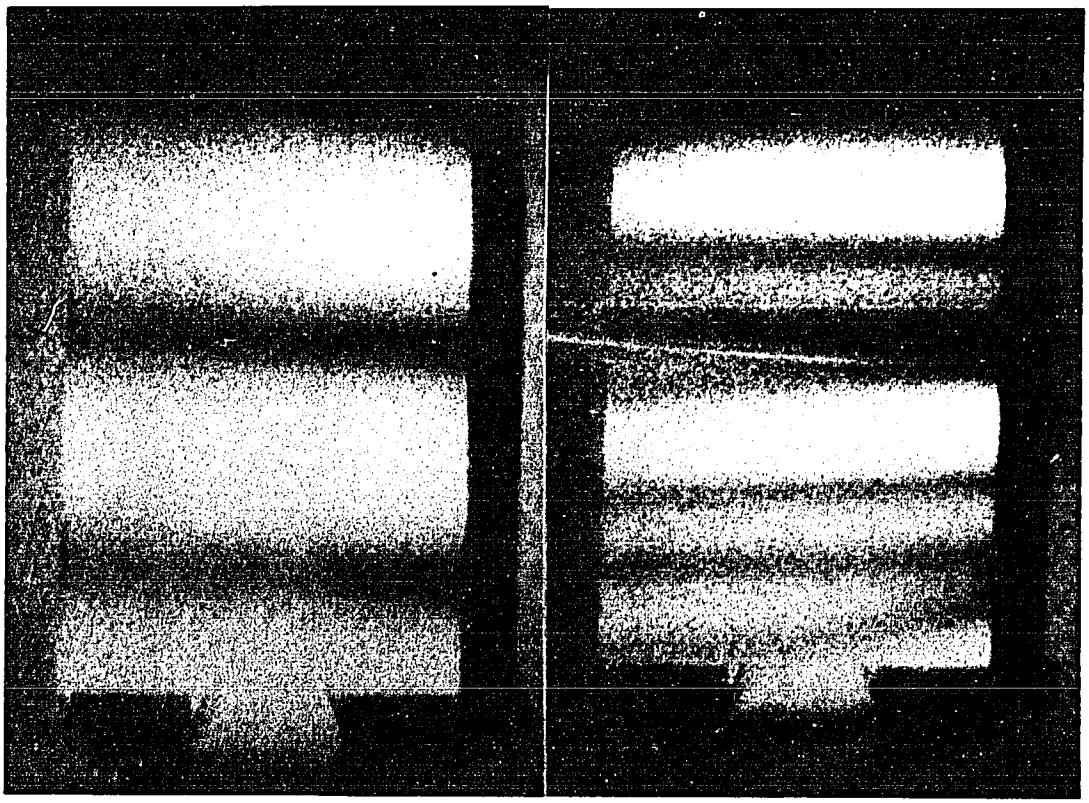

(a)

FILM AND OBJECT MOTION

(b)

OBJECT MOTION ALONE

Figure 7-9

Conventional photographs of the reconstructed image of a hologram taken with simultaneous staircase object and step film motion

TABLE 7-III

Simultaneous Film & Object Motion

Fringe Position (predicted) (cm)	Fringe Position (measured) (cm)
0 (bottom of object)	
3.5	3.5
7.0	7.0
10.5	10.5

Object Staircase Motion

0 (bottom of object)	0
1.0	1.0
2.0	2.2
3.0	3.2
5.0	5.2
6.0	6.0
7.0	7.0

CHAPTER VIII

CONCLUSIONS AND RECOMMENDATIONS

The effects of optical path perturbations during recording on the reconstructed image of a hologram has been discussed in this thesis. The situations considered were object motion alone, film motion alone, and simultaneous object and film motion occurring during the hologram recording.

Specifically, previously developed theory regarding the effects of object motion during the recording of a hologram with quasi-monochromatic illumination, on the characteristics (radiance distribution) of the holographic reconstructed image, was summarized (chapter III, section 3.1), and new experimental verification was presented (chapter VII, section 7.3).

The theory concerning object motion effects was extended to include the effects of film motion (chapter III, section 3.3 and chapter VI, section 6.1) and of simultaneus film and object motion during recording (chapter V and chapter VI, section 6.2). Experimental results (chapter VII) confirm the theory within experimental error for the cases of step film motion (section 7.5), simultaneous step film and object motion (section 7.6), simultaneous staircase

film and object motion (section 7.7) and simultaneous step film - staircase object motion (section 7.8).

The effects on a reconstructed holographic image of a change in refractive index of the medium separating the object and film during recording was discussed (chapter IV, section 4.1). Results show that the effects on the reconstructed image are identical in form to those computed for a mechanical film displacement occurring during the hologram recording.

These results, relating the effects of a change in refractive index of the medium to a film motion during hologram recording, indicate a promising and practical means of analysis of random variations of refractive index in an optical propagation medium by proper interpretation of the radiance distribution in the reconstructed image of an appropriately recorded hologram. In chapter IV, section 4.2 it is proved that the effects on the reconstructed image of a randomly varying refractive index in the medium between the object and film can be simulated by a random film plate motion during the hologram recording. The analysis leading to this conclusion requires that the random variations of the refractive index slab satisfy the usual assumptions invoked by researchers in the field of turbulence theory (gaussian statistics and local stationarity with respect to time and lateral position).

This new concept hints at a new means for the study of turbulence effects. It is shown correctly to predict some known conclusion reached by other researchers employing conventional methods of turbulence analysis. The analysis as presented confirms the trend of recent research in the field pointing out the importance of considering structure function techniques in describing the effects of atmospheric turbulence on the propagation of light.

The theory developed in this thesis concerning the effects of simultaneous film and object motion on the reconstructed holographic image implies improved possibilities of interpretation of fringe patterns in holographic interferometry for non-destructive testing. As indicated (chapter V), by taking a series of holograms this theory can yield information about complex object motions more easily and thoroughly than otherwise possible at the present state of the art. As an example, this new scheme for object motion identification should greatly simplify the process of determining the cause and origin of stresses and deformations in products undergoing non-destructive testing procedures.

Additionally, the techniques of simultaneous object and film motion have application to the possible reduction of the effects of small table motions or object motions during the recording of the hologram. It appears feasible that the use of a large (compared to the expected object

motion) step motion of the film during recording may reduce the effects of table instabilities and of object motions that are step like in nature during the hologram recording. This will of course occur at the expense of image radiance of the reconstructed image.

The experimentation presented concerning simultaneous film and object motion indicates that the possible reduction of small motion effects is a function of the correlation between the film and the object motion. This conclusion is supported by the analysis concerning an approximate solution for complex film and object motion (chapter V, section 5.6) effects and is an area which warrants further study in the future.

The calculations concerning random refractive index changes during the recording of a hologram indicates a means of simulating turbulence effects in the laboratory by carefully controlling film motion during the hologram recording. Precise simulation of turbulence effects through introduction of known distributions of film motion can now be achieved. This capability indicates that the absolute need of present day research for an atmospheric laboratory to investigate a great many research problems concerning the nature of atmospheric turbulence can be overcome. This appears to open research possibilities in this field to

many investigators by decreasing laboratory and equipment costs and by making computer controlled experimental conditions possible.

The use of a simulation test bed as indicated has other important applications. The capability to recreate the results of experimental work already reported on atmospheric turbulence effects can now be accomplished under controlled laboratory conditions. This has obvious advantage for the purpose of determining the distribution of the turbulence and precisely what values the structure function constants associated with that turbulence distribution take. This information is of utmost importance to the optical systems engineer who must design systems to account for and minimize the effects of turbulence.

Section 4.3 of chapter IV also indicates an alternative experimental approach to the problem of determining the constants associated with the structure function of atmospheric turbulence which is recommended for future work. The concepts underlying an experimental approach to utilize a hologram for the recording of data are discussed, as well as the expected difficulties of completing the experiment. Although the experiment does have certain practical difficulties, they do not appear to be insurmountable. The technique proposed does have advantages over the interferometric methods that have been employed in the past.

The holographic method can record the multitude of data required on a single exposure thus reducing the chance of experimental error in data recording while saving considerable time and effort. Data acquisition by interferometric techniques generally requires several hours of work to obtain a single set of measurements.

Several other avenues for further work presently appear to be promising. As regards the concept of fringe pattern identification for holographic non-destructive testing, a catalog of fringe positions for basic forms of simultaneous and non-simultaneous motions is needed. This catalog of responses to motions will greatly aid the engineer who is trying to modify his designs based on the data taken with this technique.

The study of refractive index changes of the medium separating the object and film planes during the hologram recording should be extended. The initial extension should be a relaxation of the restriction concerning the geometric regularity of the turbulent slab. This, in effect, would make the analysis more complex causing the consideration of a film motion which contains two basic components. One component would be the random displacement of the film parallel to the x axis, and the second component, due primarily to the relaxation of the geometric constraint,

would be a random translation of the film on a plane perpendicular to the x axis. If the complexities of the analysis can be overcome, a tool for analyzing the total effect of turbulence on holography will be forthcoming.

With the tools developed in chapter V, a theoretical study consisting of a single turbulent slab of finite thickness and its effect on the reconstructed holographic image with varying distance from the recording plane would be useful. Results here would yield quantitative information concerning reconstructed image radiance versus turbulence location and strength. A unified theory accounting for the already documented experimental results of Goodman et. al. concerning some experimental conditions (stationary turbulence limited to regions close to the film or close to the object) might then become available. This would lead to a better understanding of the observed phenomena and eventually may lead to a good means of encoding secret information.

Lastly, an optimum means of controlling film displacement to obtain film motions of specific parameters is needed. The experimentation concerning the simulation of turbulence distributions, fringe interpretations and the reduction of stray motion effects all require an efficient means of achieving rigorously controlled film motion.

APPENDIX I

THE PHOTOGRAPHIC PROCESS

A complete description of the holographic process must take into account the characteristics of the medium used to record the hologram. In most cases, this recording medium is a high resolution photographic film where the result of having light incident on the film is to modify the transparency of the processed film. The relationship between the transparency of the developed film and the light initially incident on the film is required in a description of the holographic process and forms the subject for this discussion.

The transparency, T, also called the transmittance, of the developed photographic plate after an exposure has taken place is defined as the ratio of the light intensity emerging from the film, I_e, to the light intensity incident on the film, I_i,[1]

$$T = I_e/I_i. \qquad (I\text{-}1)$$

Basically, the transparency of the developed film depends on many factors, some of the most important being the type of film emulsion, the amount of exposure given the film, the film temperature at the time of exposure and the

prevailing ambient temperature and developing chemical conditions during the development of the film.

Of particular interest in holography is the amplitude transmittance of the developed film plate, χ, defined as the ratio of the complex amplitude of the wave emerging from the film α_e, to the complex amplitude of the wave incident on the film, $\alpha_i{}^2$, then,

$$\chi = \alpha_e/\alpha_i \qquad \text{(I-2)}$$

Notice that the amplitude transmittance is a complex function of the new coordinate. The relationship between the transparency of the film as defined by equation I-1 and the amplitude transmittance of the film as defined by equation I-2 is given by,

$$T = \chi\chi^* \qquad \text{(I-3)}$$

where χ^* denotes the complex conjugate function of χ.

The exposure, E, is defined as the time integral, extended to the exposure interval, of the illumination, I, for light of normal incidence on the photographic film. If during the cause of the exposure, the light intensity remains constant, the exposure simplifies to the product of the incident light intensity and the time the photographic plate is exposed to this intensity.

The density of the processed film plate can be related to the transparency of the film plate. This relationship is given by[3]

$$D = \log_{10} T. \qquad \text{(I-4)}$$

In addition, an approximate relationship between the exposure and the density of the processed film is expressable as,[4]

$$D = D_o + \Gamma \log_{10} (E/E_o) \qquad \text{(I-5)}$$

where D is the density, E is the exposure, D_o and E_o are constants of the film and Γ is the slope of the linear section of the curve represented by equation I-5.

The curve that results from the plot of D versus $\log_{10}E$ is today referred to as the Hurter and Driffield curve (H & D curve) after the two men who first proposed the relationship. For most films, the H and D curve comprises a "TOE" or region of increasing slope with increasing exposure, followed by a section of nearly constant slope with increasing exposure, and then a "SHOULDER" region which is a section of decreasing slope with increasing exposure indicating that the density of the processed film is asymptomatically approaching a saturation value.

Now, by substituting equation I-4 into equation I-5 we find that the relationship between the transparency of the developed film plate and the exposure is,

$$T = T_o \ (E/E_o)^{-\Gamma} \tag{I-6}$$

Continuing, using equation I-3 and substituting into equation I-6 results in,

$$\chi\chi^* = \chi_o\chi_o^* \ (E/E_o)^{-\Gamma}. \tag{I-7}$$

Consequently, equation I-6 becomes,

$$|\chi|^2 = |\chi_o|^2 \ (E/E_o)^{-\Gamma}, \tag{I-8}$$

and equation I-7 becomes,

$$|\chi| = |\chi_o| \ (E/E_o)^{-\Gamma/2}. \tag{I-9}$$

Equation I-9 is an expression which relates the exposure of the film to the magnitude of the amplitude transmittance that results after proper processing of the exposed film plate. Then, in general, equation I-9 can be represented as

$$|\chi| = K \ E^{-\Gamma/2} \tag{I-10}$$

where K is a constant of proportionality.

Equation I-10 indicates that with proper exposure and processing of the film, the amplitude transmittance of the processed film and the exposure can be made to be linearly related. This is the desired condition for the holographic process. To achieve this, the gamma (Γ) of the processed film must be controlled to a value of minus two. This can be usually accomplished by careful development and exposure of the photographic plate.

REFERENCES

1. C.E. Mees and T.H. James, Theory of the Photographic Process, The MacMillan Company, 816 (1966)

2. M. Born and E. Wolf, Principles of Optics, third edition, Pergamon Press, N.Y., 455 (1965)

3. Kodak Plates and Films, Eastman Kodak Company, 3 (1973)

4. C.E. Mees and T.H. James, op. cit., 817

APPENDIX II

THE STRUCTURE FUNCTION

We shall denote a random process by X(t) where X(t) represents an ensemble of time functions, and, for a specific t_s, $X(t_s)$ is a random variable.

Associated with the random process X(t)is a distribution function, $F(x;t_s)$ for the random variable $X(t_s)$. This distribution function is defined as

$$F(x;t_s) = P\{X(t_s) \leq x\} \qquad \text{(II-1)}$$

where the statement of equation II-1 is that for a given x and t_s, the function $F(x;t_s)$ represents the probability of the event $X(t_s) \leq x$ occurring. The distribution defined in equation II-1 is a first order distribution for X(t).

Associated with the distribution function is a density function denoted as $f(x;t_s)$. The density function can be obtained from the distribution function by differentiation with respect to x. This will result in the following

$$f(x;t_s) = \partial F(x;t_s)/\partial x. \qquad \text{(II-2)}$$

To have a complete description of the random process X(t) generally requires that one must go beyond a first order distribution function for the process. Knowledge

of the complete multi-dimensional nth order probability distribution is required. This distribution function is defined as,

$$F(x_1, x_2, \ldots, x_n; t_1, t_2, \ldots, t_n) = P\{X(t_1) \leq x_1; \; X(t_2) \leq x_2; \; \ldots \; X(t_n) \leq x_n\} \tag{II-3}$$

Associated with the nth order distribution function is the nth order density function given by,

$$f(x_1, x_2, \ldots, x_n; t_1, t_2, \ldots, t_n) = \frac{\partial F(x_1, x_2, \ldots, x_n; t_1, t_2, \ldots, t_n)}{\partial x_1 x_2, \ldots \partial x_n} \tag{II-4}$$

Generally, the nth order distribution function, which is termed a statistic of the random process, is very difficult, if not entirely impossible to determine. Consequently, some simpler function of the process is considered which is practical to compute and represents some meaningful characteristic of the random process. Two such functions are the mean and the covariance of the process.

The mean value of the process X(t) is defined as the expected value of the random variable $X(t_s)$, i.e.,

$$\eta(t_s) = E\{X(t_s)\} = \int_{-\infty}^{\infty} xf(x;t_s)dx \qquad \text{(II-5)}$$

In general, the mean value, $\eta(t_s)$, will be a function of the time t_s chosen for evaluation.

The covariance of the process X(t) is essentially the covariance of the random variables $X(t_1)$ and $X(t_2)$ defined by

$$C_X(t_1, t_2) = E\{[X(t_1) - \eta(t_1)][X(t_2) - \eta(t_2)]\}. \qquad \text{(II-6)}$$

Again, in general, the covariance function, $C_X(t_1, t_2)$, will depend on the times t_1 and t_2 chosen for evaluation.

Generally, for the computation of the mean and the covariance from a set of data points obtained from an experiment, one must still make some simplifying assumptions concerning the random process under investigation. One very important assumption often used is the principle of stationarity. Essentially, a random process is considered stationary in the wide sense (weakly stationary) if its expected value (mean value) is a constant and its covariance depends on time difference rather than specific times. Then for a wide sense stationary random process we have that,

$$\eta(t_s) = \text{constant}$$

$$C_X(t_1, t_2) = C_X(t_1 - t_2) = C_X(\tau). \qquad \text{(II-7)}$$

Unfortunately, for a great many physical problems even the use of these simpler functions is limited because the assumptions which make the calculations valid are not always representative of the process at hand. Still, there is another function, other than the mean and the covariance, which can be used to overcome these problems. This function, called the structure function, was initially introduced by Komogorov to handle the problems associated with non-stationary random processes.

Assume now that X(t) represents a non-stationary random process. Consider the difference function Y(t) defined as

$$Y(t) = X(t + \tau) - X(t) \qquad \text{(II-8)}$$

where for small values of τ, slow changes in the function X(t) do not appreciably affect the difference function Y(t). Essentially, Y(t) can be considered, under these conditions, an approximately stationary function. When in fact Y(t) is a stationary function, X(t) is termed a random process with stationary first increments.

An interesting function is the correlation function of $Y(t)$, denoted as $C_Y(t_1, t_2)$ and defined as

$$C_Y(t_1, t_2) = E\{Y(t_1)Y(t_2)\}$$

$$= E\{[X(t_1 + \tau) - X(t_1)][X(t_2 + \tau) - X(t_2)]\}. \qquad \text{(II-9)}$$

By making use of the algebraic identity

$$(a-b)(c-d) = \frac{1}{2}\{(a-d)^2 + (b-c)^2 - (a-c)^2 - (b-d)^2\} \qquad \text{(II-10)}$$

equation II-9 can be rewritten as

$$\begin{aligned} C_Y(t_1, t_2) = {} & \frac{1}{2} E\{[X(t_1 + \tau) - X(t_2)]^2\} \\ & + \frac{1}{2} E\{[X(t_1) - X(t_2 + \tau)]^2\} \\ & - \frac{1}{2} E\{[X(t_1 + \tau) - X(t_2 + \tau)]^2\} \\ & - \frac{1}{2} E\{[X(t_1) - X(t_2)]^2\} \end{aligned} \qquad \text{(II-11)}$$

Equation II-11 indicates that $C_Y(t_1, t_2)$ can be represented as a linear combination of the functions $E\{[X(t_i) - X(t_j)]^2\}$. We shall now define the structure function for the random process $X(t)$ as,

$$D_X(t_i, t_j) = E\{[X(t_i) - X(t_j)]^2\}. \qquad \text{(II-12)}$$

Then, the correlation function for the difference function Y(t) of the random process X(t) is expressible as a linear combination of structure functions.

If Y(t) is a stationary function, i.e., the random process X(t) has stationary first increments, we can then write that

$$D_X(t_i, t_j) = D_X(t_i - t_j). \qquad \text{(II-13)}$$

Attention has been focused on the time dependence of the random process, and, we will now consider the space dependence of the process. For situations which require consideration of random fields, the counterpart of the concept of stationarity is the concept of homogeneity. A random field is considered homogeneous if its expected value is a constant with respect to space and the covariance function for the random field does not change for translations of the pair of points $\bar{r}_1$, and $\bar{r}_2$ by equal amounts in the same direction. More specifically, the conditions for a homogeneous field are,

$$\eta(\bar{r}) = E\{X(\bar{r})\} = \text{constant}$$

$$C_X(\bar{r}_1, \bar{r}_2) = C_X(\bar{r}_1 + \bar{r}_0, \bar{r}_2 + \bar{r}_0) \qquad \text{(II-14)}$$

From equations II-14, we can imply that for a homogeneous field the covariance function will only depend on the distance between the points $\bar{r}_1$ and $\bar{r}_2$, i.e.,

$$C_X(\bar{r}_1, \bar{r}_2) = C_X(\bar{r}_1 - \bar{r}_2) = C_X(\bar{r}). \qquad \text{(II-15)}$$

Continuing, a homogeneous field is called isotropic if the covariance function depends on just the magnitude of the distance vector $\bar{r}$ and is independent of direction, i.e.,

$$C_X(\bar{r}) = C_X(|\bar{r}|) = C_X(r) \qquad \text{(II-16)}$$

where $r = |\bar{r}|$ represents the magnitude of the distance between observation points.

Experience indicates that homogeneous and isotropic fields are very rough approximations to most physical processes (e.g. the refractive index perturbations of a turbulent atmosphere), hence, we are again led to consider a difference function of the random process.

Forming the difference function $Y(\bar{r})$ at two points $\bar{r}_1$, and $\bar{r}_2$,

$$Y(\bar{r}) = X(\bar{r}_1) - X(\bar{r}_2) \qquad \text{(II-17)}$$

we have that $Y(\bar{r})$ is chiefly affected by the inhomogeneities of the field within the distance $|\bar{r}_1 - \bar{r}_2|$. When this distance is not too large, the largest inhomogeneities will have little effect on the function $Y(\bar{r})$. Consequently, we can define a field as locally homogeneous in a region G if the distribution function of the random variable $Y(\bar{r})$ is invariant with respect to shifts of the pair of points $\bar{r}_1$ and $\bar{r}_2$ providing these shifts and the points of consideration are located within the region G.

The correlation function associated with the difference function which is now defined as

$$Y(\bar{r}) = X(\bar{r}_1 + \bar{r}_0) - X(\bar{r}_1) \qquad \text{(II-18)}$$

can be expressed as

$$C_X(\bar{r}_1 - \bar{r}_2) = E\{[X(\bar{r}_1 + \bar{r}_0) - X(\bar{r}_1)][X(\bar{r}_2 + \bar{r}_0) - X(\bar{r}_2)]\}. \qquad \text{(II-19)}$$

Also, as was shown for the time varying situation, this correlation function can be expressed as a linear combination of functions termed space structure functions defined as,

$$D_X(\bar{r}_i, \bar{r}_j) = E\{[X(\bar{r}_i) - X(\bar{r}_j)]^2\}. \qquad \text{(II-20)}$$

If the random function $Y(\bar{r})$ is locally homogeneous we can write that,

$$D_X(\bar{r}_i, \bar{r}_j) = D_X(\bar{r}_i - \bar{r}_j) = D_X(\bar{r}_\Delta). \qquad \text{(II-21)}$$

When, in addition to being locally homogeneous, the random function is locally isotropic, it follows that

$$D_X(\bar{r}_i - \bar{r}_j) = D_X(|\bar{r}_i - \bar{r}_j|) = D_X(|\bar{r}_\Delta|). \qquad \text{(II-22)}$$

To summarize, if the random function X is non-stationary (non-homogeneous) the covariance function may be very difficult to compute. For these cases, a new function, termed the structure function, is more easily calculated and has the aforementioned properties. Then, the structure function, under the restrictive conditions mentioned, can be useful in describing the fluctuations of the random function.

REFERENCES

1. Athanasios Papoulis, Probability, Random Variables and Stochastic Processes, McGraw-Hill Book Company, (1965)

2. V.I. Tatarski, Wave Propagation in a Turbulent Medium, McGraw-Hill Book Co., (1961)

REFERENCES

Athanasios Papoulis, Probability, Random Variables and Stochastic Processes, McGraw-Hill Book Company, (1965)

C.E. Mees and T.H. James, Theory of the Photographic Process, The MacMillan Company, 318 (1966)

D.L. Fried, J. Opt. Soc. Am., 56, 1372 (1966)

D. Gabor, Nature, 161, 777 (1948)

D. Gabor, Nature, 162, 764 (1948)

Edward L. O'Neill, Introduction to Statistical Optics, Addison-Wesley Publishing Company, 15 (1963)

E. Leith and J. Upatnieks, J. Opt. Soc. Am., 52, 1123 (1962)

E. Leith and J. Upatnieks, J. Opt. Soc. Am., 53, 1377 (1963)

E. Leith and J. Upatnieks, J. Opt. Soc. Am., 54, 1295 (1964)

G.O. Reynolds and T.J. Skinner, J. Opt. Soc. Am., 54, 1302 (1964)

G.R. Heidbreader, J. Opt. Soc. Am., 57, 1477 (1967)

Grant R. Fowles, Introduction to Modern Optics, Holt, Rinehart and Winston, Inc., 144 (1968)

H.M.A. El-Sum, Science and Technology, 71, 50 (1967)

H. Hodara, Proc. IEEE, 54, 368 (1966)

H.M. Smith, Principles of Holography, Wiley-Interscience, (1969)

J.B. De Velis and G.O. Reynolds, Theory and Applications of Holography, Addison-Wesley Publishing Company, (1967)

J.D. Gaskill, J. Opt. Soc. Am., 58, 600 (1968)

J.M. Stone, Radiation and Optics, McGraw Hill Book Company, 299 (1963)

J.W. Goodman, W.H. Huntly Jr., D.W. Jackson, and M. Lehmann, Appl. Phys. Letters, 8, 311 (1966)

Kodak Plates and Films, Eastman Kodak Company, 2 (1973)

L.O. Heflinger, R.F. Wuerker, and R.F. Brooks, J. Appl. Phys., 37, 642 (1966)

M.J. Beran and G.B. Parrent Jr., Theory of Partial Coherence, Prentice-Hall Inc., 12 (1965)

M. Born and E. Wolf, Principles of Optics, third edition, Pergamon Press, N.Y., 453 (1965)

M. Lurie, J. Opt. Soc. Am., 56, 1369 (1966)

M. Lurie, Effects of Partial Coherence on Holography, Doctoral Thesis, Newark College of Engineering, (1967)

M. Zambuto and M. Lurie, Applied Optics, 9, 2066 (1966)

M. Zambuto and M. Lurie, Applied Optics, 9, 2066 (1970)

Philip F. Panter, Modulation, Noise, and Spectral Analysis, McGraw-Hill Book Company, 198 (1965)

R.E. Hufnagel and N.R. Stanley, J. Opt. Soc. Am., 54, 52 (1964)

R.L. Powell and K.A. Stetson, J. Opt. Soc. Am., 55, 1593 (1965)

R.J. Collier and K.S. Pennington, Applied Optics, 6, 1091 (1967)

R.J. Collier, C.B. Burckhardt, L.H. Lin, Optical Holography, Academic Press, (1971)

V.I. Tatarski, Wave Propagation in a Turbulent Medium, McGraw-Hill Book Company, (1961)

W.P. Brown Jr., J. Opt. Soc. Am., 57, 1539 (1967)

W.T. Cathey, Optical Information Processing and Holography, Wiley-Interscience, (1974)

Y.W. Lee, Statistical Theory of Communication, John Wiley and Sons, Inc., 58 (1960)

VITA

1965	B.S.E.E., Magna Cum Laude, Newark College of Engineering, Newark, New Jersey
1968	M.S., Brown University, Providence, Rhode Island

Professional Background

1965-1967	Teaching and Research Assistant, Brown University
1967-1970	Teaching Fellow, Newark College of Engineering
1970-present	Employed by Lockheed Electronics Co. Inc., Plainfield, New Jersey

This research was conducted at Newark College of Engineering during the years 1968-1970 and while employed by Lockheed Electronics Co. Inc. during the years 1970-1975.